# PERFORMANCE OF CONCRETE IN DIFFERENT MARINE EXPOSURE ZONES UTILIZING CEMENTITIOUS MATERIALS AND CHEMICAL ADDITIVES

BY

Ibrahim Nabil Ali Al-Duais

A Thesis Presented to the
DEANSHIP OF GRADUATE STUDIES

**KING FAHD UNIVERSITY OF PETROLEUM & MINERALS**

DHAHRAN, SAUDI ARABIA

In Partial Fulfillment of the
Requirements for the Degree of

# MASTER OF SCIENCE

**In**

CIVIL ENGINEERING

March 2017

KING FAHD UNIVERSITY OF PETROLEUM & MINERALS

DHAHRAN- 31261, SAUDI ARABIA

**DEANSHIP OF GRADUATE STUDIES**

This thesis, written by **Ibrahim Nabil Ali Al-Duais** under the direction his thesis advisor and approved by his thesis committee, has been presented and accepted by the Dean of Graduate Studies, in partial fulfillment of the requirements for the degree of **MASTER OF SCIENCE IN CIVIL ENGINEERING**

Dr. Salah O. Al-Dulaijan
Department Chairman

Dr. Salam A. Zummo
Dean of Graduate Studies

28/5/17

Date

Dr. Salah O. Al-Dulaijan
(Advisor)

Dr. Ahmed Abd El Fattah
(Co-Advisor)

Dr. Mesfer M. Al-Zahrani
(Member)

Dr. Mohammed A. Al-Osta
(Member)

Dr. Shamsad Ahmad
(Member)

© Ibrahim Nabil Ali Al-Duais

2017

[I dedicate this to my mother and father; amare et sapere vix deo conceditur. ]

# ACKNOWLEDGEMENT

First of all, I would like to thank God for guiding me throughout my life and leading me to this point where my dream of perusing scientific research is granted.

Second, I would like to thank my advisors, Dr. Salah Al-Dualijan in the Civil Engineering Department at KFUPM and Dr. Ahmed Abd El Fattah from the college of environmental design at KFUPM. The door to their offices was always open and they helped me immensely while allowing this project to be my own work at the same time. Without their guidance and dedication, my research would not have been possible.

I would like to also thank my thesis committee members, Dr. Mesfer Al-Zahrani, Dr. Mohammed Al-Osta and Dr. Shamshad Ahmad from the Civil Engineering department at KFUPM for their dedication and their patience.

I would also like to thank the maintenance department at KFUPM and the Research Institute as well for allowing me to use their equipment throughout the research duration.

This work would not have been possible without the help of my colleagues Mohammed Al-Sagga, Khalid Al-Shigari and Mohammed Al-Shayea from the Civil Engineering department at KFUPM in addition to the help from my colleague and friend Abdulwahab Al-Luhaibi from the Physics department at KFUPM.

Finally, I would like to express my deepest gratitude to my parents(Nabil and Fadheela Al-Duais), my brothers(Khalid, Majed, Maher, Mohammed, Abdulghani and Ali Al-Duais) and my friends for without their support I would not have been able to pursue my academic goals.

# TABLE OF CONTENTS

ACKNOWLEDGEMENT ..... V

LIST OF FIGURES ..... X

LIST OF TABLES ..... XIV

ABSTRACT ..... XV

ملخص الرسالة ..... XVII

CHAPTER 1.INTRODUCTION ..... 1

CHAPTER 2.OBJECTIVES ..... 9

CHAPTER 3.LITERATURE REVIEW ..... 11

3.1.General literature ..... 11

3.2.Laboratory literature ..... 14

3.3.Exposure literature ..... 24

CHAPTER 4.MATERIALS AND EXPOSURE SITE SETUP ..... 35

4.1.Materials ..... 35

4.2.Mix proportions ..... 37

4.3.Laboratory samples preparation ..... 39

4.4.Exposure sites ..... 40

4.4.1.Location ..... 40

4.4.2.Casting of exposure samples and construction of sites ..... 43

CHAPTER 5.EXPERIMENTS ..... 46

5.1.Physical properties ..... 47

5.1.1.Density, absorption and void ratio test ..... 47

5.1.2.Sorptivity ..... 50

5.1.3.Compressive strength ..... 52

5.2.Lab experiments ..... 54

5.2.1.Rapid chloride permeability test (RCPT) ..... 54

5.2.2.Bulk diffusion ..... 56

5.2.3.Chloride binding ..... 63

5.3.Exposure studies ..... 65

5.3.1.Chloride profiling ..... 66

5.3.2.Linear polarization resistance ..... 68

CHAPTER 6.RESULTS ..... 72

6.1.Compressive strength ..... 72

6.2.Rapid chloride permeability test ..... 73

6.3.Density, absorption and void ratio ..... 75
6.4.Sorptivity ..... 78
6.5.Binding capacity ..... 81
6.6.Bulk diffusion ..... 83
6.7.Chloride profiling ..... 93
6.8.Linear polarization resistance ..... 103
CHAPTER 7.DISCUSSION ..... 116
7.1.Chloride binding models ..... 116
7.2.Chloride threshold and corrosion status ..... 120
7.3.Overall performance of mixes ..... 122
CHAPTER 8.CONCLUSION ..... 126
CHAPTER 9.RECOMMENDATIONS ..... 130
REFERENCES ..... 131
Vitae ..... 144

# LIST OF FIGURES

Figure 1-1: corrosion products and their relative volume: ....4

Figure 1-2: exposure zones breakdown ....5

Figure 4-1: Geographical location of the city of Khobar (Google maps) ....41

Figure 4-2: Satellite images of the exposure beach (left) and exact locations of the tidal, splash and atmospheric zones(right) (Google Satellite)....41

Figure 4-3: Gulf water temperature variance across the depth ....42

Figure 4-4:Gulf water salinity variance across the depth....43

Figure 4-5: Casting process of exposure samples(left) linear polarization resistance sample (middle) and chloride profiling sample (right) ....44

Figure 4-6: burlap curing (left) and shading during curing (right) ....44

Figure 4-7: Atmospheric samples (left) and tidal samples (right) ....45

Figure 5-1: Phase diagram example ....48

Figure 5-2: boiling and cooling of samples for density test ....49

Figure 5-3: suspension weighing setup for density test....50

Figure 5-4: Oven conditioning using KBr solution(left) and sorptivity test setup (right).51

Figure 5-5: Capping of samples(left) and a typical stress-strain curve for plain concrete(right) ....53

Figure 5-6: RCPT cell components(left) and RCPT setup (right) ....56

Figure 5-7: coated samples(left) neutralization in calcium hydroxide (middle) salt water basin with samples exposed in it (right).....58
Figure 5-8:Profile grinding setup(Left) Photospectrometer (middle) Filtration of HNO3 soaked samples (right) .....58
Figure 5-9: example of an absorbance graph.....60
Figure 5-10: potentiometric titration setup .....62
Figure 5-11: example of potentiometric titration voltage graph .....63
Figure 5-12: casting of paste samples (left) wet grinding of samples(right).....65
Figure 5-13: desiccation of samples using silica gel (left) samples after total conditioning(right).....65
Figure 5-14: batching of cored slabs(left) Profile grinder ring setup on site(middle) Profile grinding and dust collecting setup(Right) .....67
Figure 5-15: example of the potential vs. current plot for LPR test.....69
Figure 5-16: example of the Tafel plot and finding the Tafel slopes. .....70
Figure 5-17: Gamry Reference 3000 potentiostat setup(left)connection of the potentionstat to the rebars for LPR testing(right).....71
Figure 6-1: 28-days compressive strength results.....73
Figure 6-2: visual representation of RCPT results(left) relative improvement/decline (right) .....74
Figure 6-3: Bulk Density results compared to the standard mix .....77

Figure 6-4: Void ratio results compared to the standard mix ..... 77

Figure 6-5: Total absorption results compared to the standard mix..... 78

Figure 6-6: Sorptivity curves ..... 79

Figure 6-7:Comparison of the different rates of absorption ..... 81

Figure 6-8: binding capacity test results. ..... 83

Figure 6-9: 35 days ponding profiles ..... 86

Figure 6-10: 6 months ponding profiles ..... 87

Figure 6-11: 12 months ponding profiles ..... 88

Figure 6-12: pinding profiles for each mix vs. exposure duration..... 91

Figure 6-13: Surface chloride and diffusion coefficient from ponding tests..... 92

Figure 6-14: 6-month tidal chloride profiles..... 95

Figure 6-15: 12-month tidal chloride profiles..... 96

Figure 6-16: 12 and 6 months tidal chloride profiles for each mix..... 98

Figure 6-17: 6-month atmospheric chloride profiles..... 99

Figure 6-18: 12-month atmospheric chloride profiles..... 100

Figure 6-19:12 and 6 months atmospheric chloride profiles for each mix..... 102

Figure 6-20: Diffusion coefficient comparison atmospheric(right), tidal (left)..... 102

Figure 6-21: Surface Chloride atmospheric (right), tidal (left)..... 103

Figure 6-22: Corrosion current density readings after 12 months in the tidal zone..... 104

Figure 6-23:Corrosion current density readings after 12 months in the splash zone..... 105

Figure 6-24: Corrosion current density reading for all of the zones for each mix ..... 115

Figure 7-1:Binding models example ..... 119

# LIST OF TABLES

Table 4-1: Chemical composition and physical properties of the materials used. ..... 35

Table 4-2: Mix proportioning ..... 38

Table 4-3: Laboratory sample breakdown ..... 39

Table 5-1: periods at which the mass was recorded in Sorptivity test ..... 52

Table 5-2: RCPT categorization system ..... 54

Table 6-1: RCPT results ..... 74

Table 6-2: Density, absorption and void ratio data ..... 76

Table 6-3: Sorptivity rates ..... 80

Table 7-1: Curve fitting results for the binding models ..... 118

Table 7-2: chloride concentration at activation depth ..... 121

Table 7-3: Overall performance ..... 123

Table 7-4: categorization of the performance of the laboratory mixes. ..... 124

Table 7-5: Performance ranking based on the exposure testing ..... 125

# ABSTRACT

Full Name : Ibrahim Nabil Ali Al-Duais

Thesis Title : Performance of concrete in different marine exposure zones utilizing cementitious materials and chemical additives

Major Field : Civil and Environmental Engineering

Date of Degree : March 2017

Corrosion in reinforced concrete is one of the main causes of deterioration especially in marine zones where chloride is abundant and the relative humidity is relatively higher than non-marine environments. SCMs and chemical additives are used to mitigate the danger caused by such harsh environments. However, results of the use of such materials vary in the literature.

This study covered an exposure and laboratory study in order to evaluate the performance of silica fume, fly ash, ground slag cement and type V cement in addition to type I cement reinforced by Calcium Nitrite Corrosion-Inhibitor, Migrating Corrosion Inhibitor and Caltite in terms of chloride diffusion, chloride permeability, water absorption and sorptivity, compressive strength, linear polarization resistance, and chloride binding capacity testing. In addition, this study focused on the comparison between the performances of the mixtures in the laboratory and exposure sites in addition to focusing

on comparing the results with the literature. The study also aimed to examine the performance of the concrete mixes in relation to their durability aspects.

Another aspect that this study covered was to study the difference in corrosion behavior between different zones in exposures site that were limited, in this study, to the atmospheric, splash and tidal zones.

The study found that the performance of Ground Granulated Blast-Furnace Slag (GGFBS) concrete and fly ash concrete reported the best improvement in terms of chloride binding and overall durability related characteristics.

The study also found a slight performance improvement with the addition of chemical additives especially with the use of deeper cover depths.

# ملخص الرسالة

**الاسم الكامل**: إبراهيم نبيل علي الدعيس

**عنوان الرسالة:** أداء الخرسانة في مناطق التعرض البحري المختلفة باستخدام المواد الإسمنتية والكيميائية

**التخصص:** الهندسة المدنية والبيئية

**تاريخ الدرجة العلمية**: مارس 2017

يعتبر الصدأ في الخرسانة المسلحة أحد الأسباب الرئيسية للتدهور خاصة في المناطق البحرية حيث يكون الكلورايد وفيرا والرطوبة النسبية أعلى من البيئات غير البحرية. تستخدم المواد الإسمنتية المضافة والمواد المضافة الكيميائية لتخفيف الخطر الناجم عن هذه البيئات القاسية. ومع ذلك، تختلف نتائج استخدام هذه المواد في الوسط العلمي.

شملت هذه الدراسة دراسة التعرض والمختبر لتقييم أداء السيليكا فيوم والرماد المتطاير وخبث الحديد المطحون والاسمنت من النوع الخامس بالإضافة إلى الاسمنت الأول المقوى بالكالسيوم نايتريت المانع للصدأ والمهاجرة التآكل المانع والكالتايت من حيث انتشار الكلورايد، نفاذية الكلورايد، امتصاص الماء و معدل الامتصاص، قوة الضغط، مقاومة الاستقطاب الخطي.
بالإضافة إلى ذلك، ركزت هذه الدراسة على المقارنة بين النتائج التي تم جمعها من المختبر ومواقع التعرض بالإضافة إلى التركيز على مقارنة النتائج مع ما تم نشره في الوسط العلمي. كما هدفت الدراسة إلى دراسة أداء الخلطات الخرسانية فيما يتعلق بجوانب الديمومة.

ومن الجوانب الأخرى التي تناولتها الدراسة هو الفرق في سلوك التآكل بين المناطق المختلفة في موقع التعرض المحدودة في هذه الدراسة، إلى مناطق الغلاف الجوي ومناطق الرذاذ ومناطق المد والجزر.وقد توصلت الدراسة إلى أن أداء الخلطات الخرسانية المحتوية لخبث الحديد والرماد المتطاير كان الأفضل من ناحية خاصية ربط الكلورايد ومن ناحية الخصائص المتعلقة بالديمومة بشكل عام.مما توصلت إليه الرسالة أيضا أن استعمال المواد الكيميائية كان له أثر طفيف من ناحية تحسين الخصائص المتعلقة بالديمومة بالأخص عند زيادة حجم الغطاء الخرساني

# CHAPTER 1.INTRODUCTION

Concrete durability in harsh environments has been the main focus of numerous studies around the world in recent history with the Arabian Gulf area being classified as one of most hostile environments for concrete structures. Due to its shallowness, semi-closure and high rate of evaporation (equivalent to 1.5 m/year), the Gulf water can have a salinity content up to 40 ppt. Concrete deterioration in marine environments mainly manifests in one of two forms, either in the form of steel corrosion, with chloride ingress being one of the main causes, or in the form of deterioration of the concrete matrix structure on the molecular scale by reacting chemically with harmful material in the soil or in the atmosphere such as sulfate. One of the main outcomes in the literature is the improvement of the durability characteristics of concrete by the addition of Supplementary Cementitious Materials and/or chemical agents to concrete mixtures. The literature varies on the effectiveness of that addition and that has been a major area of study in recent years.

Corrosion of reinforcing steel is the most common cause of reinforced concrete deterioration and repair. Due to the considerably elevated pH of concrete (ranging from 12.6 to 13.5), embedded steel forms a regenerative passive layer of ferric oxides ($\gamma$-$Fe_2O_3$) that adheres tightly to the surface and prevents further oxidization of the steel,

thus preventing corrosion [1]. Corrosion mainly manifests in concrete in one of two forms. The first form is uniform corrosion and it is when the pH of the concrete is lowered uniformly by the ingress of carbon dioxide through diffusion that reacts with the calcium hydroxide inside the concrete forming Calcium Carbonate. As a result, the whole reinforcement is de-passivated and corrosion cells are formed in succession where anodes and cathodes are next to each other in the same reinforcement bar. The second form is mainly associated with chloride ingress and mainly manifests in the form of localized (pitting) corrosion.

The mechanism of chloride-induced corrosion is described by Neville[2] as the local reaction between the passivated layer of reinforcement and chloride ions that activates the steel ions forming an anode. The adjacent passive layer of the same reinforcement becomes the cathode with the water in the concrete forming the electrolyte to connect them as shown in Equations 1 to 3:

$$Fe \rightarrow Fe^{+2} + 2e \quad (1)$$

$$Fe^{+2} + 2Cl^{-} \rightarrow FeCl_2 \quad (2)$$

$$FeCl_2 + 2H2O \rightarrow Fe(OH)_2 + 2HCl \quad (3)$$

Thus, the chloride ions are regenerated and are free to de-passivate more reinforcement. Ferric hydroxide ($Fe(OH)_3$) is formed at the anode while water and oxygen react with the released electrons at the cathode to form hydroxyl ions that are free to react with steel to activate it again in a continuous reaction resulting in the deposit of more iron rust. In order for this process to initiate, it is required that the chloride reaches a certain critical concentration at the reinforcement level identified as the “chloride threshold”.

The main issue with this process, in addition to the weakening of the reinforcement, lies in the fact that the corrosion reaction products occupy larger volume which creates internal stress within the concrete leading to the formation of cracks within concrete that allow for more chloride-laden water to penetrate and increase expansion and damage as shown in Figure 1-1.

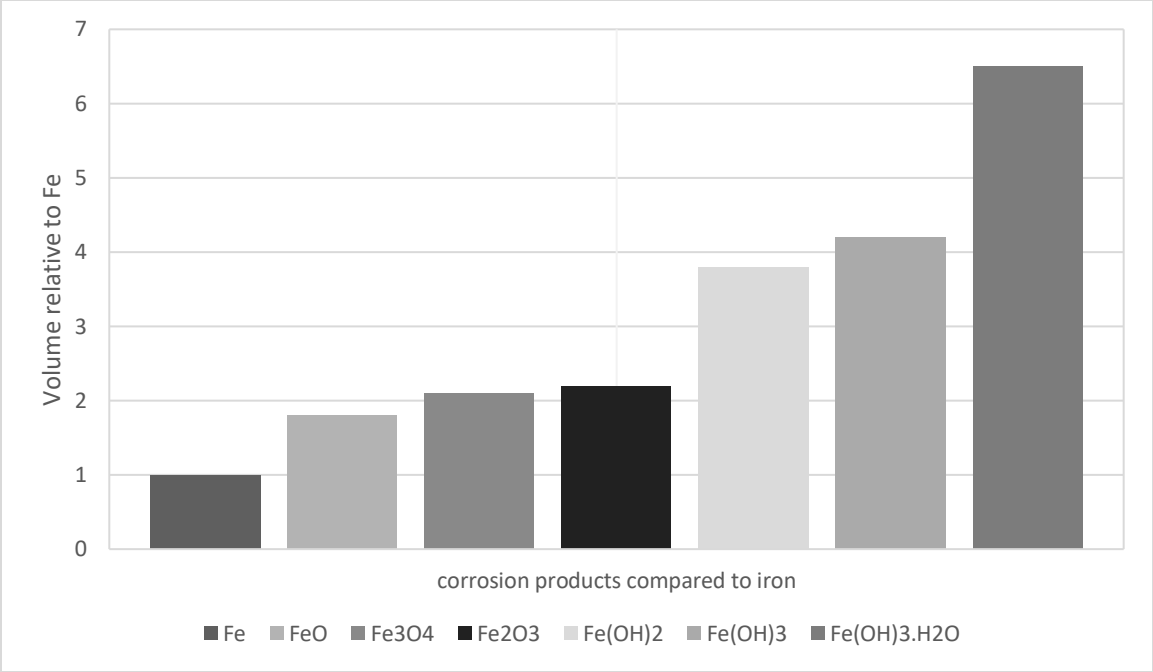


*Figure 1-1: corrosion products and their relative volume:*

Durability studies are usually conducted in one of two forms, either in laboratories with controlled environments where actual exposure conditions are simulated or are conducted on real exposure sites in selected marine environments. In most exposure studies the marine environment is divided into four main zones in relation to the interaction between concrete and seawater as shown in Figure 2. The first zone is the atmospheric zone and it is defined as the area of the site where concrete is not in direct contact with water and only airborne chlorides interact with the concrete. The next zone is the splash zone and it is characterized as the zone where water splashing caused by the tide waves crashing comes into contact with concrete. The third zone (tidal zone) has been labeled as the

worst zones for concrete by many researcher and it is defined as the area that lies between the high and low tide levels. Concrete in this zone is subjected to cyclic drying and wetting throughout the day which creates chemical differentials that expedites the migration of chlorides into concrete. The submerged zone which as the name suggests lies under the low tide level and concrete in this zone is totally submerged in seawater at all times. This area has minimal effects on corrosion since it has low oxygen levels which is a requirement for the corrosion reaction.

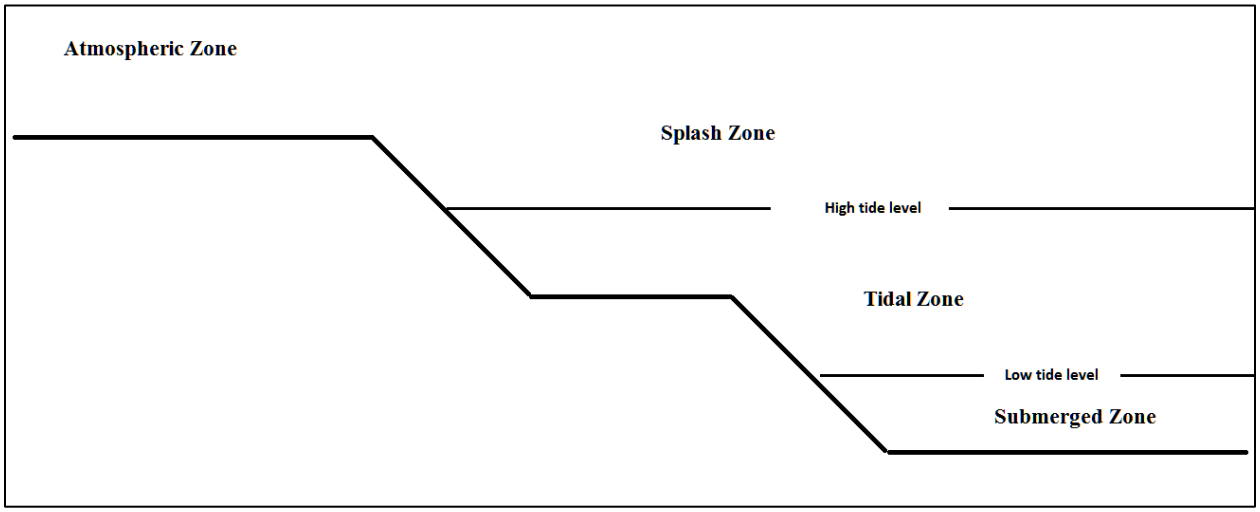


*Figure 1-2: exposure zones breakdown*

One of the best ways to protect concrete reinforcing steel from corrosion is to reduce the concrete porosity and permeability. A concrete microstructure that is less porous increases the amount of time required for the chloride concentration to reach the chloride threshold, and consequently expands concrete service life. Concrete permeability and

diffusivity can be reduced by the use of supplementary cementitious materials (SCMs) such as GGBFS, fly ash, or silica fume or use of a lower water-to-cementitious materials ratio (w/cm) [3]. The effectiveness of such materials have been the main focus of numerous studies [4]–[12] where the diffusion is studied and the corrosion activity is monitored. The possibility and rate of corrosion are controlled by two main factors: the ease of chloride ingress into the surface of the reinforcement and the concentration required to initiate the reaction and maintain it. Chloride ingress typically follows three forms according to Malikakkal and Neville [2], [13] that include: ingress by diffusion, ingress by capillary suction and ingress by absorption and permeation with the former two forms being more impactful than the latter.

Diffusion is described as the movement of chloride (or other water soluble ions) under a chemical differential. In marine environments, concrete is subjected to chloride diffusion from the sea water. The rate of diffusion is influenced by the diffusion coefficient as described by Fick's second law of diffusion [14]–[16]. Chloride diffusion and the influence of adding SCMs and additives while varying the water-to-cementitious material ratio (w/cm) is a major study subject in contemporary literature [17]–[28].

Capillary suction (sorptivity) is described as the movement of water under capillary action without the application of a pressure nor a chemical differential. It is a material property that is associated with the internal structure of porous materials such as concrete.

Since water plays the role of an electrolyte in the corrosion cell, control of water movement has been a major focal point in recent published researches [21], [22], [29]–[36]. Pore refinement in the transition zone (area near the interface between coarse aggregates and cement) by the addition of SCMs is reported to decrease the permeability and sorptivity while producing higher strength concretes as well due to the pozzolanic reaction[1], [2].

Calcium Nitrite corrosion inhibitor ($CaNO_2$) has been used in mitigating corrosion since the 1970s and has been recommended as a replacement for Sodium Nitrite and Sodium Benzoate since the latter two have been reported to reduce the strength of concretes made incorporating them [37]. The mechanism of CNI was explained by Kim et al. [38] and it is described by the formation of more Iron Oxides, particularly $Fe_2O_3$, which play a role similar to the passive layer on the surface of the reinforcement. In addition, CNI raises the anodic polarization towards a safer one thus increasing the chloride threshold and delaying the corrosion initiation and propagation. On the other hand, organic Migrating corrosion inhibitors started to gain popularity as either surface treatment agents or as admixtures during batching. MCIs usually consist of chains that have polar and no-polar sides as Morris and Vazquez [39] explain. The polar side of the chain travels through the concrete and adheres to the surface of the reinforcement while the non-polar end is aligned normal to the surface. This results in forming a protective layer on the surface of the reinforcement which limits its exposure to chloride ions in addition to the nonpolar

side of the MCI chain repelling chloride ions as well. Finally, the role of caltite as either a surface treatment agent or an admixture revolves around adding a hydrophobic nature to the concrete which in turn slows the movement of chlorides and other chemicals that are dissolved in water.

# CHAPTER 2.OBJECTIVES

According to the reviewed literature, no specific SCM is reported to have the best effect on the durability aspects of concrete. Moreover, the literature contains varying results regarding the SCMs chosen in this study where part of the research claims an advantage to the implementation of a certain SCM while other studies reports that SCM to be of little to no effect in terms of durability aspects. The variation can be owed to numerous reasons such as: differences in exposure conditions, differences in exposure periods and differences in mixture proportions. This work studies the effect of the aforementioned SCMs and chemical additives in the Arabian Gulf and verify the results in the literature of the same exposure conditions. In addition, with the Gulf area being reported as a severely harsh environment, research is required in order to enhance the durability of concrete subjected to such environment.

The primary objective of this study is to monitor the performance of concrete with different local SCMs and chemical additives exposed to the Arabian Gulf deteriorative marine environment in terms of corrosion related tests and compare the results to the available literature. In addition, the study aims to investigate the differences between the performances of mixtures in laboratory tests and the tests conducted on the chosen

exposure sites (tidal, splash and/or atmospheric) in terms of chloride ingress and corrosion results.

Furthermore, the study aims to identify the most hostile exposure type since researchers in the same region such as Valipour [40] who suggested that the splash zone was the most aggressive in the Arabian Gulf region despite other studies that show the tidal zone being the most aggressive.

In order to achieve the previously mentioned objectives, the following milestones have to be achieved:

1. Casting and curing of laboratory and exposure samples.
2. Construction of two well-located exposure sites in the Arabian Gulf.
3. Planning, scheduling and procuring the required equipment for the tests.
4. Testing of the samples both on-site and in the laboratory.
5. Compilation and representation of the data and benchmarking it against literature.

# CHAPTER 3.LITERATURE REVIEW

This chapter addresses the works found in the literature regarding the theory of diffusion, the chloride thresholds and the application of SCMs and chemical admixtures in corrosion monitoring in laboratory and exposure studies. It is divided into three sections in terms of the literature subject which are: theoretical and review literature that cover the theory of diffusion and chloride threshold studies, laboratory studies related to the application of SCMs in corrosion-related properties, and exposure studies that address the use of SCMs and chemical admixtures in exposure sites around the world. Some of the studies may include laboratory and exposure parts which will be mentioned if applicable. It is worth mentioning that the contemporary literature regarding the use of corrosion inhibitors and hydrophobic agents in chloride binding, chloride profiling, chloride diffusion and water absorption and sorptivity are quite scarce.

## 3.1. General literature

Angst et al.[41] published a review on the value of chloride content that was deemed critical in various studies spanning over 30 years from the 1980s to the 2000s. The authors divided the critical values into two categories based on the damage caused due to corrosion; chloride contents that signaled the initiation of corrosion and chloride contents that at which a considerable damage to the concrete is attained. The authors stated that

the exposure conditions may affect the critical contents at which corrosion is initiated. The publication also included the results of addition of supplementary cementitious materials from different studies worldwide. It was reported that the addition of Silica Fume (SF) generally resulted in lowering the critical chloride content while the addition of Ground Granulated Blast-furnace Slag (GGBFS) on the other hand reported mixed results in the literature. It is noted that the paper generalized the addition of supplementary cementitious materials and did not take into consideration the amounts at which they were added in the reviewed experiments. Values of the chloride threshold varied from 0.4% to 0.8% by weight of binder for OPC concrete, 0.2 % to 1.2% for GGBFS concrete, 0.4% to 1.2% for fly ash concrete and 0.2% to 0.68% for silica fume concrete.

Andrade and Alonso [42][43], [44] published three journal articles on the various methods of monitoring corrosion in the laboratory and on site. The papers first started by defining the corrosion rate in civil engineering and its relationship with time and their importance in assessing the state of reinforcement steel embedded in concrete. The papers also defined the method by which chloride-induced corrosion initiate which is described as the deposition of chloride salts on the surface of the concrete that dry during the drying cycle of the climate thus increasing the chloride concentration at the surface creating a chemical differential that drives the chloride deeper into the concrete. The cycle of depositing chloride on the surface, drying it and then diffusing it through the

concrete is repeated daily and seasonally until sufficient chloride reaches the surface of the rebars and depassivate it leading to the initiation of corrosion. Both papers then proceeded to discuss the difference between the Alternating Current (AC) and Direct Current (DC) methods and their respective advantages and disadvantages in addition to their applications. The methods included corrosion potential monitoring which evaluates the risk of corrosion and the resistivity method which only gives a qualitative assessment of the concrete state. The publications also explained some complementary methods and on site methods. They concluded that the most important method of corrosion monitoring was the linear polarized resistance method and the weight loss method. The paper suggested a categorization criterion that would classify the corrosion based on severity using the corrosion current readings. The papers also proposed that a minimum of four measurements of the polarized resistance ($R_p$) and current density ($I_{corr}$) should be taken to negate the effects of dry and rainy periods on the results respectively.

Ann et al. [45] studied the effect of concrete surface chloride concentration (Cs) on the time to corrosion in different concrete structures. The study mainly focused on modelling the surface concentration and studying the effect on the time to corrosion using chloride bulk diffusion data gathered at different exposure period for different exposure conditions. The study proposed four different models for the concrete surface concentration in which Cs was related to exposure time. The constant model, which is used a solution for Fick's second law of diffusion, reported the highest surface

concentration which resulted in the highest corrosion risk and the shortest time to corrosion period unlike the linear and square root models. However, it is noted that the assumption of constant Cs leads to the most conservative results by reporting higher corrosion risk. The authors also studied the effect of adding SCMs on the diffusion coefficients and reached a conclusion that the addition generally results in a reduction of the apparent diffusion coefficients ($D_a$) which is owed to the enhancement of the pore structure due the pozzolanic reaction. Another factor for the previous mentioned decrease is the higher chloride binding capacity especially in GGBFS. Moreover, it was highlighted in the paper that rate of diffusion decreases with time until it reaches a minimum value at which it maintains that plateau level despite the type of concrete or the exposure conditions.

## 3.2. Laboratory literature

Kayali and Zhu [17] conducted a fourteen-month project in which medium strength concrete (w/b=0.6) and high strength concrete (w/b=0.3) containing 10% silica fume were partially submerged in 3.5% NaCl solution. The samples were cast as slabs with reinforcement being embedded 25 mm from the surface of the concrete. Moreover, the samples were placed in 10 mm deep NaCl solution that was agitated to simulate the tidal zone conditions. The authors conducted bulk diffusion, corrosion potential and corrosion current density tests. Medium strength concrete was reported to have an active corrosion

after only 240 days with a corrosion potential more negative than -500 mV while the high strength concrete maintained a potential less than -200 mV and a current density of 0.2 $\mu A/cm^2$ which indicated a low chance of corrosion.

Matsumura et al. [18] conducted a 256 day-long experiment on OPC concrete in order to examine the effect of temperature and water-to-cement ratio on the chloride diffusivity. Cylindrical samples were cast and cured and then sealed from all sides except for one where a groove is made and a salt solution is poured. The authors reported a significant increase in the diffusivity with increased temperature as well as with increased water-to-cement ratio.

Ramezanionpour and Malhotra [29] tested the mechanical properties and chloride resistance of mixes with different supplementary cementitious materials (SCMs) modified concretes. Silica fume, fly ash and ground granulated blast-furnace slag were added separately at different replacement ratios (SF at 10%, GGBFS at 25% and 50%, FA at 25% and 58% with lower W/C ratio of 0.35) to ordinary Portland cement concrete with a water-to-cementitious materials ratio of 0.5. Concrete with SF showed the highest rate of strength development and largest overall strength at 180 days followed by the control mix. It was reported that the mix with 50% GGBFS exhibited the lowest rate of strength development and overall strength. However, they showed the best pore refinement out of all the tested samples. The chloride resistance was measured using

ASTM1202 in which a voltage was applied through the test cell and the charges passed over the period of six hours was recorded. All of the modified concretes showed a general improvement in the resistivity with the SF concrete exhibiting the lowest RCPT number.

Dhir et al. [19] studied the effects of adding fly ash at different replacement contents on the diffusivity and binding capacity of concrete. Fly ash was added at different contents ranging from 17 to 67% by weigh of the binder. The study showed the addition of fly ash results in a sharp decrease in the diffusion coefficient up to 70% and a remarkable increase in the binding capacity up to 200%. Moreover, the study reported that the optimum fly ash content was around 33% by binder weight since any further increase up to 50% did not cause any significant change while any addition more than that caused negative effects on the binding and diffusive properties of the specimens.

Song and Kwon [20] Conducted a lab experiment on the chloride ingress in concrete utilizing a neural network algorithm and the micro pore structure system. Samples with different fly ash, silica fume and GGBFS contents were submerged, after wet curing for different periods, in a concentrated NaCl solution for six months and the chloride profile was extracted by grinding the samples at different depths. The study reported an overall decrease in the diffusion coefficient with the addition of the aforementioned SCMs. In addition, chloride ingress was found to be lowest in the case of the concrete with 50% GGBFS.

Tamimi et al. [21] conducted a 21-month long lab experiment in which normal concrete made with type I cement and high performance concrete containing GGBFS at a replacement content of 40% by weight of binder were exposed to concentrated NaCl solution in accordance to ASTM C 1556. The chloride profile and diffusion coefficient were calculated using Fick's 2$^{nd}$ law of diffusion. The study showed a sharp reduction in the chloride penetration and concentration as high as 50% with the addition of GGBFS. Moreover, the authors conducted an experiment in which the initial absorption of concrete was measured and found that the value decreased with the addition of GGBFS in the early stages of the test.

Luping and Nilsson[46] developed a method to study the binding capacity of OPC pastes and mortars subjected to saline environments. The study used repeated cycles of binding and unbinding of crushed and conditioned paste and mortar samples at different water-to-cement ratios. The study reported that the binding capacity is dependent on the water-to-cement ratio if the binding capacity is to be expressed per unit weight of the binder and independent to the water-to-cement ratio if it is expressed per unit of CSH gel. The study also found that the binding capacity and its irreversibility are proportional to the free chloride ($C_f$). The study also tried to model the binding capacity using the Langmuir isotherm model and the Freundlich binding isotherm model and reported that both models were fit as long as the free chloride concentration is less than 1 Molar.

Thomas et al. [47] conducted a study in which the chloride binding capacity of pastes containing different SCMs was measured using the method suggested by Luping and Nilsson[46] . The study included investigating the relationship between the bound chloride and the free chloride (water soluble) in addition to the mechanism of chloride binding and irreversibility of the bound chloride. Moreover, the authors investigated the relationship of the water-to-binder ratio to the binding capacity. The addition of SCMs with higher Alumina compounds showed the greatest increase in binding capacity such as Metakaolin while other SCMs with lower Alumina compounds showed less improvement which was the case with silica fume. In addition, the study showed that lowering the water-to-binder ratio decreased the binding capacity in all paste specimens while increasing the NaCl concentration in the exposure solution increased the irreversibility of the binding process by converting larger portion of the bound chloride to Friedel's salt.

Islam and Islam [48] investigated the physical and chemical durability characteristics of concretes blended with fly ash at different replacement contents ranging from 10% to 70% by weight of binder. The study included the Rapid Chloride Penetration Test at different concrete ages. Addition of the fly ash showed a remarkable increase in the charges passed beyond the 4000 coulombs limit in the early ages that increased with higher fly ash contents. However, the values of the RCPT test kept decreasing with age with the optimum fly ash content being 30% which showed a remarkable decrease of 50% compared to the OPC concrete samples.

Valipour et al. [22] conduct a lab experiment in which concretes with zeolite, metakaolin , natural pozzolans and silica fume were compared to each other in terms of the values of strength, strength development, water absorption, water sorptivity and chloride diffusion tests. All SCMs were added at multiple replacement contents. The study showed a remarkable improvement in most aspects with the concrete having 10% silica being the most improved in terms of lower chloride diffusion coefficient (22%), gas permeability (40%), sorptivity (83%), volume of voids (91%) and water absorption (75%) in addition to higher electrical resistivity (184%) and compressive strength (128%).

Yun and Kyum [24] studied the effects of adding GGBFS to concrete in terms of chloride permeability and corrosion resistivity. They tested concrete samples that were cured for 28 days and for 50 days for the rapid chloride permeability characteristics and found that adding GGBFS decreased the charge passed during the test. They also concluded that replacing cement with GGBFS at replacement ratios of 40% and higher or by weight of cement increased the corrosion resistivity 200% and reduced the area of reinforcement corroded by half. They also reported that concrete made with type V cement was inferior to type I concrete or GGBFS concrete in terms of RCPT values, Half cell potential and corrosion current density values.

Nokken et al. [25] studied the long term and short term effect of adding pozzolanic materials (silica fume, GGBFS, fly ash and high reactivity metakaolin) at different

replacement ratios on the diffusion coefficients for samples submerged in 1 Molar NaCl solution. The study found that the diffusion coefficient was reduced significantly with the addition of the pozzolanic materials and the largest decrease was reported with the silica fume and GGBFS mixture added at 8% and 25% respectively. Also, the study found that the diffusion coefficient decrease followed a pattern that could be modeled for the laboratory samples.

Siddique [27] studied the effect of adding fly ash and coal bottom ash to concrete in terms of compressive strength, abrasion resistance, RCPT and sorptivity. The study reported a sharp decrease in the RCPT values at 90 days and at 360 days for the samples the fly ash that resulted in classifying the chloride permeability of the samples in the "very low" category. The study also reported an increase in the sorptivity for the fly ash mixes that was proportional to the replacement ratio.

Hooton et al. [28] studied the effect of adding silica fume at different ratios (0, 7 and 12%) to concretes having different water-to-cementitious materials ratios ranging for 0.35 to 0.45 on the bulk diffusion and RCPT values. It was reported that the samples were steam cured which may have had an effect on the results if compared to samples made with the same constituents but are cured via a different method. The study reported an overall improvement in the performance of the 7% silica fume samples in terms of

reducing both the diffusion coefficient and RCPT values in addition to reducing the overall diffusion values.

Dhir et al. [49] studied the binding properties of concretes containing GGBFS at different replacement percentages ranging from 0 % to 67 % by weight of cement. The samples were tested after immersion in Sodium Chloride solutions that had different concentrations ranging from 0.1 Molar (mol/L) to 5 Molar. The study reported a substantial increase in the binding capacity with the increase of Slag cement content and with the increase of the concentration of the free chloride in the solution. The study also reported that a replacement percentage of 60% and higher would be useful in hindering the movement of chlorides especially in high-salinity marine environments.

Luo et al. [9] studied the effect of adding Gypsum (5 % by weight of binder) and GGBFS (65% and 70% by weight of binder) on the diffusion and chloride binding properties of such concretes. The study reported a 30% decrease in the total chloride diffusion coefficient and a 40% decrease in the free chloride diffusion coefficient in the mixtures that contained both the gypsum and GGBFS. The study also reported a noticeable increase in the bound chloride content of the previously mentioned concretes compared to the normal mixtures.

Delagrave et al. [50] studied the effect of silica fume on the binding capacity of concrete subjected to an environment that has a relatively high saline content. The study reported a

slight decrease in the binding capacity of cement pastes made with 6% silica fume. In addition, the study claimed that when the bound chloride is expressed per unit mass of the CSH gel available in the sample that is become independent of the water-to-binder ratio.

Yuan et al. [51] published a review journal on the effects of adding various supplementary cementitious materials on the binding capacity and reported that in the case of silica fume the general trend in the literature was that it decreased the binding capacity due to the reduction of the pH and due to lowering the calcium-to-silicate ratio in the mixture because of the pozzolanic reaction which depletes part of the Calcium from the concrete in spite of some studies reporting an increase in the binding capacity with silica fume concretes. In addition, they reported that in the case of fly ash and GGBFS concretes, the literature mostly agrees that their addition increases the binding capacity substantially due to high alumina content and due to the sulphate dilution effect.

Demirel [31] studied the effect of pumice and silica content on the sorptivity of concrete tested at different temperatures. The study reported that the addition of pumice on its own as a SCM increased the sorptivity and reduced the compressive strength while the addition of pumice and silica fume reduced the sorptivity by 50% in the case of the mixture with 10% silica fume and 5% pumice. Moreover, the study reported that while keeping the silica fume at a constant percentage and increasing the pumice content, the

sorptivity kept on increasing which indicates that the reduction gained by ternary blend is most likely a result of the silica fume and not the pumice.

Uysal and Akyuncu [32] studied the effect of adding Class F and C fly ash to concrete in terms of chloride resistivity and sorptivity. The study reported a drastic decrease in the RCPT value with the addition of 34% class F fly ash (more than 80% reduction) and reported similar but less drastic reductions at other fly ash contents and for both classes of fly ash. In addition, the study reported a decrease in the sorptivity for both classes but were more prominent at higher cement content and with the use class F fly ash.

Li et al. [33] studied the effects of adding silica fume and silica flour on the RCPT values and density values for concrete made with such materials at different replacement contents ranging from 0% to 30% for both silica based materials. The study reported a drastic improvement in the chloride resistivity that was proportional to the silica fume and silica flour contents especially at later ages. The study also reported an increase in the density which can be owed to the pozzolanic reaction filling the spaces by forming more CSH crystals thus reforming the internal structure.

Leung et al. [34] studied the effect of adding different amounts of fly ash and silica fume to self compacting concrete in terms of sorptivity and strength development. The study reported a general increase in the total water absorbed with time. The study also reported a decrease in the water sorptivity with the addition of fly ash that was noticeable at 20%

fly ash content and higher. In addition, the study reported substantial decrease in the total water absorbed with the addition of silica fume.

Hung et al [35] studied the short and long term effects of GGBFS on the water absorption, sorptivity and free shrinkage in concretes made incorporating such materials. The study reported a similar water absorption and sorptivity at 28 days in all mixes while at 90 days the values of the total absorption, sorptivity and shrinkage were reduced significantly especially with GGBFS content of over 40%. The study concluded that the effect of GGBFS in reducing the sorptivity and overall enhancing the water-related aspects of concrete are more pronounced in the long term.

Nath and Sarker [36] studied the effects of class F fly ash content on the sorptivity, chloride resistance and shrinkage of concrete at different ages. The study reported a general decrease in the sorptivity and RCPT values in early ages as well as later ages with the addition of fly ash and noted that the decrease in both were proportional to the fly ash content.

## 3.3. Exposure literature

Akiyama et al. [52] Studied the effect of airborne chloride on the probability of corrosion induced cracking in ordinary Portland cement. The study was conducted in the atmospheric zone in multiple locations on the coast of different main islands in Japan. Moreover, the study proposed a design method for calculating the cracking occurrence

probability and the probability of steel corrosion that would be initiated due to atmospheric chlorides. It is noted that the authors design method did not take into consideration the effect of rain level and humidity in addition to the differences in corrosion rates within a given structure on the hazard imposed by airborne chloride.

Andrade et al. [53] conducted a year-long exposure experiment off the coast of Madrid in Spain where OPC samples were subjected to the natural environmental weathering process that manifested mainly through rain and change in temperature in 1997. The chloride was introduced in the concrete via the addition of two different salts that were studied separately; Calcium Di-Chloride ($CaCl_2$) and Sodium Chloride (NaCl). Both chemicals were added as 3% by weight of concrete and Corrosion potential, resistivity in terms of polarized resistance, corrosion rate, internal relative humidity and external relative humidity were monitored periodically throughout the exposure period using Coppper/Copper Sulphate reference electrodes for the electrochemical tests. A moisture factor was assigned to samples based on the moisture conditions and later was found to better relate to the values of the corrosion rate than internal relative humidity or the temperature which the experiment was unsuccessful in finding a relationship with. It was found also that the resistivity was the most comprehensive test that described the state of the concrete.

Costa and Appleton [15], [16] conducted an exposure study on concrete samples with different mixes and water-to-binder ratios off the coast of Portugal on the Atlantic Ocean that lasted for 3 years for some samples and 5 years for the rest. The exposure was carried out in five different zones (spray, tidal, atmospheric and two dockyards) to study the weathering process of each one. OPC with a water-to-cement ratio of 0.3 and 0.5 was used in addition to OPC samples with 4.12% SF replacement by weight of binder and a w/b ratio of 0.35. Bulk diffusion data collected over the exposure period was used to derive an advanced exponential diffusion model of Fick's law that correlated well with the original model. In addition, an empirical model for the surface concentration was proposed and used in formulating the previously mentioned advanced Fick's model. The study noted that in the early ages a rapid chloride penetration is observed the attenuates over time leading to an increase in the surface chloride concentration. Moreover, the study conclude that the cover depth was a very integral component in concrete durability even with high performance concretes and that an effective cover depth that is less than 40 mm is inadequate. However, it is noted that curing time was relatively short lasting only 7 days unlike the standard curing period. The authors also published an earlier paper in which the values of $D_a$ of the three aforementioned mixtures were determined in addition to the Cs values. It was reported the value of Cs increased over time in spite of the exposure zone with the tidal zone having the highest one in addition to the highest penetration followed by the spray and atmospherics zone respectively. It is worth noting

the change in Cs values were not affected by the mix properties as much as the exposure type which seemed to be greatly influencing them. SF mixes was recorded to have the lowest diffusion coefficient which was 50% less than the OPC mix with w/b of 0.5. However, the reduction in $D_a$ in the SF mix was marginal the OPC mix which had a w/b of 0.3. It is noted that the authors compared the performance of SF to OPC that had a lower w/b ratio instead of comparing its performance to a mix with the same w/b ratio. Moreover, the authors tested the SF mix in the atmospheric zone and one of the dockyards only unlike the other two mixes which were tested for all zones.

Ganjian and Pouya [4] Studied the effect of adding silica fume and blast furnace slag to concrete in samples exposed to the weathering action in the Persian Gulf. The study included four different mixes; standard type II Portland cement concrete, 7.5% silica fume concrete, 10% silica fume concrete, and 10% silica fume with 50% GGBFS concrete. The samples were evaluated over the period of six months in the tidal zone of the Persian Gulf and in simulation ponds. It was reported that the mix with 10% SF had the highest rate of strength development and overall strength while exhibiting the lowest strength loss rate followed by the 7.5% SF mix. Moreover, the ternary blend concrete (GGBFS and SF) exhibited the lowest strength development rate and the highest rate of strength loss across both exposure media. However, it is noted that the GGBFS did not pass the ASTM standard.

Shekarchi et al. [54] conducted a three-year long experiment on the effect of the tidal zone weathering on concrete with SF. Concrete mixes with a water-to-cement ratio varying from 0.35 to 0.5 and a SF replacement percentages varying from 5% to 12.5% were tested for the Chloride bulk diffusion to study the effect of varying water-to-binder ratio in addition to studying the effect of the addition of the SF. Lowering the water-to-binder ratio was reported to increase the durability of the by significally reducing the diffusivity of chloride in concrete up to 75%. However, this reduction became less significant as the water-to-binder ratio was lowered beyond 0.4. Moreover, the authors attributed this reduction in the diffusivity to the enhanced pore structure formed with lower ratios. On the other hand, the authors reported a noticeable decrease, up to 50% for the same w/b ratio, in diffusivity with the addition of SF. However, the behavior of mixes containing SF was not predicTable and varied across different water-to-cement ratios. Nonetheless, the experiment reported a general improvement in durability with the addition of SF. In addition, the authors reported the optimum SF content to be around 7.5% as further addition did not cause any significant change in the diffusivity.

Valipour et al. [40] published a paper that summarized their study on the effect of adding silica fume, metakaolin and zeolite to type II Portland cement concrete on the durability aspects when exposed to the chloride ingress in the Persian Gulf. The study was conducted for nine months and included different exposure zones (soil, atmospheric, splash and tidal zones). Four type II concrete mixes with varying water-to-cement ratios

were cast and cured for two days in addition to three mixes with 5% SF, 5% Metakaolin and 10% Zeolite respectively. The study reported a noticeable improvement in durability that manifested by the reduction in the diffusion coefficient and chloride content up to 30% in the case of 0.35 w/c concrete. However, the improvement was only noticeable in lower water-to-cement ratios (0.4 to 0.35). The paper reported similar performances in all concretes with SCMs that manifested by a significant reduction in the diffusion coefficient up to 80% in the tidal zone and 25% in the splash. It is noted that the authors reported the splash zone to be the most critical in terms of durability instead of the tidal zone which is the one reported to be the most critical in most the literature covered.

Mustafa and Yosuf [55] conducted a year-long experiment off the coast of Port Dickson in Malaysia in the atmospheric zone. The study used OPC concrete samples with a water-to-cement ratio of 0.5. The specimens were divided into four groups depending on their distance from the sea shore and elevation from the sea line. The bulk diffusion test was carried out on the samples every three months to monitor the development of the surface chloride content (Cs) and the apparent diffusion coefficient (Da) in accordance with Fick's law of diffusion. A general trend was reported by the authors in which Cs would increase over time and Da would decrease. The final 1 year readings were below the critical chloride content. However, it can be noted that the samples closest to the sea shore were exposed to splashing action by the sea during strong winds which violates the exposure condition set in the beginning of the study.

Meira et al. [56] exposed OPC concrete samples with varying water-to-cement ratios (0.5, 0.57 and 0.65) to the atmospheric zone weathering off the coast of Jaoa Pessoa in Brazil. The chloride concentration in the air was monitored using the wet candle device. The study was carried for four years where samples were placed at different distances from the sea shore were tested at different time intervals for the chloride bulk diffusion. Samples were cured for seven days before being exposed which simulates actual construction conditions. The study reported trends of Cs, Da and chloride concentrations similar to those discussed previously in which Cs and chloride concentrations increased over time while Da declined.

Pack et al. [57] studied chloride ingress in bridge piers with varying age on the western coast of South Korea. The piers were variant in age and in composition but were divided into two groups: OPC piers and GGBFS piers. The age of the bridges varied from six months to 48 years. All Samples were extracted from the same area in each bridge to be comparable. The area chosen was between the high and low tide lines so it would represent the tidal zone exposure. It was reported the GGBFS bridges showed generally lower values of Da and Cs compared to the OPC ones.

Roy et al. [58] conducted an exposure study off the coast of Pulau Brani to the south of Singapore in which OPC concrete samples were set in different exposure zones (Atmospheric, tidal and submerged) and exposed for 80 weeks. During the exposure

period, the bulk diffusion test was carried out at twenty-week intervals. The results of the study were in good agreement with other experiments carried out in the same region and showed trends that were in agreement with the literature as well where the surface concentration increased and diffusion coefficient decreased with time. The study also concluded that the chloride diffusion coefficient is more dependent on the w/c ratio than on other parameters such as the fineness of cement or addition of water reducers and superplasticizers. Moreover, the study reported that the slightest increase in reinforcement cover depth greatly affects the time to corrosion initiation.

Safehian and Ramezanianpour [30] conducted a study in which precast piers and cast-in-place concrete elements subjected to the marine activity 50 kilometers away from the mouth of the Persian Gulf were rehabilitated using concrete with silica fume content of 14%. The elements in question were placed in three different exposure zones (Tidal, Splash and Atmospheric) and the long term performance against deterioration was studied. The addition of the silica fume was reported to decrease the charges passed in the Rapid Chloride Permeability Test (RCPT) by 30% which may indicate a denser microstructure. In addition, the study found that the most aggressive exposure zone in terms of surface chloride concentration and chloride diffusion coefficient was the tidal zone followed by the splash and atmospheric zones respectively.

Sandberg et al. [59] conducted a 5-year study on the chloride ingress in concretes subjected to different exposure conditions off the west coast of Sweden. The specimens were cast with different w/b ratios ranging from 0.25 to 0.5 and with different silica fume and fly ash contents varying from 5 to 10% and 10 to 20% respectively. In addition, type I cement and type V were used in order to study the effect of the sulfate resisting cement on the chloride properties. The study showed that the chloride diffusion coefficient decreases with time following a linear fashion while the chloride surface concentration increased following a non-linear trend. Moreover, the authors found that the addition of silica fume and fly ash reduced the diffusion coefficient by 50% in the case of 5% silica fume and over 60% in the case of 20% fly ash.

Schueremans et al. [12] conducted a field study on the long-term effectiveness of hydrophobic silanes treatment in preventing chloride ingress through capillary suction and diffusion. The specimens were tested for carbonation and chloride ingress in the tidal and splash zones and the service life was estimated based on the results. The addition of the hydrophobic agents showed a drastic decrease in the diffusion coefficient up to 88% after 12 years of exposure and a sharp increase in the expected service life from 16.5 years to 107 years.

Rincon et al.[60] conducted an exposure study on the durability of OPC concrete elements subjected to the marine activity of the atmospheric zones of eleven different

countries most of which are located in South America. The study included the investigation of the time to initiation of corrosion in addition to studying the corrosion current($I_{corr}$) using the linear polarization resistance method and electrochemical corrosion potential ($E_{corr}$) of the samples in all exposure sites. The study found reported samples in the harshest marine environments (Cabo Raso, Portugal and La Voz, Venezuela) started corroding after 10 months of exposure with the $I_{corr}$ values exceeding 0.2 $\mu A/cm^2$, $E_{corr}$ being lower than -250 mV and the free chloride level exceeding 0.4%. In addition, core samples of the exposed concrete were used in order to test for the bulk diffusion as well. The study suggested that the chloride threshold was mostly influenced by the environmental factors and not only by the physical properties of concrete.

Thomas and Bamforth [26] conducted an exposure study for reinforced concrete blocks made with Portland cement as the standard mix in addition to block made with 25% fly ash and 70% GGBFS that were subjected to the marine activity of the splash zone. The blocks were tested for chloride diffusion. In addition, the study included testing the diffusion for a sea wall in addition to laboratory samples made with the same constituents as the blocks. The study reported that fly ash and GGBFS samples exhibited higher chloride concentrations at the surface but decreased rapidly over the depth. In addition, the study reported a significant decrease in the diffusion coefficient for all the samples that incorporated fly ash and GGBFS indicating that the service life could be increased substantially with the addition of those two SCMs to concrete.

Pech-Canul and Castro [61] studied the effect of varied water-to-cement ratios on the corrosion behavior of samples exposed to the atmospheric zone in the peninsula of Yucatan in Mexico. The study monitored the corrosion rates of OPC samples having water-to-cement ratios of 0.46, 0.5 and 0.7 using three electrochemical methods (LPR, $E_{corr}$ monitoring and EIS) in addition to studying the chloride profile of such samples. The study duration lasted for 56 months. The study reported that the corrosion initiation time was inversely proportional to the water-to-cement ratio. For the water-to-cement ratio of 0.4, it took more than 24 months for the samples to start corroding with the $I_{corr}$ value exceeding 0.2 $\mu A/cm^2$ and the total chloride value at the rebar level exceeding 0.4%.

Kondratova et al.[62] studied the effects of adding CNI to uncracked and precracked slabs exposed to the marine environment in the bay of Fundy, Maine. The study monitored the chloride profile and corrosion current density ($I_{corr}$) over the duration of the research project. The study reported a decrease in the chloride level for both cracked and cracked samples with use of CNI and a noticeable overall decrease in the $I_{corr}$ values for the uncracked samples only. The effect of CNI on the $I_{corr}$ values for the precracked slabs were slight and nonuniform as the study reported indicating that CNI was only effective if the matrix of the concrete is intact and undamaged.

# CHAPTER 4. MATERIALS AND EXPOSURE SITE SETUP

This chapter describes the materials used throughout the thesis research and the mix proportions for the eight concrete mixes. In addition, the chapter also illustrates the properties of the exposure sites chosen and the construction of the sites as well.

## 4.1. Materials

As mentioned previously, Portland cement type I was used as the standard mixture and it was provided by the ready-mix plant after it was tested to pass through the ASTM standards for quality. Moreover, the cement, fine aggregates, coarse aggregates were tested before using them to ensure a good quality. Three SCMs were used as well in three mixes that are: silica fume, fly ash and ground granulated blast-furnace slag and their chemical composition and physical properties are illustrated in Table 4-1. In addition, type V cement was used as well in one of the mixtures and its properties are illustrated in the same Table. Finally, three chemical admixtures were used which are: Migrating Corrosion Inhibitor (MCI), Calcium Nitrite Inhibitor (CNI) and Caltite. The proportions and dosages of all SCMs and chemical admixtures are illustrated in the following section.

*Table 4-1: Chemical composition and physical properties of the materials used.*

| Chemical | OPC | Cement | Silica Fume | Fly Ash | GGBFS |
|---|---|---|---|---|---|

| | | | | | |
|---|---|---|---|---|---|
| and Physical analysis (%) | | Type V | | | |
| $SiO_2$ | 20.8 | 20.97 | 85 | 51.47 | 34.8 |
| $Al_2O_3$ | 5.37 | 3.91 | | 24.31 | 13.4 |
| $Fe_2O_3$ | 3.32 | 4.8 | | 8.87 | 0.62 |
| $TiO_2$ | | | | 1.02 | |
| CaO | 63.77 | 64.27 | | 5.15 | 43.4 |
| MgO | 2.08 | 1.97 | | 3.50 | 5.44 |
| $SO_3$ | 2.63 | 1.86 | | 0.23 | 0.34 |
| Loss on Ignition (L.O.I) | 1.34 | 2.16 | 6.00 | 0.53 | |
| Insoluble residue (I.R.) | 0.39 | 0.60 | | | 0.34 |
| $Na_2O_{eq}$ | 0.52 | 0.48 | | | 0.56 |
| $K_2O$ | | | | 1.47 | |
| $P_2O_5$ | | | | 0.257 | |
| $C_3S$ | 53.20 | 63.84 | | | |
| $C_2S$ | 19.50 | 11.96 | | | |

| | | | | | |
|---|---|---|---|---|---|
| $C_3A$ | 8.61 | 2.24 | | | |
| $C_4AF$ | 10.10 | 14.61 | | | |
| $C_3AF + 2C_3A$ | 27.33 | 19.09 | | | |
| Fineness, Air permeability Test ($m^2/Kg$) | 323 | 315 | | | |

## 4.2. Mix proportions

After revising the literature, a water-to-binder ratio of 0.4 was chosen in the mix proportioning since it represented most medium-strength concretes that are used in the construction industry and scientific research. Eight different mixes were prepared to be tested which are described in Table 4-2. The cement content was chosen as 400 $kg/m^3$ and the unit weight of the concrete was 2400 $kg/m^3$. Silica fume, fly ash and GGBFS were used at replacement ratios of 6%, 25% and 70% by weight of cement, respectively. Furthermore, MCI, CNI and Caltite were used at liquid dosages of 0.6 L, 20 L and 30 L for every cubic meter of concrete respectively and their weights were added to the mixing water weight so the w/b ratio was not exceeded as shown in Table 4-2. All lab samples

were wet cured in potable water basins while exposure samples were cured using layers of wet burlap in addition to having the curing area shaded using plastic sheets.

*Table 4-2: Mix proportioning*

| Mix | W/B | Cement ($Kg/m^3$) | Coarse Aggregate ($Kg/m^3$) | Sand ($Kg/m^3$) | Water ($Kg/m^3$) | Silica Fume ($Kg/m^3$) | Fly Ash ($Kg/m^3$) | GGBFS ($Kg/m^3$) | Notes |
|---|---|---|---|---|---|---|---|---|---|
| 1 | 0.4 | 340 | *1070* | *775* | 136 | - | - | - | Type I |
| 2 | | 340 | 1070 | 775 | 136 | - | - | - | Type V |
| 3 | | 320 | 1100 | 735 | 136 | 21 | - | - | SF |
| 4 | | 255 | 1090 | 735 | 136 | - | 85 | - | FA |
| 5 | | 100 | 1095 | 735 | 136 | - | - | 240 | GGBFS |
| 6 | | 340 | 1070 | 775 | 136 | - | - | - | MCI at 0.6 $L/m^3$ of concrete |
| 7 | | 400 | 1070 | 775 | 136 | - | - | - | CNI at 20 $L/m^3$ of concrete |
| 8 | | 400 | 1070 | 775 | 136 | - | - | - | Caltite at 30 $L/m^3$ of |

| | | | | | | | | | |
|---|---|---|---|---|---|---|---|---|---|
| | | | | | | | | | concrete |

## 4.3. Laboratory samples preparation

As illustrated in Table 4-3, the samples were made and cured in accordance to each test reference. The samples were made by a ready-mix concrete plant except for the binding samples which were made by the research author.

*Table 4-3: Laboratory sample breakdown*

| Test name | Reference | Sample size[1] | Sample type |
|---|---|---|---|
| Void, density and absorption | ASTM 642 [63] | 100 X 200 cylinders | Concrete |
| Water sorptivity | ASTM 1585 [64] | 100 X 200 cylinders | Concrete |
| Chloride bulk diffusion | ASTM 1556 [65] | 75 X 150 cylinders and cores | Concrete |
| Compressive strength | ASTM C39 [66] | 150 X 300 Cylinders | Concrete |
| Chloride binding capacity | Tang and Nilsson [46] | 75 X 150 cylinders | Paste |

[1] Size in millimeter.

| | | | |
|---|---|---|---|
| Linear polarized resistance | Gamry Instruments [67] | 230 X 460 X 1200 slabs | Concrete |
| Rapid chloride permeability | ASTM 1202 [68] | 75 X 150 Cylinders | Concrete |

## 4.4. Exposure sites

Three zones (tidal, splash and atmospheric) were chosen for the exposure sites with two of the zones being in one location. Both of the sites were located in the Arabian Gulf.

### 4.4.1. Location

The exposure zone was chosen at a private beach belonging to King Fahd University for Petroleum and Minerals University on the Half-Moon bay located in the city of Khobar in the Eastern province of the Kingdom of Saudi Arabia as shown in Figure 4-1. The location chosen is part of a semi-enclosed body of the Arabian Gulf as illustrated by Figure 4-2. The Eastern Province has been labeled by the Saudi Building Committee as one of the most aggressive environments for concrete in Saudi Arabia and in the Gulf region due to its closeness to the Arabian Gulf, its high-temperature and high-humidity weather, and due to its sulfur-rich soil in addition to its high temperature gradient through the day and through the seasons[69].

*Figure* 4-1*: Geographical location of the city of Khobar (Google maps)*

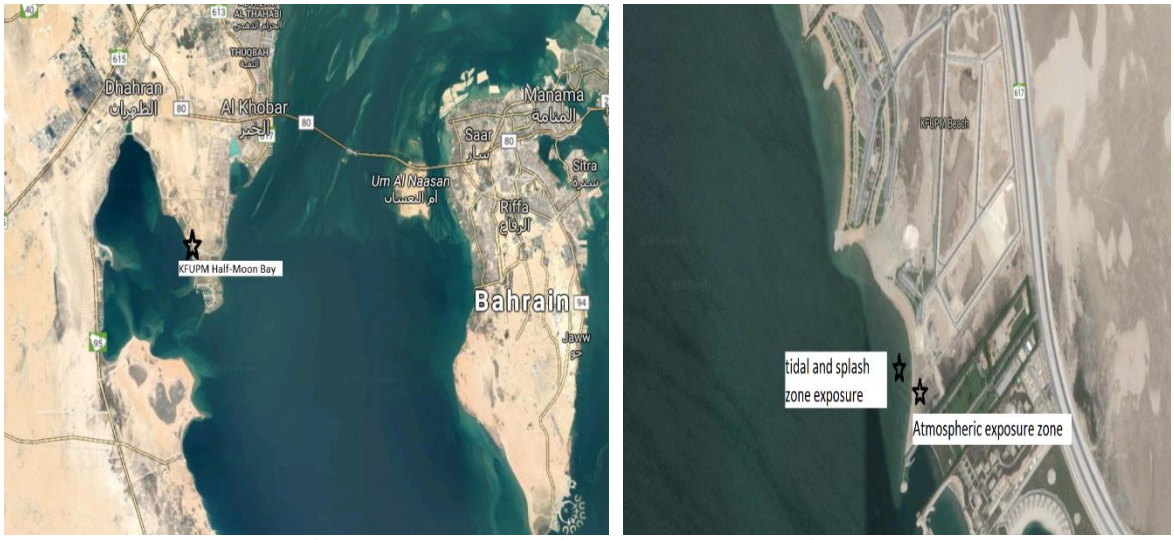


*Figure 4-2: Satellite images of the exposure beach (left) and exact locations of the tidal, splash and atmospheric zones(right) (Google Satellite)*

The salinity and temperature gradient are quite high in the gulf water as illustrated in Figures 4-3 and 4-4 with an average rate of evaporation of almost 0.02 millimeter per minute and an average temperature gradient of 28 °C in the summer. The exposure site

has a local temperature ranging from 5 to 50°C throughout the year. The average relative humidity usually fluctuates between 10% and 80%. Periods of high rainfall occur from November to April. Monthly average value of wind speed is 4.5 m/s coming mainly from North and North West. The average difference between high and low tide is one meter.

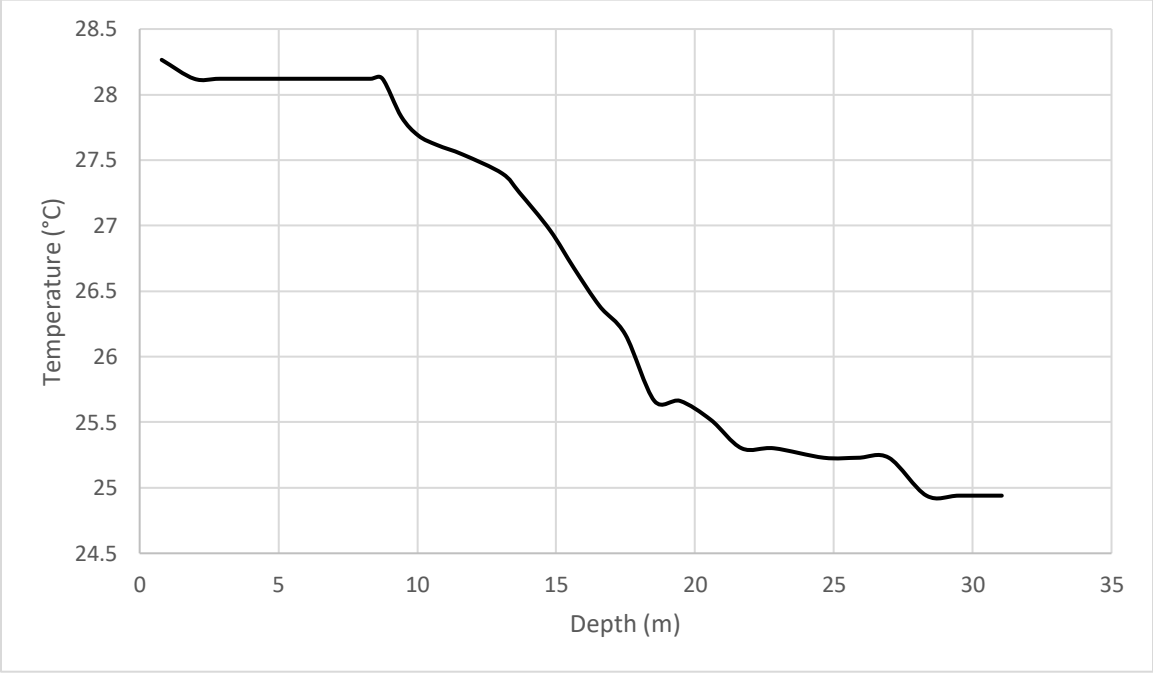


*Figure 4-3: Gulf water temperature variance across the depth (Mosaddad and Delphi*[70]*)*

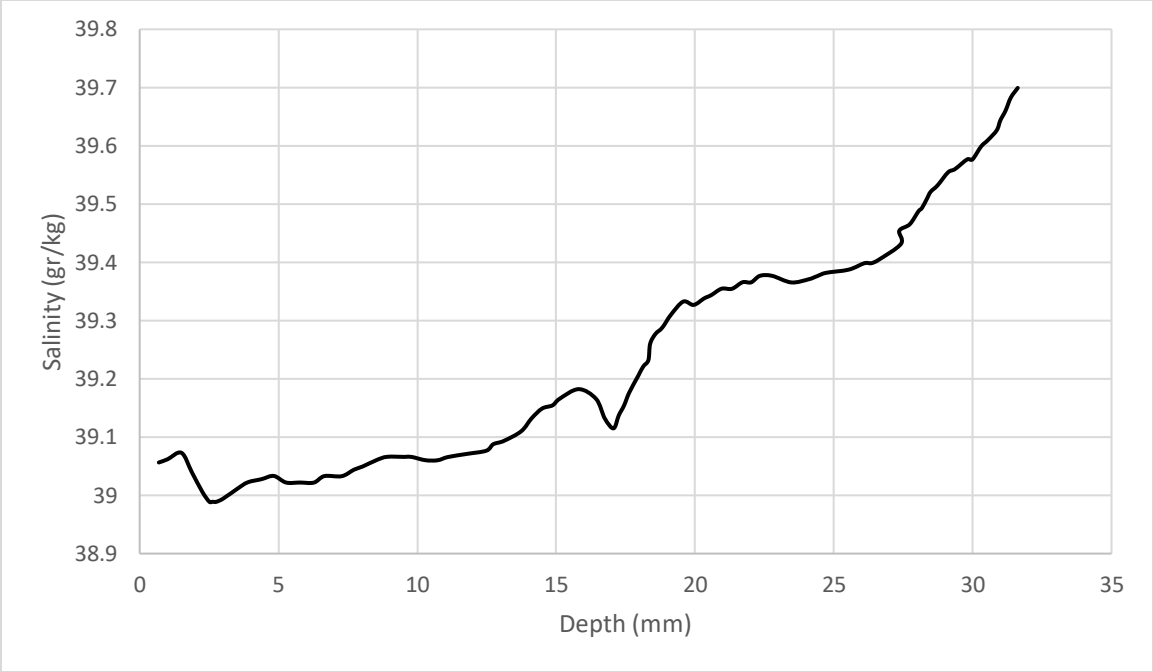


*Figure 4-4:Gulf water salinity variance across the depth (Mosaddad and Delphi*[70]*)*

### 4.4.2. Casting of exposure samples and construction of sites

Four 23 cm x 46 cm x 120 cm specimens of each mix were made, two of them have reinforcement bars at four depths, 12.7, 25.4, 38.1 and 50.8 *mm*, and the other two were plain concrete with one stainless steel bar passing through the centroid to be used for handling, hooking, and polarization measurements as illustrated in Figure 4-5. The samples were made on August, 2016 in a ready-mix plant and demolded after one day of casting. They were cured using wet burlap layers that surrounded each prism after demolding for 28 days. Plastic sheets and shading device were also used for curing process as shown in Figure 4-6 .

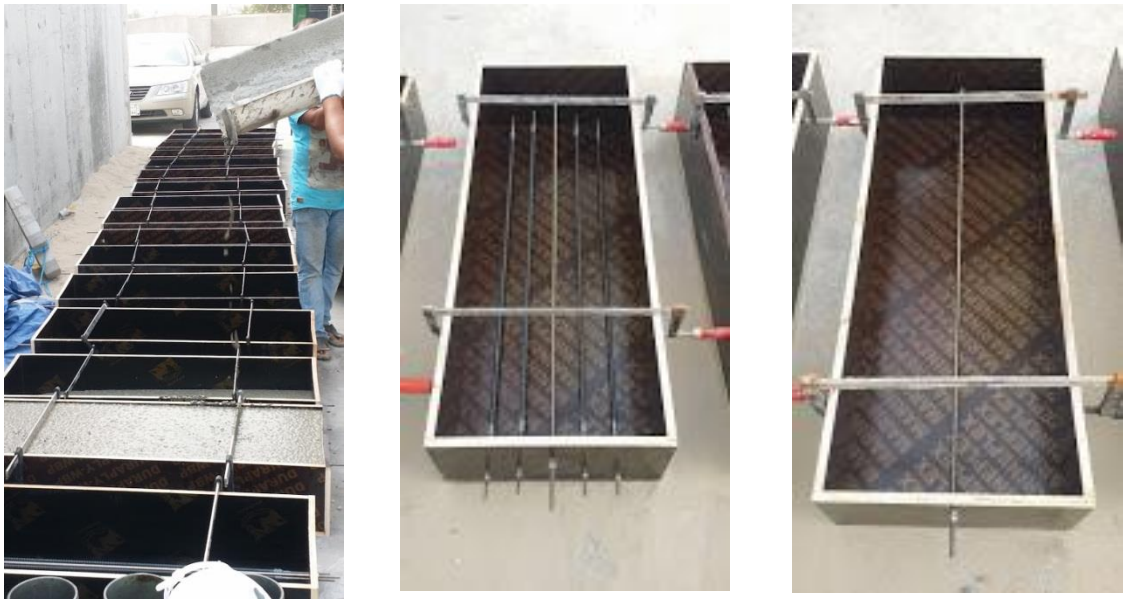

*Figure 4-5: Casting process of exposure samples(left) linear polarization resistance sample (middle) and chloride profiling sample (right)*

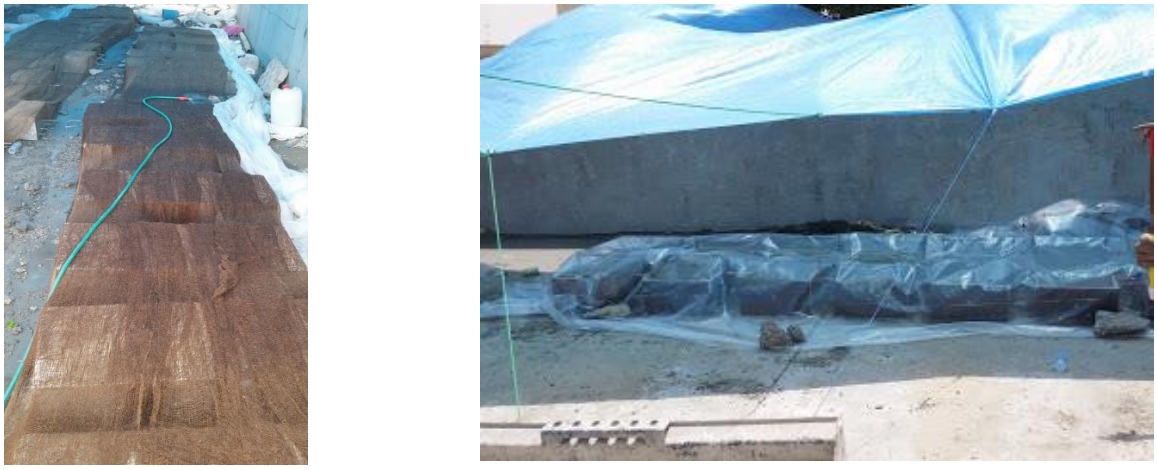

*Figure 4-6: burlap curing (left) and shading during curing (right)*

Then, the specimens were transported to the exposure zone. For the atmospheric zone, the samples were placed in four rows on hollow-core slabs of precast concrete and water resistant plywood, in order to eliminate any salt diffusion from the moist beach sand 25 meters away from the shoreline, Figure 4-2. Moreover, the samples were secured using

galvanized steel ties at the top to prevent any wind-caused swaying and damage as illustrated in Figure 4-7. On the other hand, samples in the tidal zone were stationed 8-10 meters into the gulf where the tide line would reach a maximum level equivalent to the two third the height of each specimen. The upper third of the specimens are considered to be in the splash zone, while the lower third is almost submerged in water. Specimens were arranged in two rows with the reinforced specimens being in the front and the chloride profiling and diffusion being in the back row. The samples then were secured using water-resistant plywood bases submerged in the gulf water as illustrated in Figure 4-7.

*Figure 4-7: Atmospheric samples (left) and tidal samples (right)*

# CHAPTER 5.EXPERIMENTS

This chapter discusses the main experiments that were performed on the concrete mixes in order to achieve the objectives set by the research. They were divided into three main sections in terms of their nature. The first section is the main physical properties of the concrete that are related to physical strength and structure. They serve in providing understanding of the internal structure of the concrete. These tests included: density, absorption and void ratio testing (ASTM C642)[63], water absorption rate testing (i.e. Sorptivity) (ASTM C1585)[64] and compressive strength testing (ASTM C39)[66].

The remaining two sections of testing were lab work and site work that focused on investigating chloride ingress, corrosion thresholds and corrosion status in concrete.. The lab work focused on laboratory testing where the simulation of exposure conditions occurred in a controlled laboratory environment. It included testing for chloride diffusion using the bulk diffusion test (ASTM C1556 and C1152) [65], [71] in addition to testing the chloride permeability under a constant voltage using the Rapid Chloride Permeability Test (ASTM C1202) [68]. Another test in this subcategory was the test for chloride binding capacity which was developed by Luping and Nilsson [46] in which an exact value of the binding capacity can be measured in order to subtract it from the total (acid-soluble) chloride concentration to give the free (water-soluble) concentration which is considered to be the main factor in modelling corrosion and estimating service life in concrete under Fick's 2$^{nd}$ law of diffusion.

The site work involved measuring and modelling the chloride profile in marine exposure zones and measuring the corrosion status. The first is established using a similar method to the bulk diffusion where core samples of exposed concrete samples are obtained and tested while the second is achieved using the linear polarization resistance testing.

## 5.1. Physical properties

This section discusses the sample preparation and testing for the experiments previously mentioned.

### 5.1.1. Density, absorption and void ratio test

The density is defined as the equivalent weight of a substance that occupies a certain volume. Any constructional material can be represented on the phase diagram that includes voids and solid as shown in Figure 5-1. A material is dense if the void percentage (ratio) is minimal and loose if the opposite occurs. The high void ratio facilitates penetration of gasses and liquids (such as saline water in the case of marine concrete) inside the material. A typical way to express the density is in defining it relation to that of a standard material such as water which makes it a dimensionless quantity. The relative density values for normal weight concrete range from 2.15 to 2.4 according to Nevile [8].

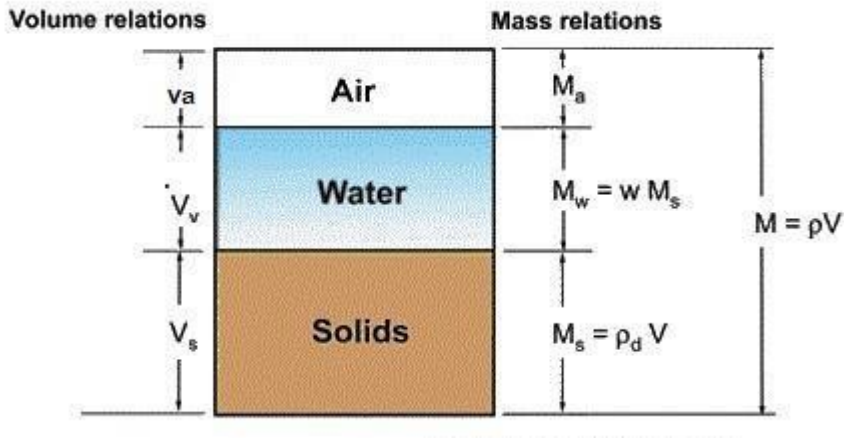


*Figure 5-1: Phase diagram example*

Another property that is used to describe concrete's affinity to water is the total absorption. It is defined as the total weight of water absorbed by the concrete after immersion in water relative to its weight. The higher the absorption percentage the more susceptible concrete becomes to corrosion as water carries chloride ions into the matrix.

Two 100 mm X 200 mm concrete cylinders were tested in accordance with the ASTM C 642 [63] standard. Two samples of each mix were made of 100mm diameter cylinders and cured in a potable water basin for 28 days. Then they were oven dried at 110 °C for twenty-four hours and the dry mass was recorded for each specimen. Then, they were submerged in water and weighed every 24 hours until no significant change in mass was observed. Then they were placed in boiling water for five hours and then the water cooled for twenty hours and the mass was recorded as shown in Figure 5-2. Finally, the specimens were transported to water tank where they were suspended and weighed using

a suspension weighing equipment as illustrated in Figure 5-3. The recorded masses where used to calculate the different densities, void ratios and total absorption.

*Figure 5-2: boiling and cooling of samples for density test*

*Figure 5-3: suspension weighing setup for density test*

### 5.1.2. Sorptivity

Sorptivity is defined as the rate of water absorption under the influence of capillary rise[72]. It is differentiated from water permeation that occurs under the influence of a differential pressure. This phenomenon was first studied by Hall [72] who coined the term “sorptivity” to describe the movement of water under capillarity effect in non-saturated concrete. Due to this property in concrete, the capillary pores work as conduits with one side being exposed to the atmosphere and one side being partially wet. The evaporation of water from the atmospheric side leads to the creation of a negative pressure that drives the water from the partially wet side towards the atmospheric side

which in turn evaporates as well leading the continuation of the cycle. This phenomenon is reported to be more related to concrete corrosion than the permeation of water under pressure differentials. Sorptivity test was conducted in this study.

Two 75 mm X 150 mm concrete cylinders specimens of each mix were first made, cured and sliced following the standard procedure described in the ASTM C 1585[64]. Then they were conditioned in a desiccator at 50 °C in an oven and a relative humidity of 80% using a saturated solution of Potassium Bromide (KBr) for three days. After that, they were moved to separate sealable containers for 15 days and ensuring that none of the faces is in contact with the container walls to allow free air flow and then they were weighed. Next, they were sealed from sides using epoxy and then one of the faces was covered using a plastic bag and rubber bands or adhesive tape. Then they were suspended with the exposed face downward and water was added up to cover 5 mm of the sides as shown in Figure 5-4. Finally, mass was recorded at several small-time intervals at the beginning and continued 7 to 9 days with larger time intervals as shown in Table 5-1.

*Figure 5-4: Oven conditioning using KBr solution(left) and sorptivity test setup (right)*

*Table 5-1: periods at which the mass was recorded in Sorptivity test*

| Time | 60 s | 5 min | 10 min | 20 min | 30 min | 60 min | Every hour up to 6 h | Once a day up to 7 days | Day 7 to 9, 1 measurement |
|---|---|---|---|---|---|---|---|---|---|
| **Tolerance** | 2 s | 10 s | 2 min | 2 min | 2 min | 2 min | 5 min | 2 h | 2 h |

The absorption (I) in millimeters was calculated at each interval using Equation 4 and the initial and secondary absorption rates were calculated for each sample using linear regression by the method of the sum of least squares. Moreover, the absorption versus the square time was plotted for every mix. The slope of the first 6 hours represents the initial rate of absorption and the slope of the 1 day to 9 days represents the secondary rate.

$$I = \frac{\Delta m_t}{A * \rho} \tag{4}$$

Where $\Delta m_t$ is the change in mass at time interval $t$ and $A$ is the exposed surface area that is in contact with water while $\rho$ is taken as the density of water at 25°C.

### 5.1.3. Compressive strength

This test mainly serves as a quality assurance measure to make sure that the strength classification of the concrete was correct. The concrete in this project was designed as a "medium strength concrete" and the compressive strength results should reflect that. The test was conducted in accordance to the ASTM C 39[66] .

First, three 150 mm X 300 mm cylindrical samples were cast and demolded after one day. The samples were then cured for 28 days in potable water basins at 25 °C. After that, each sample was capped using molten sulfur as illustrated in Figure 5-5. After that, each sample was placed in an automated load applying machine and the load rate was set to 0.25 MPa/s until failure and the pressure at which failure had occurred was recorded. The average of the three samples was taken as the compressive strength (f´c). Plain Concrete is classified as a brittle material and that is evident in the stress-strain curve for any sample as shown in Figure 5-5 where the failure occurred suddenly in the form of crushing without reaching a yielding state.

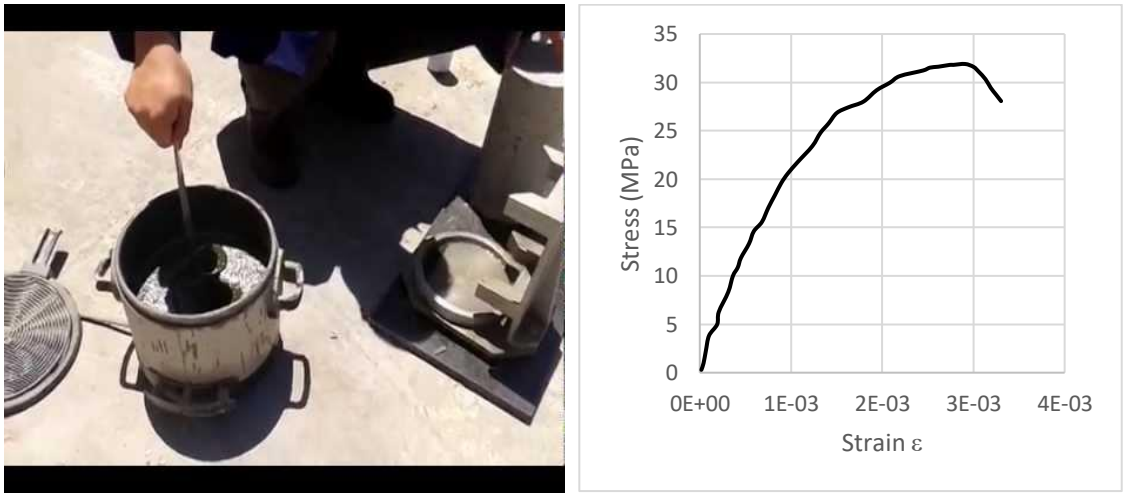


*Figure 5-5: Capping of samples(left) and aa typical stress-strain curve for plain concrete(right)*

## 5.2. Lab experiments

This section describes the corrosion and diffusion tests that were conducted on samples conditioned to test for diffusion, chloride resistivity and chloride binding properties.

### 5.2.1. Rapid chloride permeability test (RCPT)

This test was developed by the American Association of State Highway and Transportation Officials (AASHTO) and ASTM [68] as a qualitative indication of the chloride resistivity in concretes that are made using additives whose RCPT values have been correlated with long-term chloride ponding results. The test provides a chloride resistivity categorization system based on the total chloride charges that pass during the test as shown in Table 5-2.

*Table 5-2: RCPT categorization system*

| Rating | Total charge passed in Coulombs |
|---|---|
| High | >4000 or temperature > 90°C |
| Moderate | 2000-4000 |
| Low | 1000-2000 |
| Very low | 100-1000 |
| Negligible | <100 |

Two samples 100 mm X 200 mm cylinders of each concrete mix were sliced with a rotary saw after curing in accordance to ASTM C 1202[68]. After that, they were coated

on the sides with epoxy sealant with the top and bottom surface being left uncoated and allowed to cure for one day then they were submerged in de-aerated water for 18 hours after being vacuumed in the same water for 4 hours. The samples were finally installed into the RCPT cells and the test was conducted. The RCPT cells mainly consisted of two side tanks that were filled with 3% NaCl and 0.3 N NaOH solution respectively that were in direct contact with the unsealed surfaces of the concrete sample and two connection electrodes that were used to apply a constant 60 V voltage using German Instrument's Proove It™ device[73]. Moreover, each sample was fixed in the RCPT cell using a central ring in addition to two rubber gaskets on each side to ensure that no leaks in the cell exist and that the chloride ions have to pass through the concrete as illustrated in Figure 5-6. The cells then were attached to a computing station that monitors the temperature and records the current passing through the sample over a six-hour period as shown in Figure 5-6. The average of the two samples' cumulative charge was then calculated at the end of the test and the concrete was classified based on that value after adjusting it to the used diameter as shown in Equation 5.

$$Q_a = Q_i \times (\frac{3.75}{Dia})^2 \quad (5)$$

Where $Q_a$ and $Q_i$ are the adjusted and measure total charges passed while the *Dia* is the diameter in inches.

The final adjusted value serves as an indication of the permeability to chloride penetration characteristics of each mix.

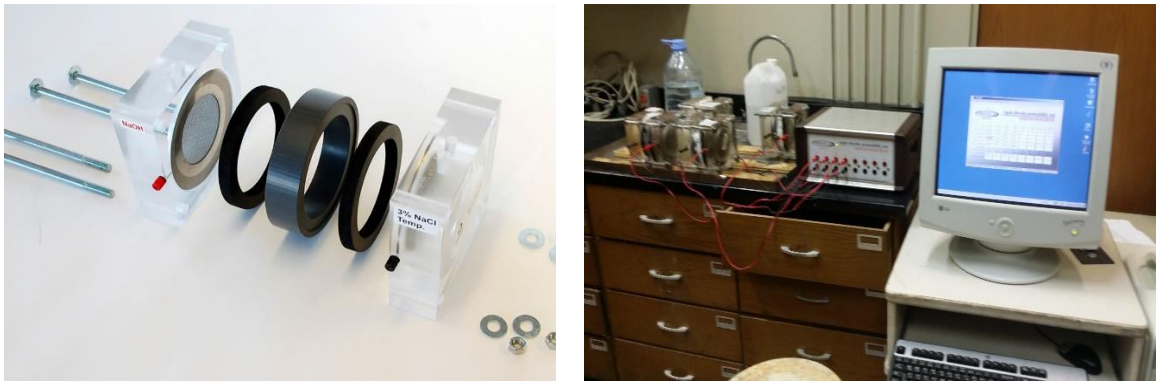


*Figure 5-6: RCPT cell components(left) and RCPT setup (right)*

### 5.2.2. Bulk diffusion

Diffusion is the movement of gasses and liquids through the materials and chemical concentration differentials. It is one of the most important factors when discussing corrosion whether it occurs in the form of carbon dioxide front diffusion or in the form of chloride ions diffusion. This study focused on the effect of chloride ions on corrosion behavior. A test was developed in order to measure the diffusion coefficient (Da) and surface chloride concentration (Cs) using the acid-soluble method. The test was conducted on samples at three different ponding periods: 35 days to show immediate effect of SCMs and chemical additives on the diffusion at early age, 6 months and 12 months to study the development advancement of chloride in the concrete.

75 mm X 150 mm concrete cylinders were sliced into halves and coated with epoxy sealant from all sides except for the cast surface which is left uncoated in accordance to ASTM C 1556 and C 1152 [65], [71] as shown in Figure 5-7 . A minimum of 20 mm from the bottom of the sample was sliced to determine the initial chloride content. Then, the coated specimens were neutralized in accordance to the test standard in a saturated calcium hydroxide solution for a minimum of two cycles(each cycle was 24 hours) until no significant weight changes were recorded. After that the specimen were exposed to a standard concentration of Sodium Chloride for 35, 183, and 365 days. Finally, a minimum of 8 layers were ground using a bench drill press and a diamond coring drill bit (Figure 5-8). Each specimen was cleaned before the grinding of the next layer to avoid contamination and ensure precise results. Each layer's powder was pulverized to pass through No. 100 standard sieve then was dissolved in 65% Nitric acid and left to be digested for at least 24 hours. After the digestion of the powder samples, the remaining solution was filtered and analyzed using the photo spectrometry method in the case of the 35 and 183 days' samples and by the method of titration against Silver Nitrate (AgNO3) in the case of the 365 days' samples.

*Figure 5-7: coated samples(left) neutralization in calcium hydroxide (middle) salt water basin with samples exposed in it (right)*

*Figure 5-8:Profile grinding setup(Left) Photospectrometer (middle) Filtration of $HNO_3$ soaked samples (right)*

The photospectrometer measures the absorbed light at certain wavelengths which then can be correlated with the concentration of certain components, chloride ions in this study. However, in order to have good correlation, an optimum light wavelength has to be set at which the absorbance due to the chloride presence is maximum as shown in Figure 5-9. Two samples were used to identify the optimum wavelength. The first is a blank sample that had no chloride ions but ferric ammonium sulphate, nitric acid and mercury (II) thiocyanide which when mixed with chloride change color thus changing the absorbed light. The second contained known concentration of chloride and then the

machine was set scan the visible and invisible light spectra ranging from 100 nm to 600 nm and the optimum, at which the absorption was maximum, was found to be at 460 nm. After that, a model was used that was developed by the KFUPM Research Institute which was correlated to find the concentration of chlorides ranging from 5 to 500 parts-per-million (PPM) as shown in the following Equation (6):

$$concentartion\ (ppm) = C1 * A^{c2} \quad (6)$$

Where A is the absorbance, C1 and C2 are constant found to be equal to 18.922 and 0.8479 respectively.

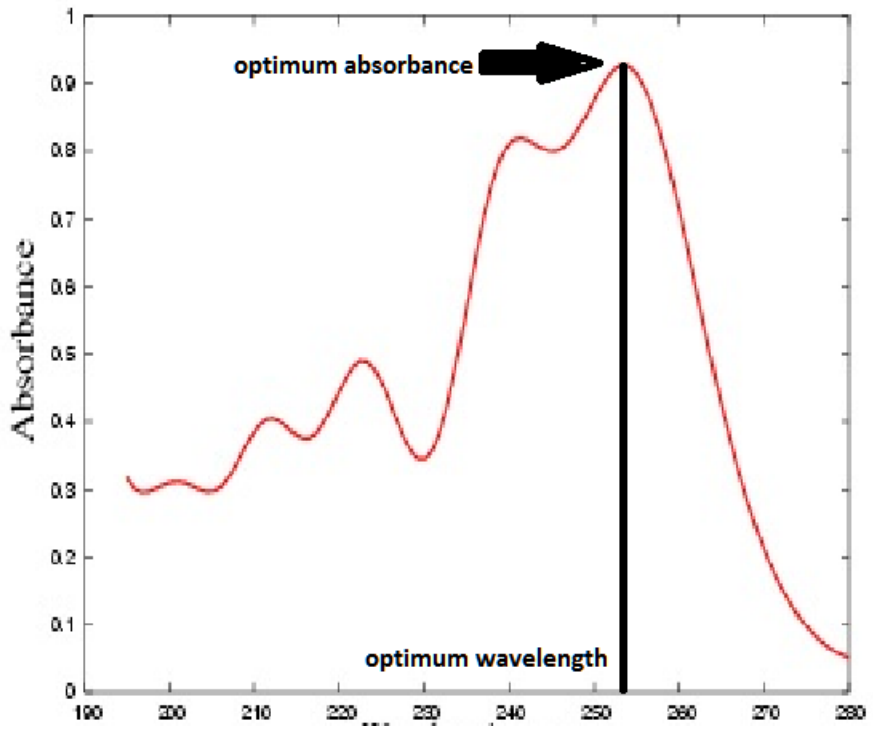


*Figure 5-9: example of an absorbance graph*

The machine was set to measure the absorbance of the 460 nanometers wavelength light wave by the sample. Before exposing the sample's filtrate to that certain wavelength, two milliliters of Mercury (II) thiocyanate and ferrous detectors were added to each solution to indicate the Chloride ion concentration through changing the filtrate color and thus its light absorbance. The spectrometer was zeroed using distilled water and a blank sample was analyzed and recorded before running the actual samples to eliminate any result disturbance from the Mercury and Ferrous detectors. Model that followed Fick's law of

diffusion was used to model the diffusion as follows (7):

$$C(x,t) = Cs - (Cs - Ci) \cdot \text{erf}\left(\frac{x}{\sqrt{4 \cdot Da \cdot t}}\right) \quad (7)$$

Where C(x,t) is the chloride concentration at different depth x(m) and time t(s) , which is measured as percent weight of concrete, $C_s$ is the chloride concentration on the surface of the concrete at the interface between the salt solution in the ponding container and concrete, $C_i$ is the initial chloride concentration before ponding, $D_a$ is the bulk diffusion coefficient ($m^2/s$), and erf is the Gauss error function described by the following expression:

$$\text{erf}(z) = 2/\pi \cdot \int_0^z \exp(-u^2)\, du. \quad (8)$$

In the case of the 12-month samples, the same model applies. The method of potentiometric titration against Silver Nitrate was followed. The method revolves around the following reaction:

$$Ag^+_{(aq)} + Cl^-_{(aq)} \rightarrow AgCl_{(s)} \quad (9)$$

Where the addition of a known silver nitrate to a solution containing chloride results in the formation of a white precipitate of silver chloride. This method measure the voltage across a solution where silver nitrate is titrated slowly into the solution containing chloride as shown in Figure 5-10. The voltage is plotted until the break point is reached. The break point is defined as the point where the amount of chloride is totally consumed by the reaction and

silver nitrate does not react anymore. At this point a voltage jump is noticed in the graph as shown in Figure 5-11. the concentration of chloride is then calculated according to the following Equation(10):

$$C_{Cl} = \frac{C_{Ag} * V_{Ag}}{V_{Cl}} \quad (10)$$

Where C is the concentration in molar and V is the volume used in liter at the break point. In this experiment, a concentration of 0.1M was used in the preparation of the silver nitrate solution.

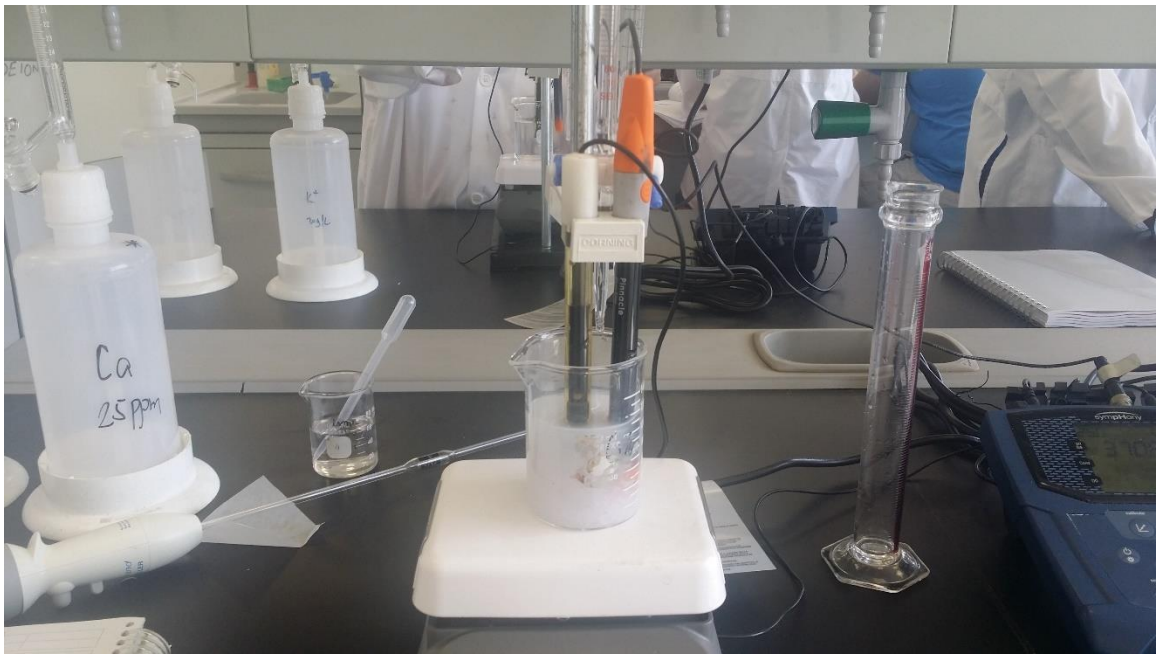


*Figure 5-10: potentiometric titration setup*

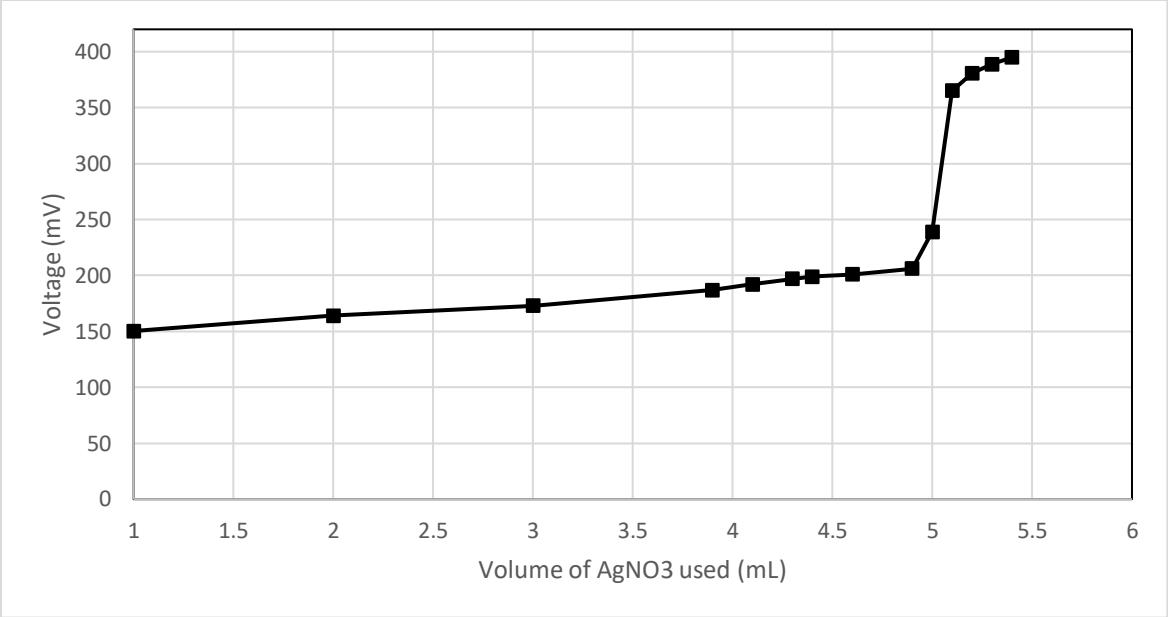


*Figure 5-11: example of potentiometric titration voltage graph*

### 5.2.3. Chloride binding

One of the main properties of concrete is its ability to bind chloride ions and thus delay its ingress into the bulk concrete. The ASTM does not provide a way to measure the exact binding capacity. ASTM provides a measure of the total chloride (free and bound) or the water-soluble chloride which contains the free and part of the bound. One of the reliable methods found in the literature that measures the chloride binding capacity is a test developed by Nilsson and Luping in 1993[46].

The method tests the binding capacity of pastes or mortars after conditioning them in cycles of binding and unbinding where chloride is bound in one cycle and then unbound in the next cycle. For the purpose of this research, only the first cycle of binding was used

since it represents the binding capacity. The test postulates that the chloride is bound in two forms: irreversibly bound chloride that reacts with the Calcium Silicate Hydrate (CSH) gel and reversibly bound chloride that can unbind when the concentration of chloride in the environment surrounding the concrete is decreased. The test also claims that with higher concentrations of chloride in the environment, the binding capacity becomes higher in addition to the irreversibility of the binding process.

First, cylindrical paste samples were cast using a 0.4 w/c and deionized water to eliminate any disturbance in the results caused by the chlorides in the mixing water. After that, the samples were cured in lime water for 14 days in de-aerated containers to avoid any carbonation. Then the central portion of each sample was wet crushed using a lathe machine as illustrated in Figure 5-12. The crushed material was sieved to pass through a No.100 sieve. After that, sieved samples were dried in a desiccator that has a bed filled with activated silica gel desiccant, that was treated at 110 °C for one day to ensure it had no moisture content prior to use, for one week under vacuum pressure. After drying, the samples were treated in a desiccator that had a relative humidity content of 11% at room temperature using a saturated solution of Lithium Chloride (LiCl) in the bed of the desiccator instead of the silica gel for two weeks in accordance to the Luping and Nilsson procedure. Finally, the conditioned paste was then exposed to a salt and lime solution at different NaCl concentrations that were: 0.1, 0.3, 0.5, 1 and 4.2 Molars respectively, for 14 days in order to reach binding capacity . Then the samples were filtered and the final

chloride concentration was measured using potentiometric titration. The binding capacity is calculated based on the difference in the chloride concentration before and after exposure.

*Figure 5-12: casting of paste samples (left) wet grinding of samples(right)*

*Figure 5-13: desiccation of samples using silica gel (left) samples after total conditioning(right)*

## 5.3. Exposure studies

This section as previously mentioned, discusses the experiment conducted in the field on exposed samples. The exposure was divided into three zones as explained in previous chapter: atmospheric, splash and tidal zones. Both tests were conducted on slabs that

were cast, cured for 28 days and then exposed on October of 2015 in the Arabian Gulf shore.

### 5.3.1. Chloride profiling

This test studies the diffusion of chloride in marine exposed samples. The methodology is similar in some aspects to the chloride ponding that was conducted in the laboratory but differs in some other aspects. The test focused on the atmospheric and tidal zones only as they covered the ends of the spectrum in exposure with atmospheric zone being the least detrimental to concrete and the tidal zone being the most detrimental according to the results collected from the literature[59], [74]–[76].

After the construction of the exposure sites, two 120 cm X 46 cm X 23 cm columns of each mix were made and cured using wet burlap for 28 days in a ready-mix plant. Then, they were transported and half of them were located in the atmospheric zone while the other half were located to splash and tidal zones. Two types of samples were cast as shown in Figure 4-5, one with a single stainless steel reinforcement in the middle of the sample that extruded from the top and was used for handling and transportation purposes. The second type had regular deformed reinforcement bars at different cover depths that ranged from 12.5 mm to 50.8 mm at 12.5 mm increments with one central stainless steel bar that was used as the counter electrode in the linear polarization test as will be explained later.

After an exposure period of 6 months, the columns in the splash and tidal zones were dredged to the shore and core samples were obtained using a 75 mm coring tip. After the cores were obtained, they were washed with deionized water and sealed until further testing while the slabs were repaired using a patch of mortar that was mixed on site as illustrated in Figure 5-14. The next day, the slabs were transported again to the exposure zones. The process was repeated after another 6 months with the only change being that the slabs were not dredged and not cored. Instead a profile grinder was used to obtain the powder at different depths in 1 mm increments directly as shown in Figure 5-14.

*Figure 5-14: batching of cored slabs(left) Profile grinder ring setup on site(middle) Profile grinding and dust collecting setup(Right)*

The core samples were transported to the lab where they pulverized following the same procedure as the chloride ponding. The powder in both cases (6 and 12 months) was digested in nitric acid and the chloride content was measured for both exposure zones utilizing both spectrometry and potentiometric titration methods. The results were then

plotted and a diffusion model was fitted for each mix, zone and exposure period following the same procedure illustrated in section 5.2.2.

### 5.3.2. Linear polarization resistance

This test was developed to measure the corrosion current density indirectly using a non-invasive measuring procedure. In contrast to the direct corrosion currents density test, this test does not require the reinforcement to be exposed and can be used to monitor the state of corrosion throughout the life of a structure. The basic principle of the test is derived from the Stern-Geary Equation where the polarization resistance ($R_P$) is disproportionally related to the corrosion. It is an enhanced form of the Tafel plot technique. In this method, a small potential is applied on the surface of the concrete ranging from -20mV to 20mV away from the corrosion Potential ($E_{corr}$) and the current is measured throughout the range. After that, a plot of the potential versus the recorded current is developed as shown in Figure 5-15 and the resistance is calculated using the following Equation (11):

$$R_P = \frac{\Delta E}{\Delta I} * A \qquad (11)$$

Where $\frac{\Delta E}{\Delta I}$ represents the slope of the linear portion of the curve and A is the area of the steel under polarization which is assumed to equal to $\pi DL$ where D is the diameter of the bar and L is the length.

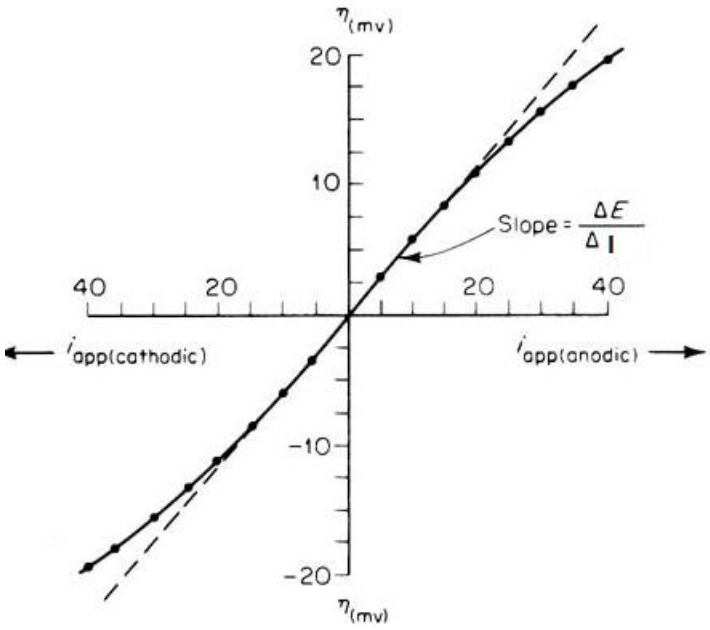


*Figure 5-15: example of the potential vs. current plot for LPR test.*

Finally, the corrosion current density ($i_{\text{corr}}$) is calculated using the following Equation(12):

$$i_{corr} = {}^{B}/_{R_P} \tag{12}$$

Where B is known as the Stern-Geary proportionality constant as is defined by Equation (13). However, it can be assumed to be equal to 50 mV in the case of active corrosion and 25 mV otherwise.

$$B = \frac{\beta_a * \beta_c}{2.3(\beta_a + \beta_c)} \tag{13}$$

Where $\beta_a$ and $\beta_c$ represent the Tafel anodic and cathodic slopes as shown by the Figure5-16.

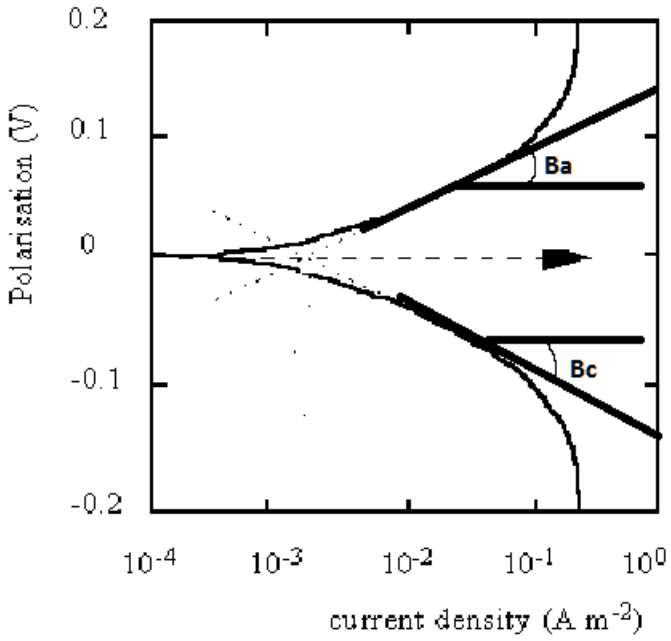


*Figure 5-16: example of the Tafel plot and finding the Tafel slopes.*

As explained previously, the samples were cast having a certain reinforcement configuration and exposed to their respective zones. The steel was connected to a non-corroding metal at end and that part protruded from the slabs at the top. After curing the slabs for 28 days they were transported to their respective exposure zones. Measurements were taken after 6 and 12 months using the Gamry Reference 3000 Potentiostat and a saturated calomel reference electrode. The polarization resistance readings were taken for each mix on site with the reinforcement passing through the centroidal axis of the

specimen being connected to the counter electrode wires of the machine and the working electrode wires being connected to the reinforcement in question at each cover depth. For the samples in the tidal and splash zones, the reference electrode is connected perpendicular to the surface of the concrete directly over the path of the reinforcement bar as illustrated in Figure 5-17. The measurements were chosen to be taken at a time of day where the tide would be at its lowest point and the wind would be as still as possible in order to minimize any noise in the data caused by wave motion.

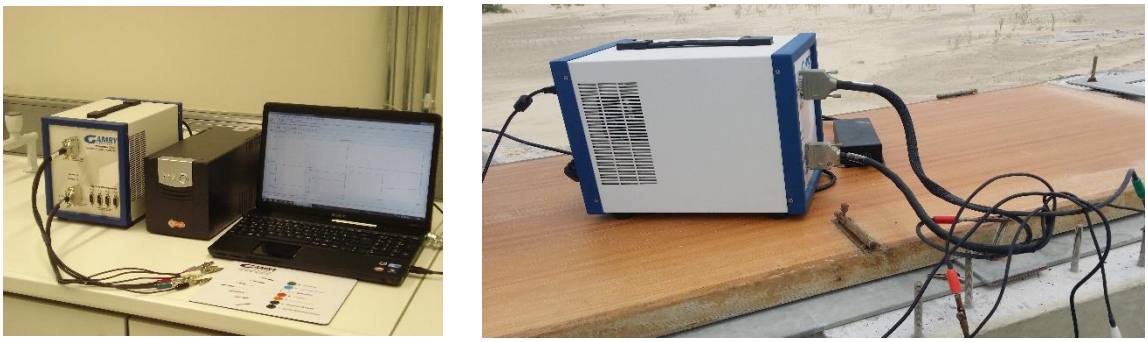

*Figure 5-17: Gamry Reference 3000 potentiostat setup(left)connection of the potentionstat to the rebars for LPR testing(right).*

# CHAPTER 6.RESULTS

This chapter illustrates and interprets the results collected over the one-year exposure and lab study. The results are divided in terms of duration to three main parts: results of tests conducted after 35 days of exposure, results of tests conducted after six months of exposure and results of tests conducted after one year of exposure.

## 6.1. Compressive strength

As illustrated in Figure 6-1, fly ash mix recorded the highest strength at 39 MPa followed by the CNI mix at 32 MPa compared to the standard mix (28.1 MPa). What was not expected was the strength recorded by the GGBFS mix (28 MPa) which was almost equal to the standard mix.

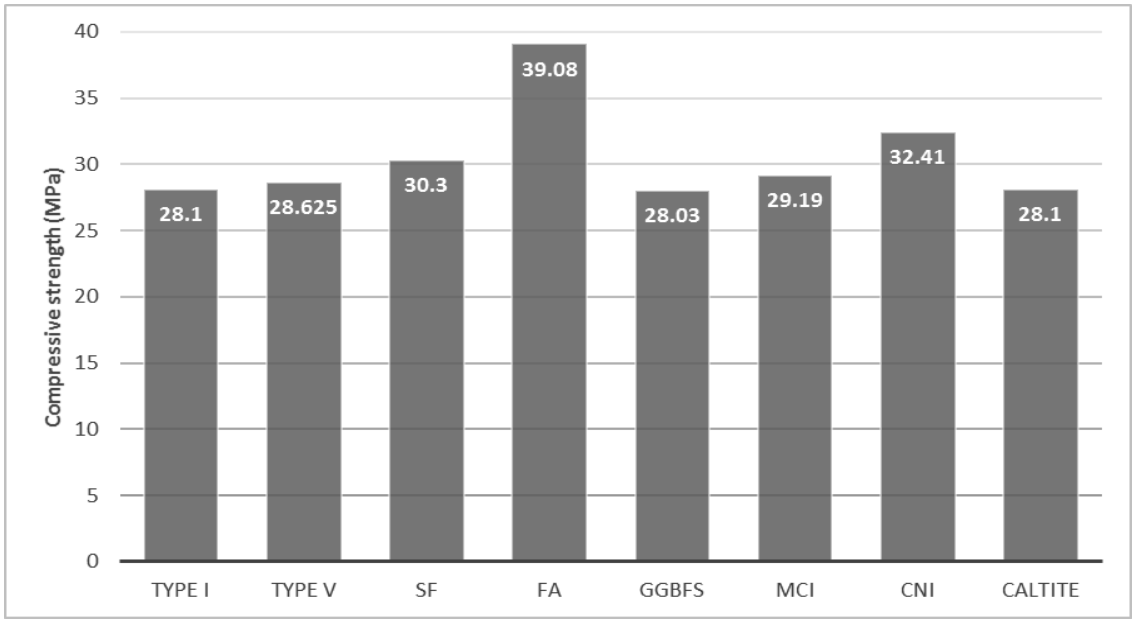


*Figure 6-1: 28-days compressive strength results*

## 6.2. Rapid chloride permeability test

As shown in Table 6-1 and Figure 6-2, type V concrete showed the highest value of charges passed coming at almost 5000 coulombs followed by CNI at 4100 coulombs. The lowest values were exhibited by the mixes containing fly ash and GGBFS with scores that labeled them in the “low” category which can be owed to those mixes containing high amounts of SCMs. It is worth noting that most mixes exhibited a relative improvement when compared to the standard mix except for type V, CNI and Caltite

mixes with decline percentages of 48%, 27% and 9% respectively. Moreover, silica fume showed a noticeable relative improvement in terms of resistivity that coincides with what was reported in the literature.

*Table 6-1: RCPT results*

| Mix | RCPT | Classification | relative improvement/decline |
|---|---|---|---|
| I | 3226 | Moderate | 0.00 |
| V | 4783 | High | -48.24 |
| SF | 1522 | Low | 52.83 |
| FA | 1140 | Low | 64.68 |
| GGBFS | 1262 | Low | 60.88 |
| MCI | 2491 | Moderate | 22.79 |
| CNI | 4094 | High | -26.89 |
| Caltite | 3509 | Moderate | -8.76 |

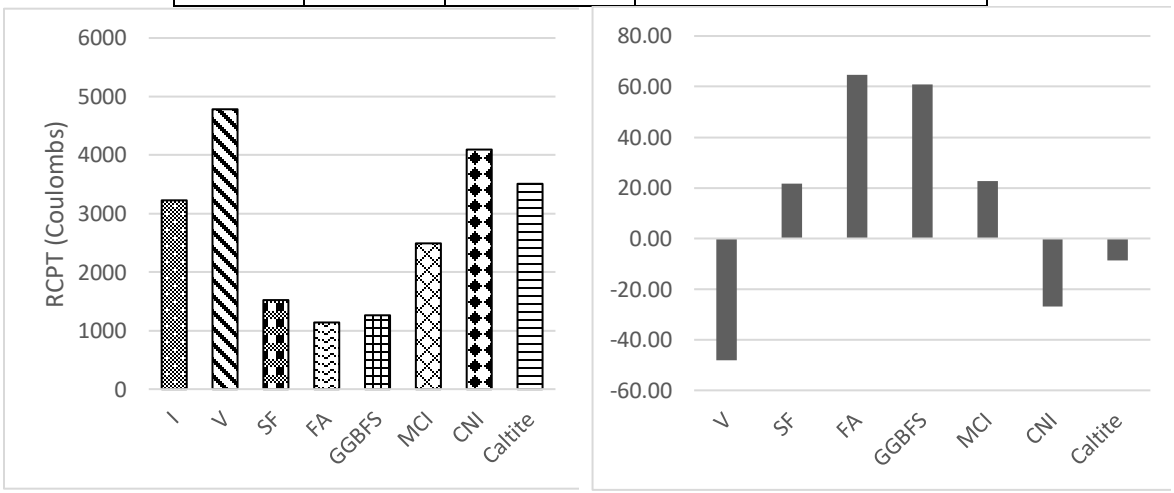


*Figure 6-2: visual representation of RCPT results(left) relative improvement/decline (right)*

## 6.3. Density, absorption and void ratio

As illustrated in Table 6-2 and Figures 6-3 to 6-5, two samples were tested for each mix =. With void ratio values of 17.13% and 16.7% in addition to absorption values of 8.15 and 7.95 respectively, GGBFS and MCI exhibited the highest void ratios and absorbed water the most. All other mixes exhibited lower values than the standard mix (13.9% void, 6.44% absorption) with Caltite, CNI and fly ash mixes showing the lowest values which coincides with the chemical admixtures' function of adding hydrophobic properties to the mixes they are used in in addition to the role of fly ash in the pozzolanic reaction that converts excess Calcium Hydroxide ($Ca(OH)_2$) to secondary calcium silicate hydrate the fills the excess pore voids in the bulk area of the concrete structure thus decreasing the volume (void) available for water to penetrate which in turn decreases absorption as well.

In terms of density, it is shown that CNI mix exhibited the highest bulk and dry densities at values of 2.33 and 2.21 g/m3 while mixes 5 (GGBFS), 6 (MCI) and 8 (Caltite) exhibited density values lower than the standard which may indicate more internal voids. However, in the case of the mix containing Caltite, the value for the absorption was lower than expected in spite of having a relatively low density which can be explained by the

hydrophobic nature of mixes containing Caltite especially at early ages that drives moisture away from the voids as Schueremans et al. suggests. [12]

*Table 6-2: Density, absorption and void ratio data*

| Sample[2] f | Mass (g) | | | | | | Absorption | Dry Bulk Dens. | Bulk Dens. | Apparent Dens. | Void %. |
|---|---|---|---|---|---|---|---|---|---|---|---|
| | OD | B.SSD | Suspended | AVG OD | AVG B.SSD | AVG Susp. | | | | | |
| Letter Des. | - | - | - | A | C | D | (C-A/A)*100 | A/(C-D)=g1 | C/(C-D) | A/(A-D)=g2 | (g2-g1)/g2*100 |
| M1-1 | 722 | 768 | 434 | 701 | 746 | 422 | 6.44 | 2.16 | 2.30 | 2.51 | 13.92 |
| M1-2 | 679 | 723 | 409 | | | | | | | | |
| M2-1 | 680 | 730 | 413 | 766 | 817 | 463 | 6.65 | 2.17 | 2.31 | 2.53 | 14.39 |
| M2-2 | 762 | 815 | 461 | | | | | | | | |
| M2-3 | 858 | 908 | 516 | | | | | | | | |
| M3-1 | 710 | 748 | 427 | 734 | 776 | 440 | 5.61 | 2.19 | 2.31 | 2.49 | 12.26 |
| M3-2 | 759 | 803 | 452 | | | | | | | | |
| M3-3 | 738 | 779 | 435 | | | | | | | | |
| M4-1 | 639 | 679 | 384 | 700 | 737 | 420 | 5.25 | 2.21 | 2.32 | 2.49 | 11.58 |
| M4-2 | 761 | 795 | 455 | | | | | | | | |
| M5-1 | 677 | 731 | 410 | 690 | 746 | 418 | 8.15 | 2.10 | 2.27 | 2.54 | 17.14 |
| M5-2 | 703 | 761 | 426 | | | | | | | | |
| M6-1 | 786 | 863 | 473 | 790 | 852 | 476 | 7.95 | 2.10 | 2.27 | 2.52 | 16.70 |
| M6-2 | 793 | 842 | 479 | | | | | | | | |
| M7-1 | 771 | 812 | 463 | 740 | 780 | 445 | 5.36 | 2.21 | 2.33 | 2.51 | 11.86 |
| M7-2 | 710 | 748 | 427 | | | | | | | | |
| M8-1 | 759 | 803 | 452 | 749 | 791 | 443 | 5.65 | 2.15 | 2.27 | 2.45 | 12.17 |
| M8-2 | 738 | 779 | 435 | | | | | | | | |

[2] M1 = Type I. M2= Type V. M3= SF. M4 = FA. M5= GGBFS. M6= MCI. M7= CNI. M8= Caltite.

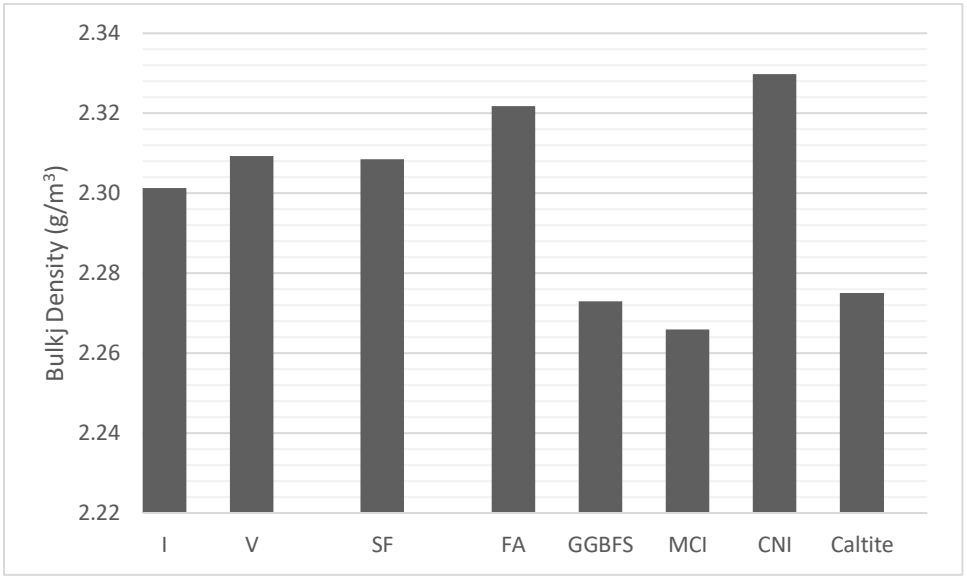


*Figure 6-3: Bulk Density results compared to the standard mix*

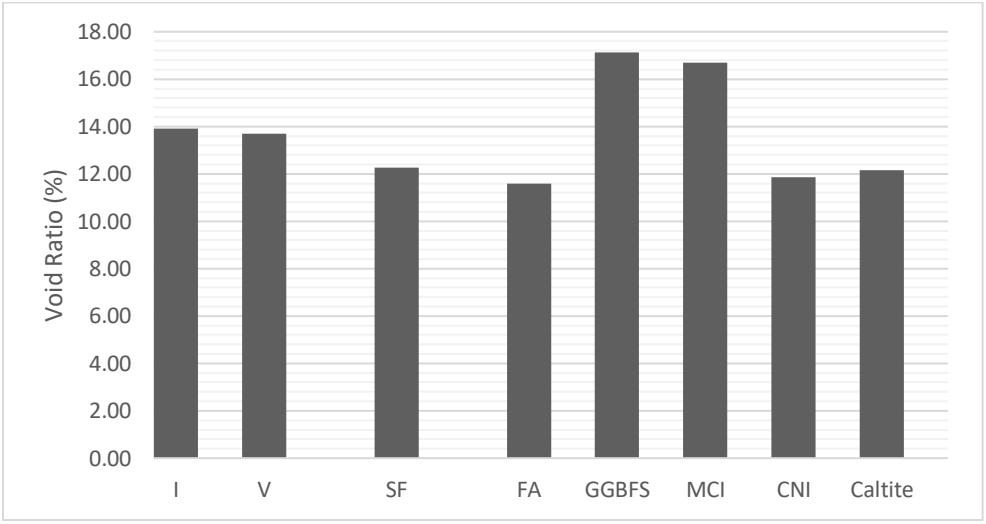


*Figure 6-4: Void ratio results compared to the standard mix*

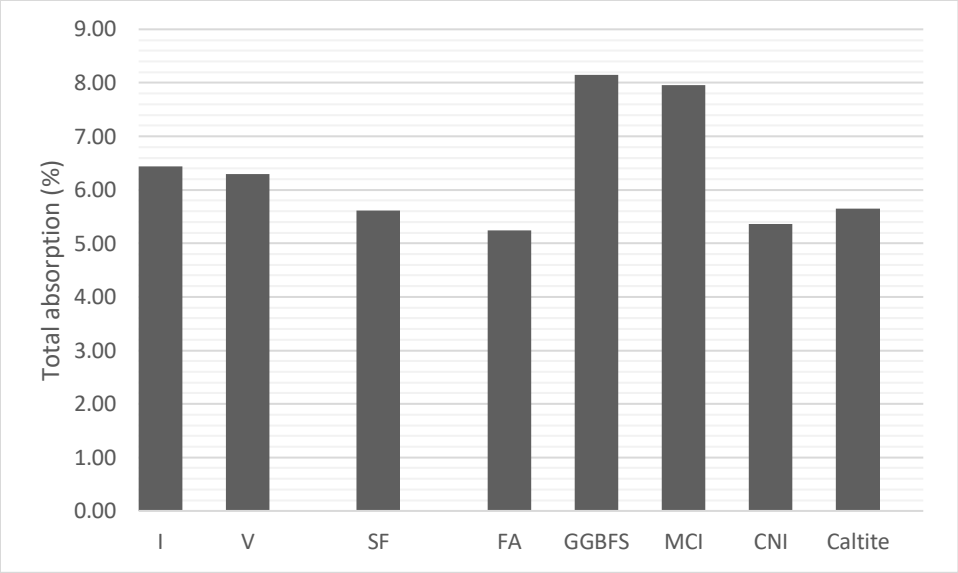


*Figure 6-5: Total absorption results compared to the standard mix*

## 6.4. Sorptivity

Illustrated in Figure 6-6 the rate of absorption test results that was conducted on two samples of each mix for 7 to 9 days. In general, the mixes followed a semi linear trend of absorption with time that was highest during the first day and kept on increasing gradually during the remaining period of testing. The rate of absorption (slope of Figure 6-5) was shown to have an inversely proportional relationship with time. The absorption was shown to be highest with GGBFS in addition to type I concrete which can be owed in the case of GGBFS to its higher void ratio as was shown in the density test. On the other hand, caltite and fly ash mixes showed the lowest overall absorption during the seven-day testing period which in the case of caltite was to be expected due to its high

hydrophobic effect especially at early ages as was further proven by the total absorption test in section 6.2. In the case of fly ash concrete, the low absorption coincides with the improved water-tight properties that were reported in the literature. It is worth noting that all mixes had a lower overall absorption than the standard mix except for GGBFS which was higher since the beginning of the testing. Silica fume reported one of the lowest profiles which can be owed to its more water-tight structure.

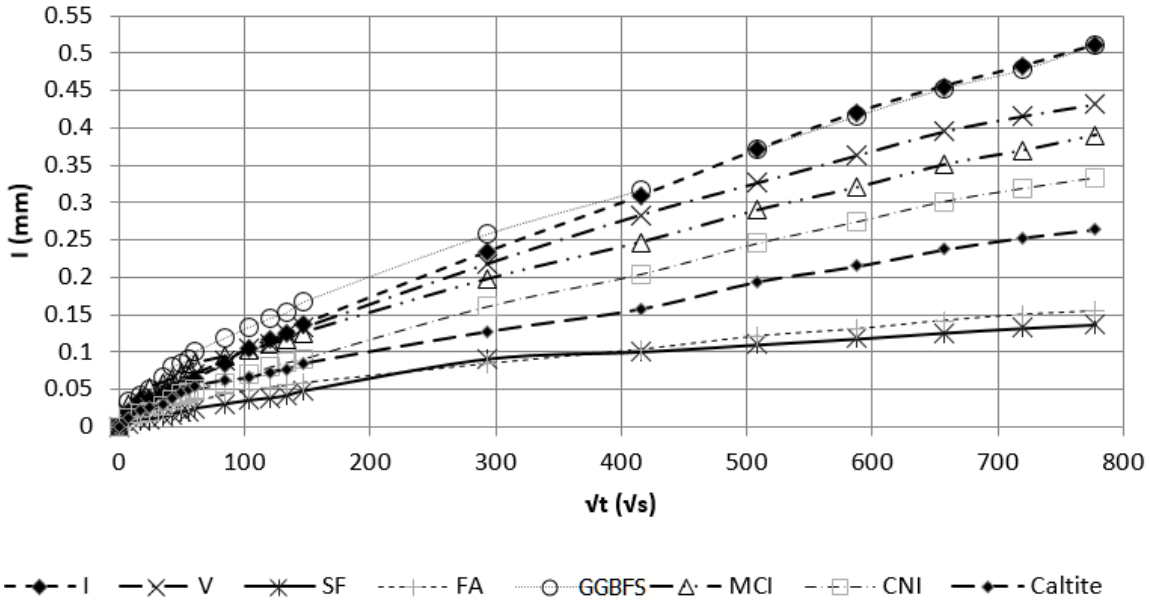


*Figure 6-6: Sorptivity curves*

As illustrated in Table 6-3 and Figure 6-7, the rate of absorption was observed to decrease significantly with time by a factor of 0.7 in cases of type I, CNI and MCI concretes which may indicate that the role of sorptivity in chloride transportation into

concrete may be limited to early exposure times. Moreover, the GGBFS mix showed the highest primary rate of absorption and could help explain the higher-than-expected chloride concentrations in the bulk diffusion testing at 35 days of exposure as shown in the bulk diffusion section. However, the secondary rate of absorption for GGBFS is shown to be improved significantly when compared to the standard mix. On the other hand, the fly ash concrete mix exhibited one of the lowest total absorption and rates of absorption which indicate an enhanced micro structure more impermeable to chloride transfer under atmospheric pressure. Moreover, silica fume reported the lowest initial and secondary rates of absorption which indicates its improved micro structure.

*Table 6-3: Sorptivity rates*

| | Type I | Type V | SF | FA | GGBFS | MCI | CNI | Caltite |
|---|---|---|---|---|---|---|---|---|
| Avg. initial rate of absorption | 8.25E-04 | 4.42E-04 | 3.03E-04 | 3.52E-04 | 9.41E-04 | 6.39E-04 | 5.75E-04 | 4.83E-04 |
| Avg.Secondary rate of absorption | 5.77E-04 | 1.77E-04 | 9.83E-05 | 1.48E-04 | 5.27E-04 | 4.02E-04 | 3.65E-04 | 2.93E-04 |

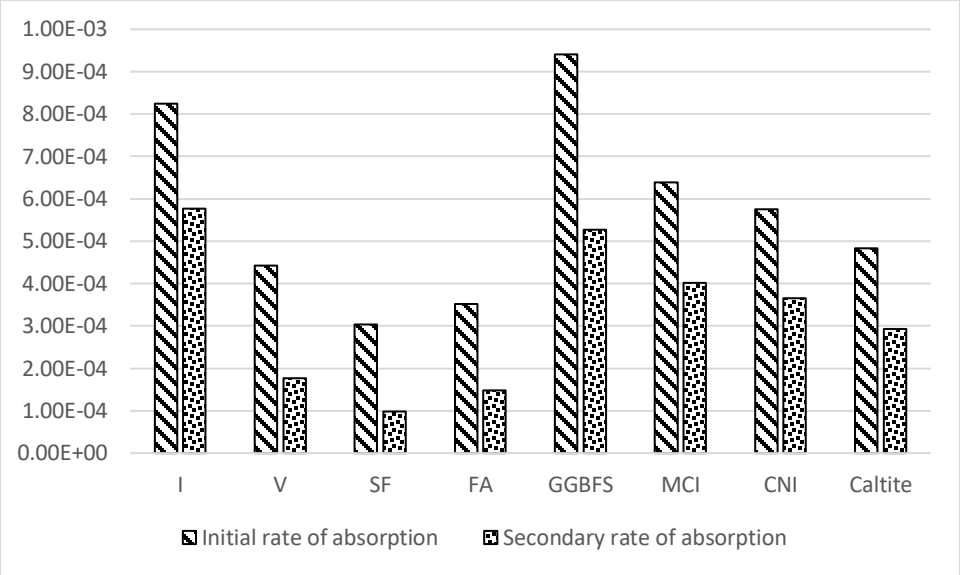


*Figure 6-7:Comparison of the different rates of absorption*

## 6.5. Binding capacity

As shown in Figure 6-8, the binding capacity was reported to be proportional with the concentration of chloride in the solution. This was exceptionally highlighted in the cases of fly ash and GGBFS concretes which both exhibited large increases in the binding capacity with the increase of free chloride in the exposure environment. Furthermore, GGBFS exhibited the highest binding capacity with increasing concentrations of NaCl in the environment compared to the standard which were double those reported by the standard mix. This increase coincides with the reported properties of GGBFS having high alumina and ferric-alumina salts which help in irreversibly binding chloride by forming

Friedal's salts [7], [46], [47], [77] . This was the case with Fly ash as well which showed an improvement in the chloride binding significantly but less than GGBFS.

On the other hand, Type V cement as expected had a lower binding capacity due to the lower amount of alumina in the cement compared to Type I cement as was reported in the literature[50], [77], [78]. Moreover, the addition of silica fume was shown to be of little to no significant effect in binding chloride which coincides with what was reported by Thomas et al[47]. in concretes with 0.5 w/c and can be owed to silica fume forming less alumina and ferric-alumina hydration products. Furthermore, the addition of CNI, MCI followed the same trend of silica fume in having slight to no effect of the binding properties especially at higher salt concentrations since their role of inhibiting corrosion has minimal effect on the hydration process and hydration results. Finally, Caltite was shown to reduce the binding significantly especially at higher concentrations of chloride in the environment which can be owed to the hydrophobic nature of concretes containing it that result in limiting the contact between hydration products and chloride thus reducing the chance of binding chloride in the first place.

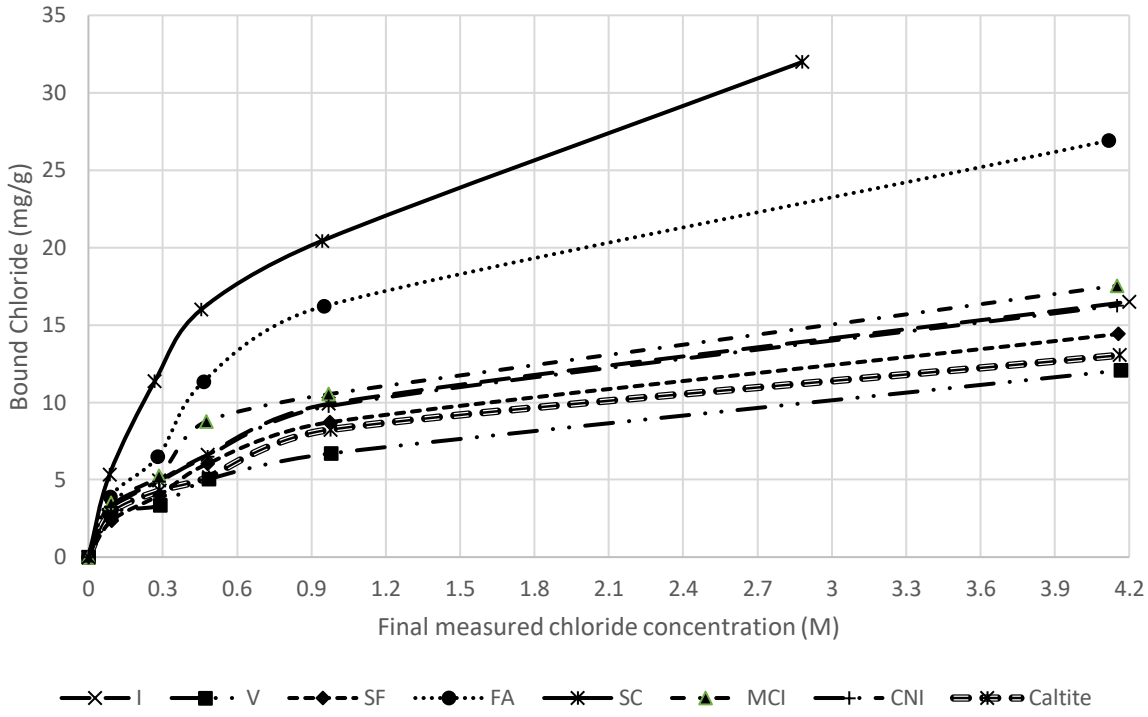


*Figure 6-8: binding capacity test results.*

## 6.6. Bulk diffusion

After testing the samples for 12 months in the laboratory, the results are illustrated in Figures 6-9 to 6-12. It is shown that GGBFS mix had always the highest concentration near the exposure surface but always declined rapidly to reach the lowest concentration before any mix which when combined with the results of the binding test and density test indicate a relatively permeable micro structure that compensates for such permeability by binding chloride effectively thus hindering the movement of chlorides inside the

concrete. This behavior is further proven when comparing the value of the surface chlorides (Cs) at any exposure period where SCMs are shown to have the highest surface chlorides but one of the lowest diffusion coefficients especially with passage of time as shown in Figure 6-12. This may indicate the role of GGBFS in hindering the diffusion of chloride improves and get more pronounced with the passage of time unlike the chemical admixtures where the opposite is shown. Moreover, fly ash concrete exhibited the same behavior throughout the testing period with the addition of having the lowest profile at all exposure periods. This fact when combined with the results of the density, sorptivity and binding test indicate that fly ash mix has the densest micro structure that when combined to effective chloride binding mechanism result in quite impervious concretes that resists the penetration of chloride.

On the other hand, the addition of silica fume at 6% by weight of cement seems to have little to no significant effect on the diffusion profile which confirms with what was reported by some researchers in the literature. Although having a dense micro structure as was reported by the density test, its water affinity and reduced binding capacity may have been the reason behind such behavior. Moreover, the diffusion coefficient that was reported for all exposure periods was higher than the standard mix and the profile was noticed to change more significantly relative to the standard mix and to the fly ash and GGBFS mix suggesting that the diffusion through this mix is easier which was unexpected.

The addition of chemical admixtures seems to have a slight positive effect on the profiles of the chloride during the ponding periods except for caltite where a significant drop in the diffusion coefficient was noticed suggesting that CNI and MCI have no effect on the diffusion on the long term unlike caltite. In terms of the surface chloride concentration (Figure 6-12), only caltite is shown to have a visible effect by reducing the concentration at the surface.

Finally, type V cement seems to have a slightly negative effect on the diffusion as its chloride ponding profile was always slightly higher than that of the standard indicating that the chloride diffusion through it is slightly easier which was to expected as type V cement reported lower binding and similar absorption and density. This is more pronounced when comparing the surface chloride concentrations and diffusion coefficients throughout the exposure periods where mix 2 (type V) reported slightly higher diffusion coefficients and lower surface chlorides except for the 35 days ponding where it reported equal surface concentration.

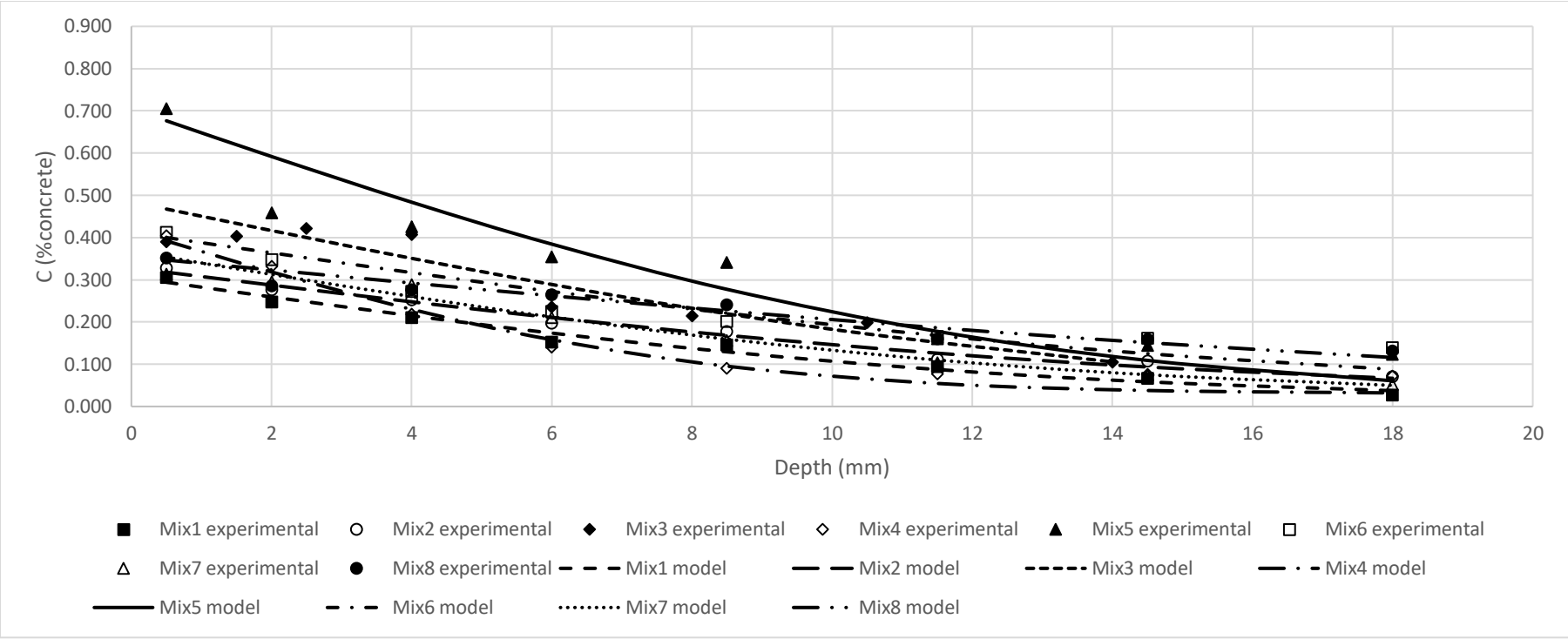


*Figure 6-9: 35 days ponding profiles*[3]

[3] Mix 1 = Type I. Mix 2= Type V. Mix 3= SF. Mix 4 = FA. Mix 5= GGBFS. Mix 6= MCI. Mix 7= CNI. Mix 8= Caltite.

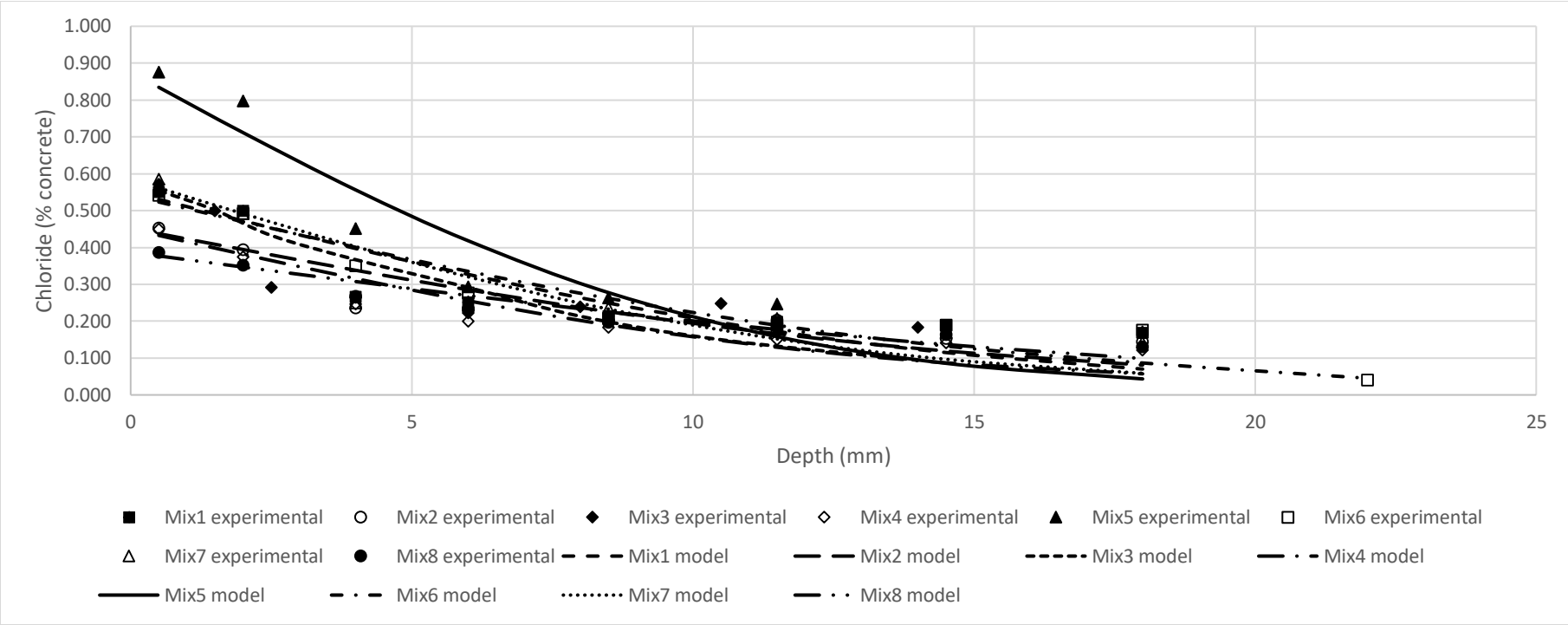


*Figure 6-10: 6 months ponding profiles*[4]

[4] Mix 1 = Type I. Mix 2= Type V. Mix 3= SF. Mix 4 = FA. Mix 5= GGBFS. Mix 6= MCI. Mix 7= CNI. Mix 8= Caltite.

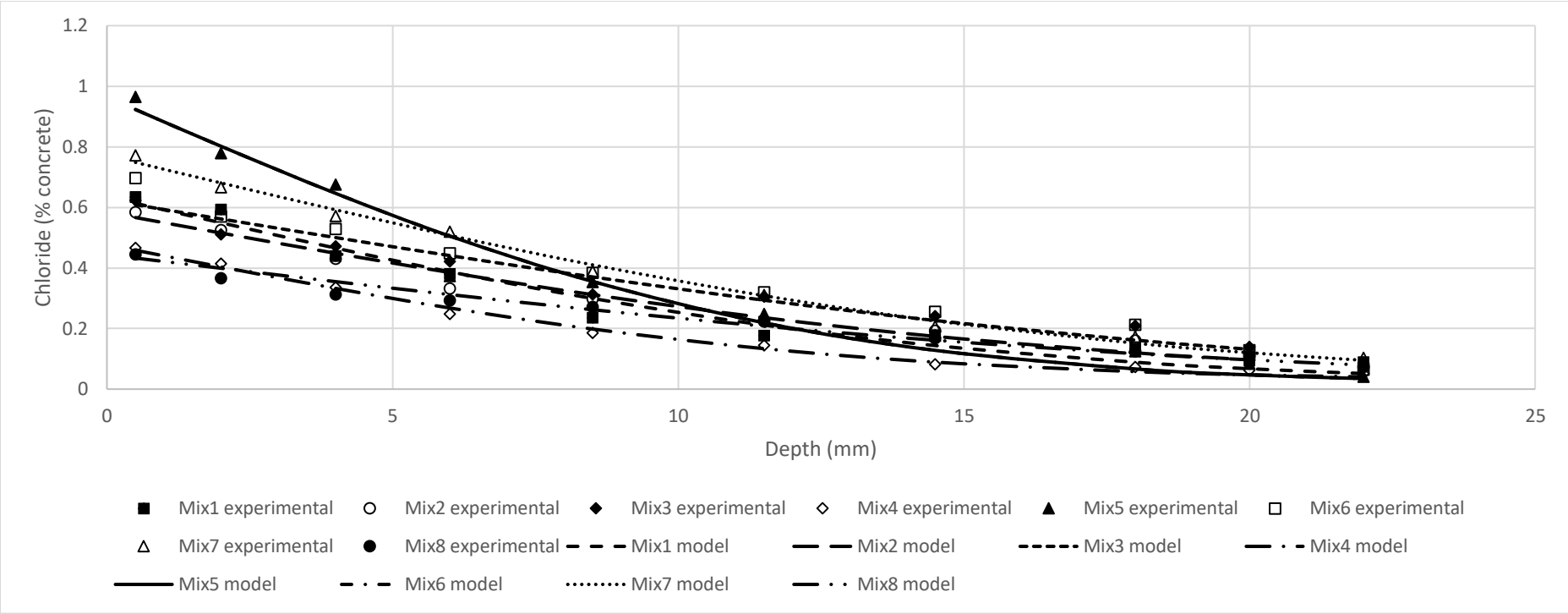


*Figure 6-11: 12 months ponding profiles*[5]

[5] Mix 1 = Type I. Mix 2= Type V. Mix 3= SF. Mix 4 = FA. Mix 5= GGBFS. Mix 6= MCI. Mix 7= CNI. Mix 8= Caltite.

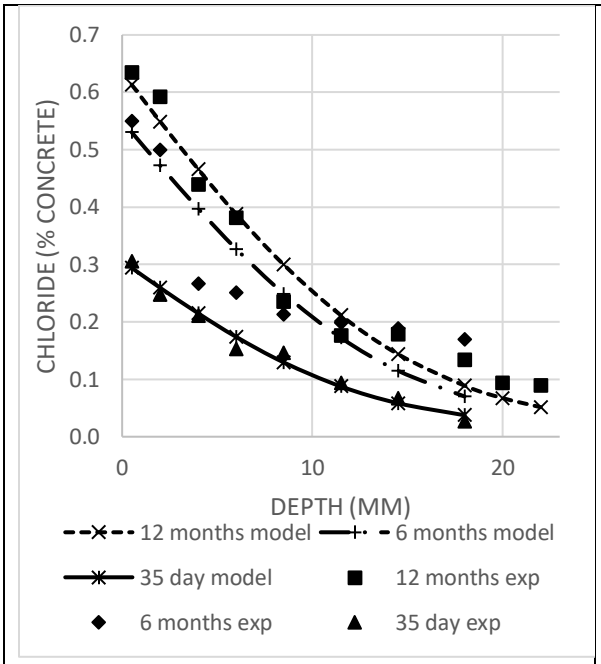
0.7
0.6
0.5
0.4
0.3
0.2
0.1
0.0
CHLORIDE (% CONCRETE)
0
10
20
DEPTH (MM)
12 months model
6 months model
35 day model
12 months exp
6 months exp
35 day exp

Type I

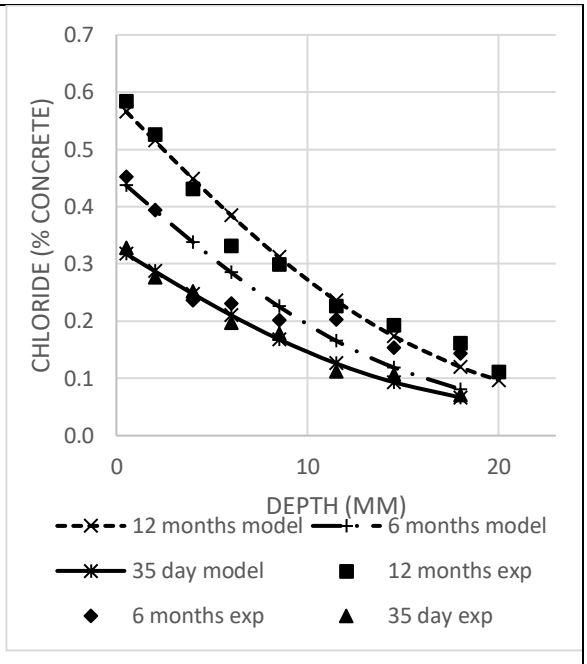
0.7
0.6
0.5
0.4
0.3
0.2
0.1
0.0
CHLORIDE (% CONCRETE)
0
10
20
DEPTH (MM)
12 months model
6 months model
35 day model
12 months exp
6 months exp
35 day exp

Type V

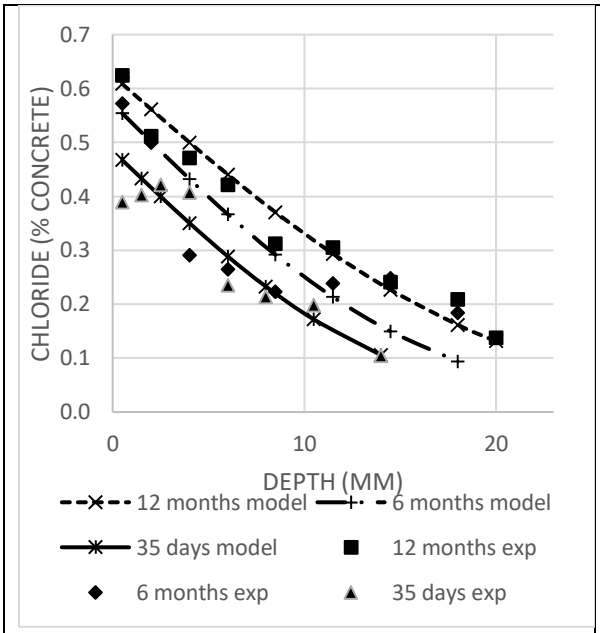
CHLORIDE (% CONCRETE)
0.7
0.6
0.5
0.4
0.3
0.2
0.1
0.0
0
10
20
DEPTH (MM)
12 months model
6 months model
35 days model
12 months exp
6 months exp
35 days exp

SF

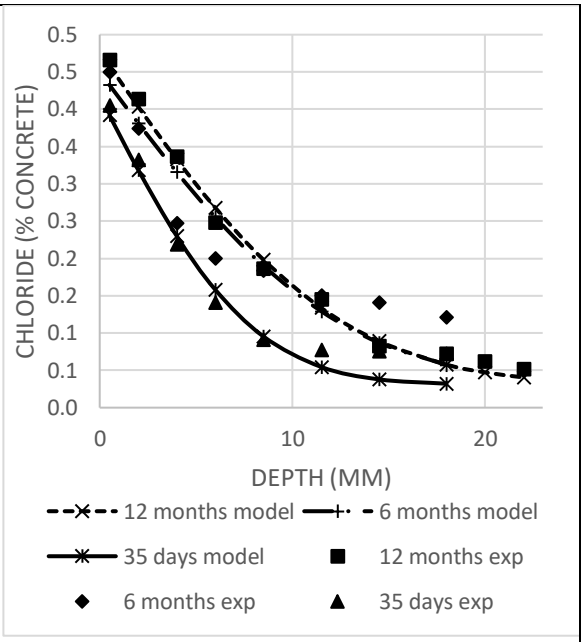
CHLORIDE (% CONCRETE)
0.5
0.5
0.4
0.4
0.3
0.3
0.2
0.2
0.1
0.1
0.0
0
10
20
DEPTH (MM)
12 months model
6 months model
35 days model
12 months exp
6 months exp
35 days exp

FA

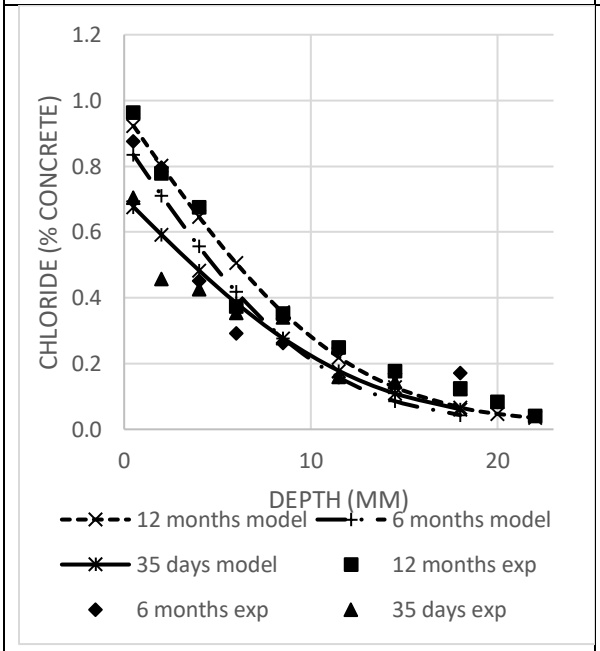
CHLORIDE (% CONCRETE)
1.2
1.0
0.8
0.6
0.4
0.2
0.0
0
10
20
DEPTH (MM)
12 months model
6 months model
35 days model
12 months exp
6 months exp
35 days exp

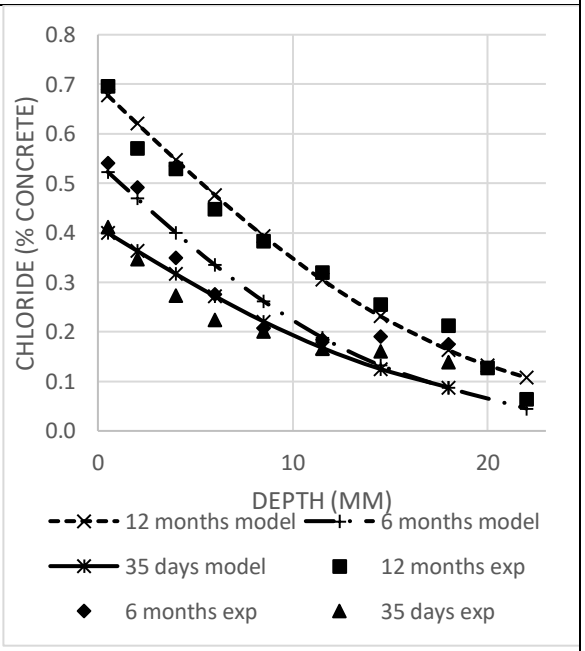
CHLORIDE (% CONCRETE)
0.8
0.7
0.6
0.5
0.4
0.3
0.2
0.1
0.0
0
10
20
DEPTH (MM)
12 months model
6 months model
35 days model
12 months exp
6 months exp
35 days exp

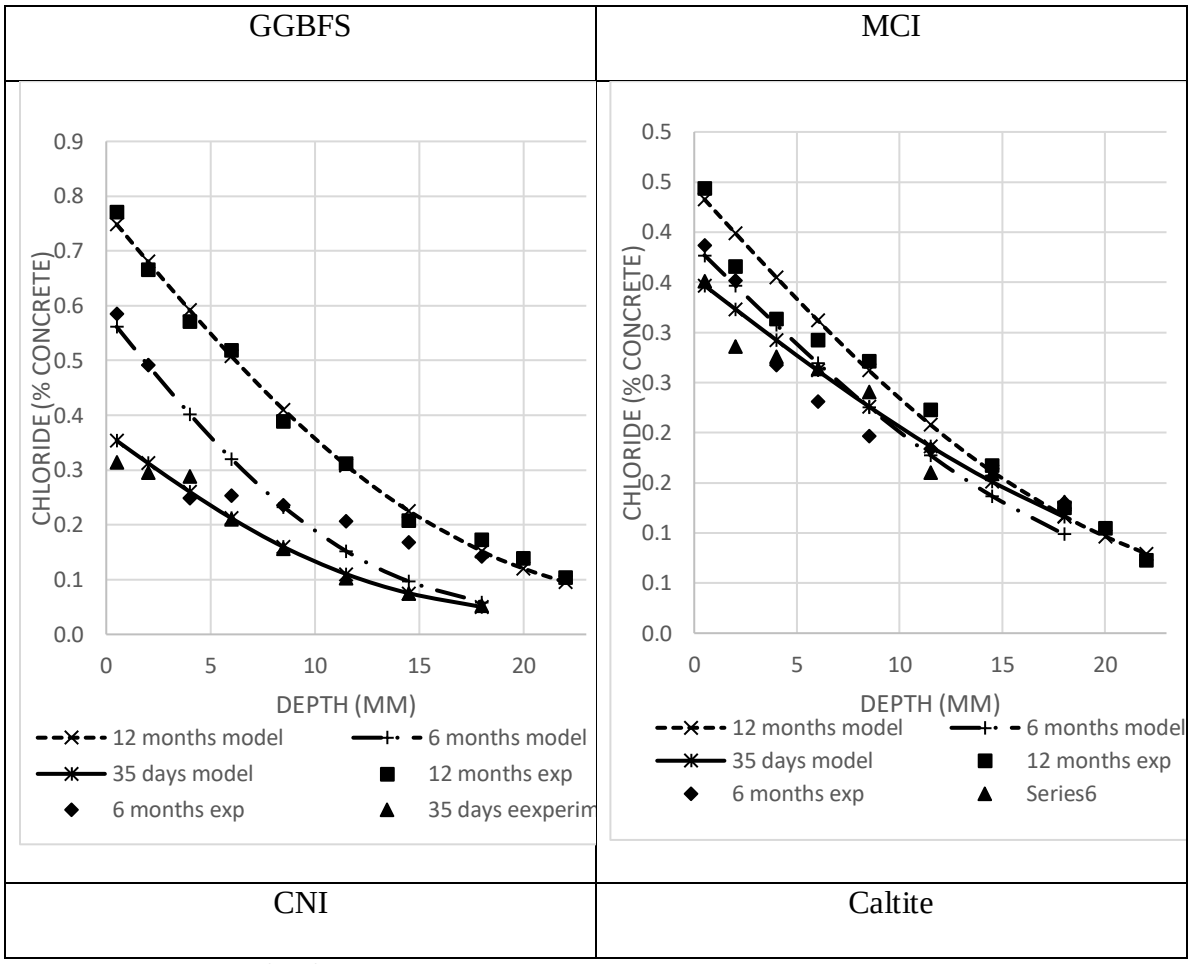


*Figure 6-12: pinding profiles for each mix vs. exposure duration*

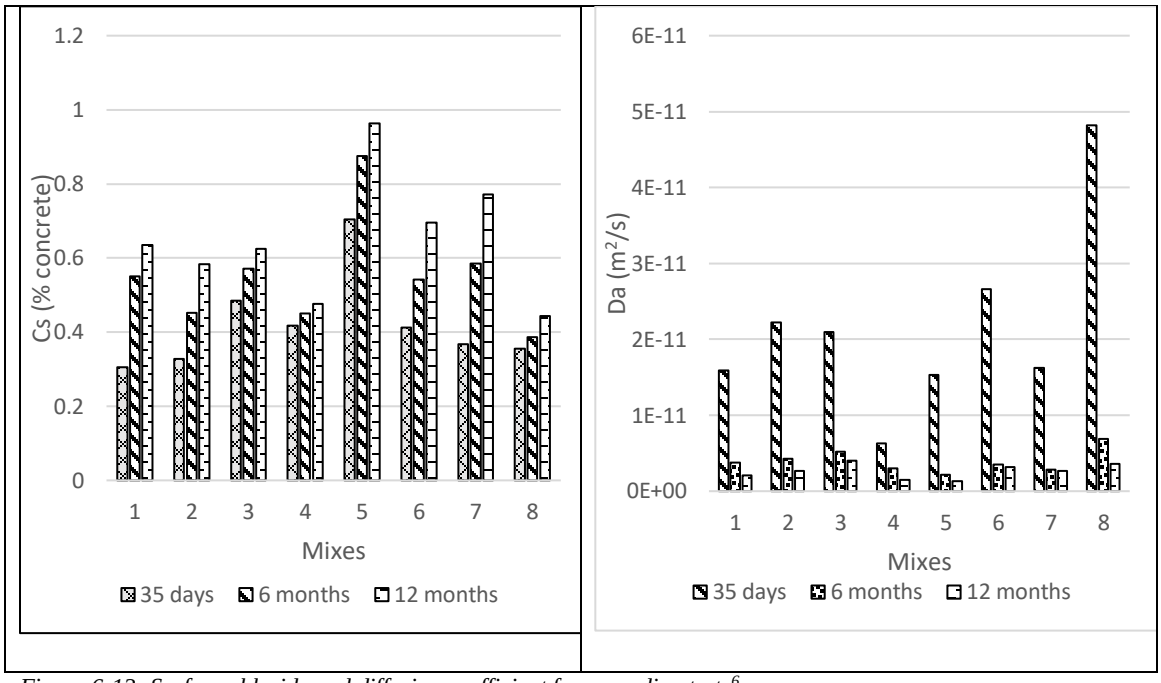


*Figure 6-13: Surface chloride and diffusion coefficient from ponding tests*[6]

In terms of the surface concentration, a general trend was observed during the testing in which values of Cs increased with the passage of time especially during the first six months which was to be expected as it was reported in the literature to be the general behavior. A suggested explanation would be that during the first 6 months, the first layer of concrete starts binding chloride at a high rate that slows down when the layer approaches its maximum binding capacity. This rate keeps on declining with the passage of time as the layer binds less chloride.

[6] Mix 1 = Type I. Mix 2= Type V. Mix 3= SF. Mix 4 = FA. Mix 5= GGBFS. Mix 6= MCI. Mix 7= CNI. Mix 8= Caltite.

On the other hand, the diffusion coefficient was noted to be inversely proportional to the exposure period with the first six months reporting the largest decrease up to 80% in the case of caltite mix which was to be expected as well since it was reported to be the case by various literature sources. An explanation of this behavior could be that the concrete becomes more saturated with chloride in deeper layers which then decreases the chemical differential thus decreasing the overall diffusion.

## 6.7. Chloride profiling

After exposing the concrete to marine activity in the Arabian Gulf water for 12 months, core samples were collected and analyzed for chloride analysis at different depths after 6 months and 12 months of exposure. As illustrated in Figures 6-14 to 6-16, samples in the tidal zone reported higher chloride profiles and required larger depths to reach layers where the chloride concentration was equal to the initial concentration. Some of the same behaviors in chloride ponding were noticed especially in the GGBFS mix (mix 5) where the highest surface concentration was reported and the diffusion coefficient was one of the lowest during both exposure durations and for exposure zones indicating a similar conclusion. Fly ash reported the second highest surface concentration preceded by mix 7 (CNI) and mix 6 (MCI) respectively unlike the ponding results where they had no effect on the profile. The effect of adding both chemical admixtures seem to be more detrimental than the chloride ponding where in this case they reported higher overall

profiles in the 6 and 12 months exposures in the tidal zone. The rest seem to have similar effects on the chloride profiles in the tidal zone as was the case for the chloride ponding except for caltite where it was in the tidal zone less effective in reducing the chloride profile opposite to what was recorded in the ponding results.

In terms of surface concentration in the tidal zone, most mixes in the 6-month tidal exposure reported a value in the range of 0.18 % to 0.25% for all mixes except for mix 5 (GGBFS) and mix 6 (MCI) were higher values were reported. However, the same trend was reported in term of the values increasing with the passage of time for all mixes similar to the trend reported in the ponding results.

As for the diffusion coefficient (Figure 6-20), a decreasing trend was noticed as was the case in the ponding results but the values of diffusion coefficients were higher in all cases and for both exposure periods compared to those reported in the ponding tests. This indicate a higher chloride diffusion activity in the tidal zone which is thus more dangerous to concrete structures exposed to tidal exposure. An explanation for this increase would be that the variation of drying and wetting of the water in the shallow layers of the concrete during low tide periods and hotter weather that results in a temporary sharp increase in the concentration of chloride that then drives chloride deeper into concrete at a much higher rate compared to the relatively steady rate in the ponding exposure.

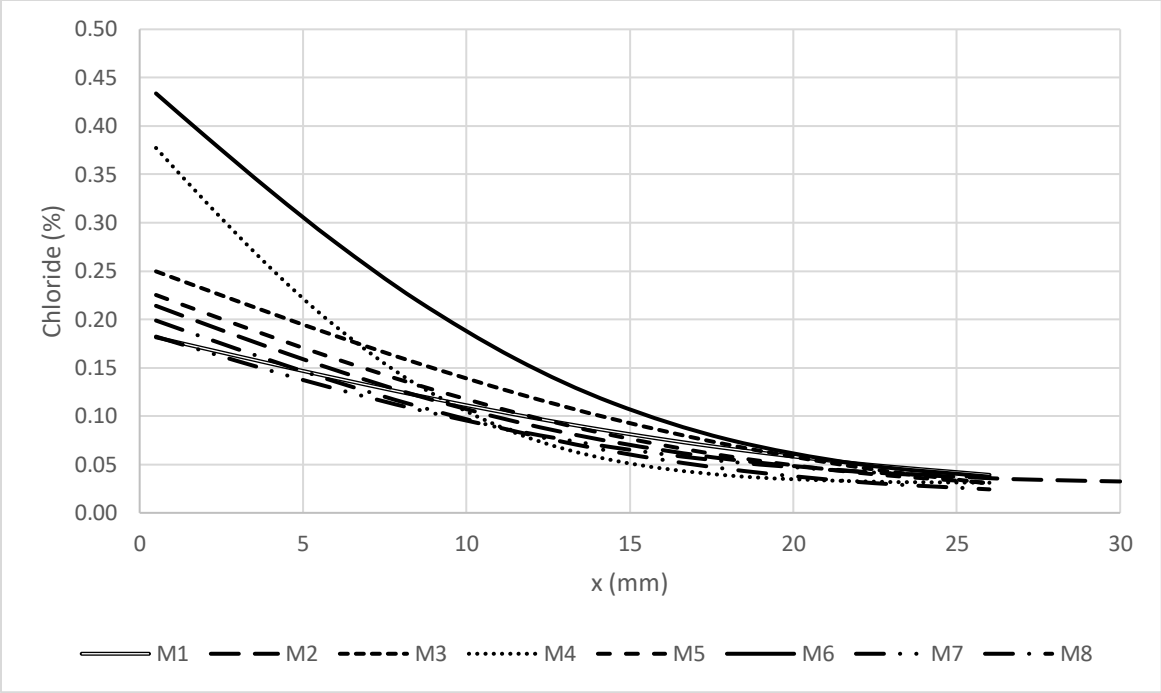


*Figure 6-14: 6-month tidal chloride profiles*[7]

[7] M1 = Type I. M2= Type V. M3= SF. M4 = FA. M5= GGBFS. M6= MCI. M7= CNI. M8= Caltite.

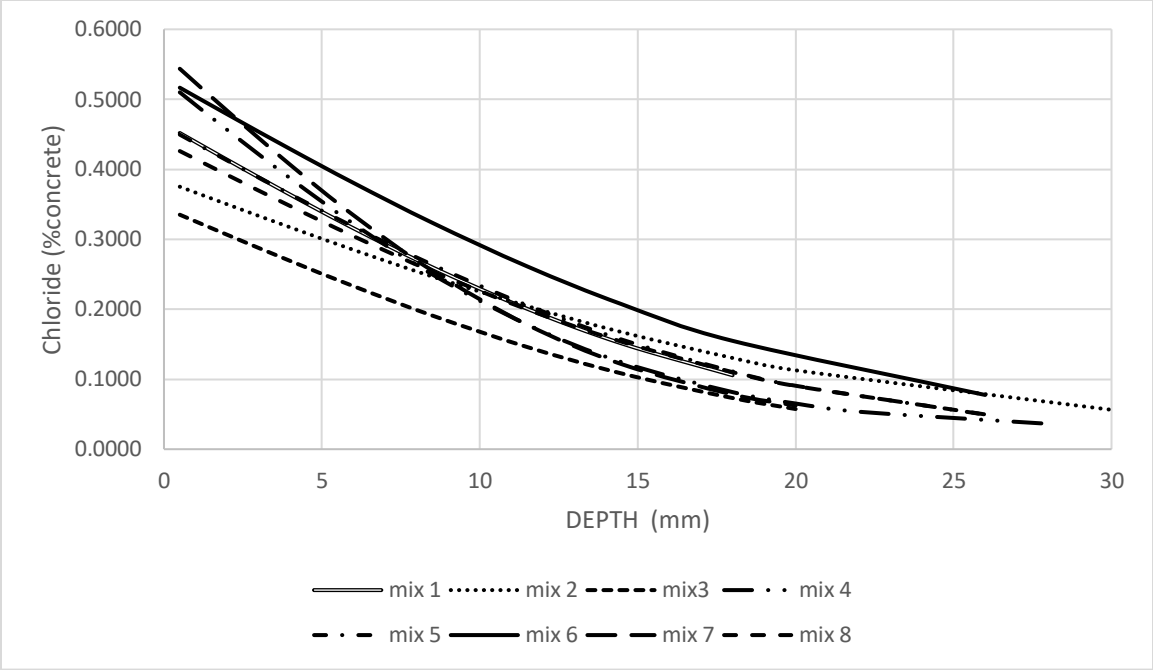


*Figure 6-15: 12-month tidal chloride profiles*[8]

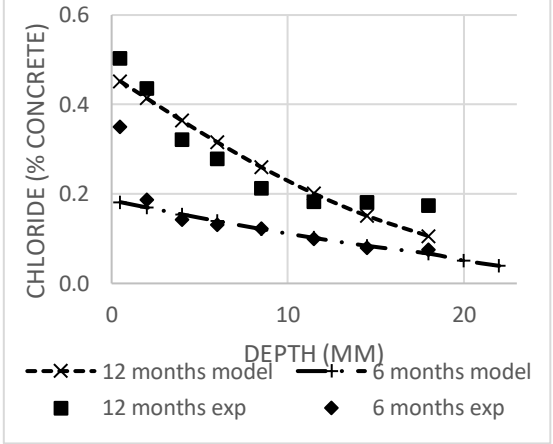


Type I

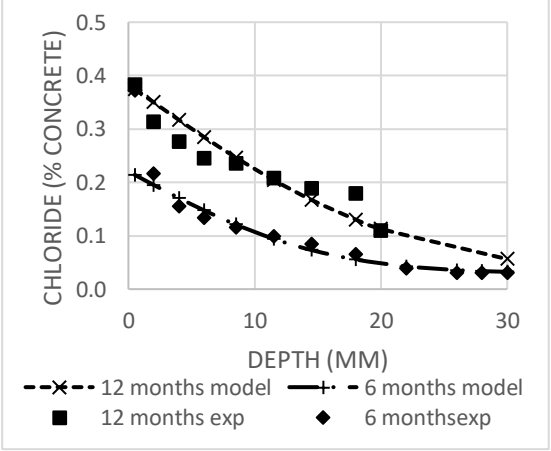


Type V

[8] Mix 1 = Type I. Mix 2= Type V. Mix 3= SF. Mix 4 = FA. Mix 5= GGBFS. Mix 6= MCI. Mix 7= CNI. Mix 8= Caltite.

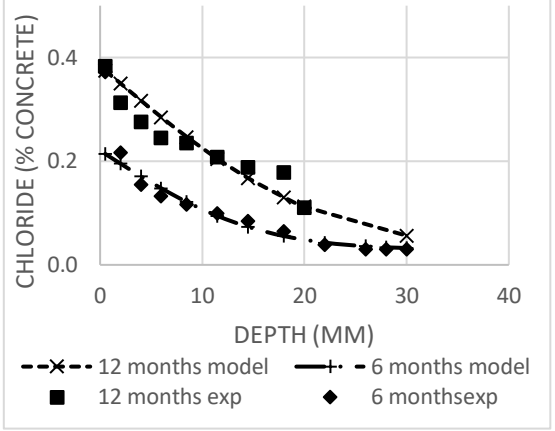


SF

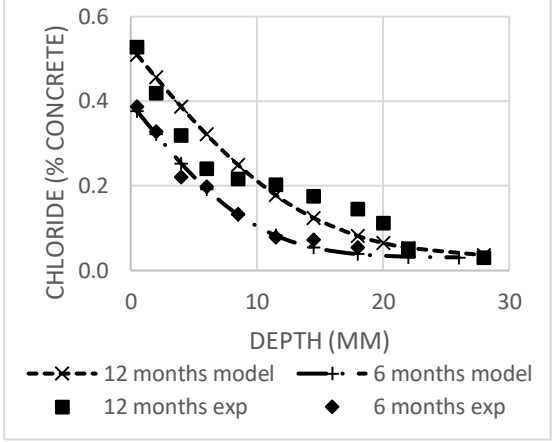


FA

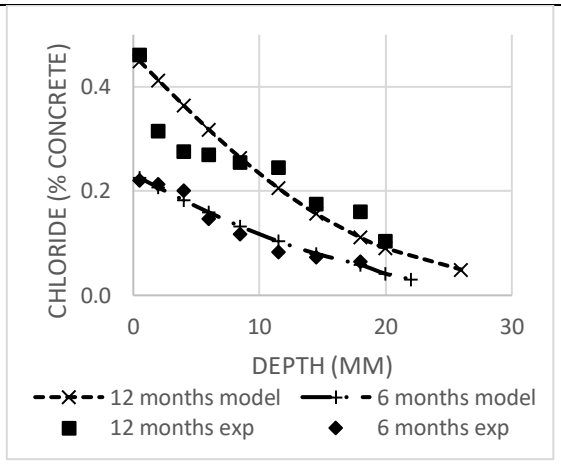


GGBFS

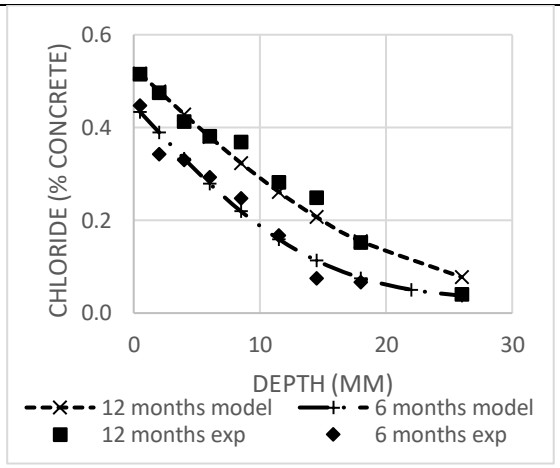


MCI

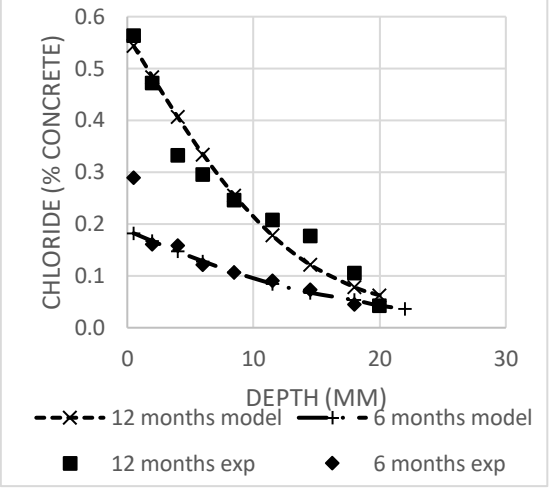


CNI

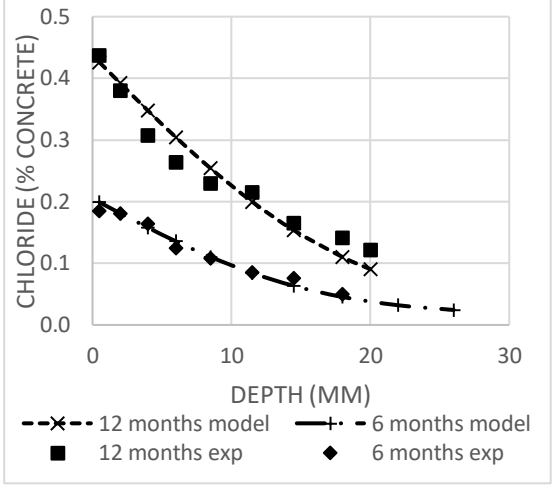


Caltite

*Figure 6-16: 12 and 6 months tidal chloride profiles for each mix*

As for the chloride analysis in the atmospheric zone, the results are illustrated in Figures 6-16 to 6-18. The same trends were reported as the tidal zone results but at much lower value for the profile values and surface concentrations which is expected as the concentration of chloride in the atmospheric zone is considerably low compared to the tidal zone. The same trend in terms of increasing Cs and decreasing Da with time as was reported in the tidal and ponding results and could be explained following the same logic previously explained. Another trend that was recorded in terms of chloride profiles is that the profiles had little to no change indicating a very slow diffusion activity thus a much lower risk of corrosion in structures exposed to atmospheric marine environments compared to any other exposure condition or zone as was reported by numerous studies

in the literature. This point is further proven by the linear polarization resistance test as will be illustrated in the following section.

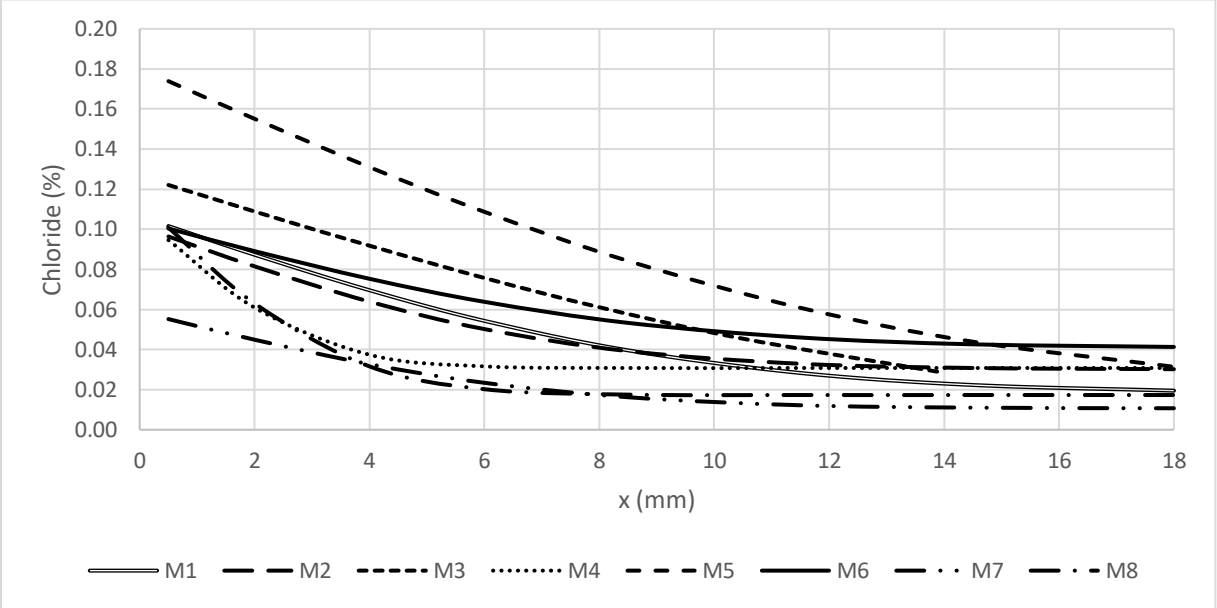


*Figure 6-17: 6-month atmospheric chloride profiles*[9]

[9] M1 = Type I. M2= Type V. M3= SF. M4 = FA. M5= GGBFS. M6= MCI. M7= CNI. M8= Caltite.

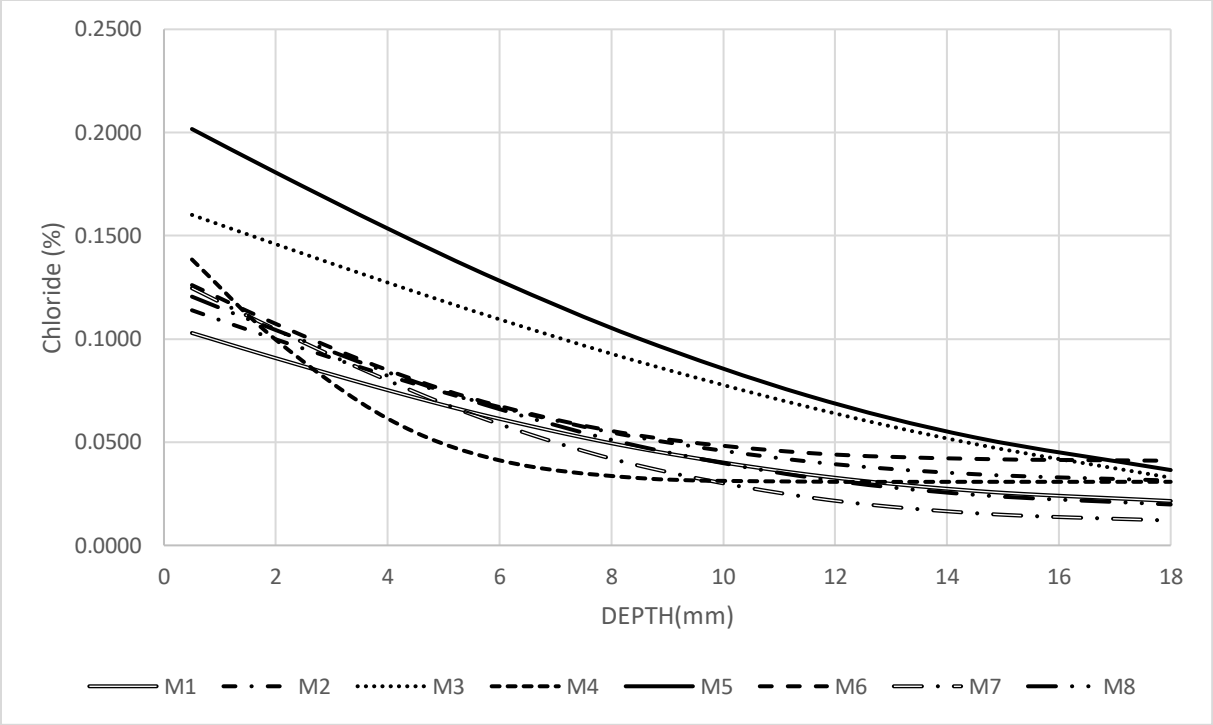


*Figure 6-18: 12-month atmospheric chloride profiles*[10]

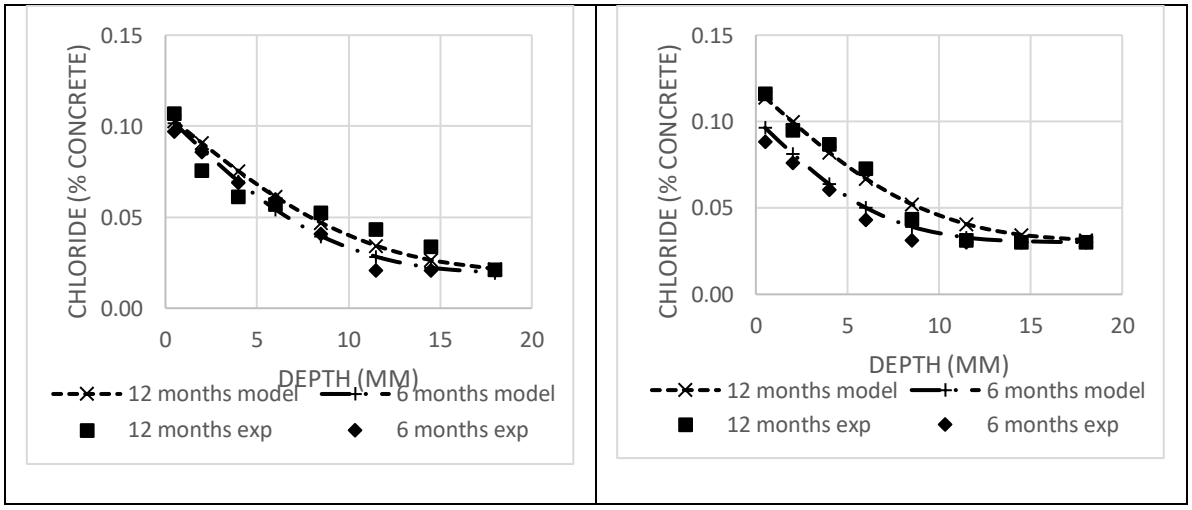


[10] M1 = Type I. M2= Type V. M3= SF. M4 = FA. M5= GGBFS. M6= MCI. M7= CNI. M8= Caltite.

| Type I | Type V |
| --- | --- |
| 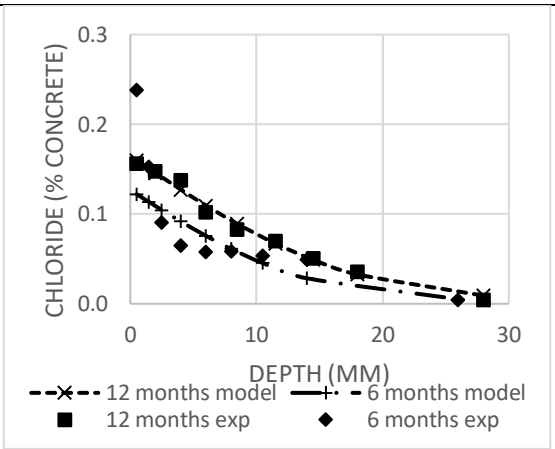 | 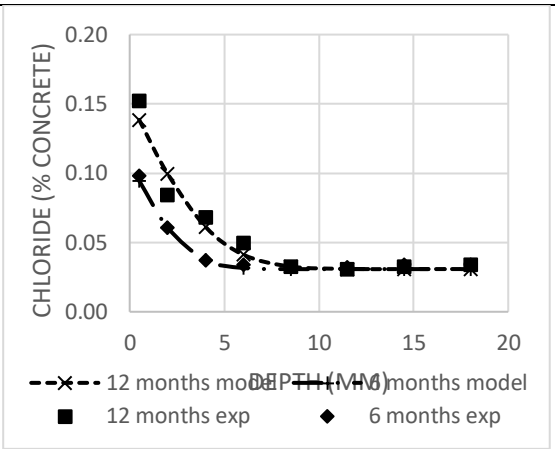 |
| SF | FA |
| 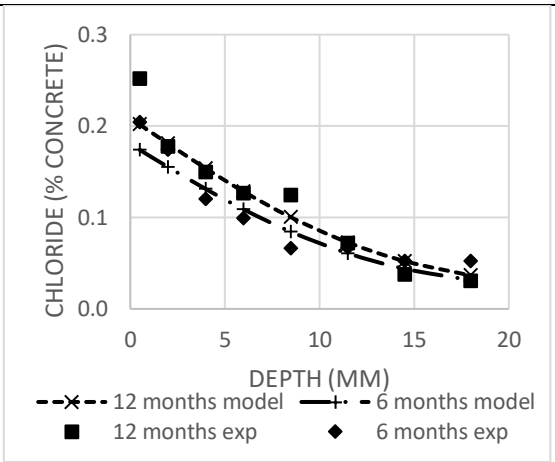 | 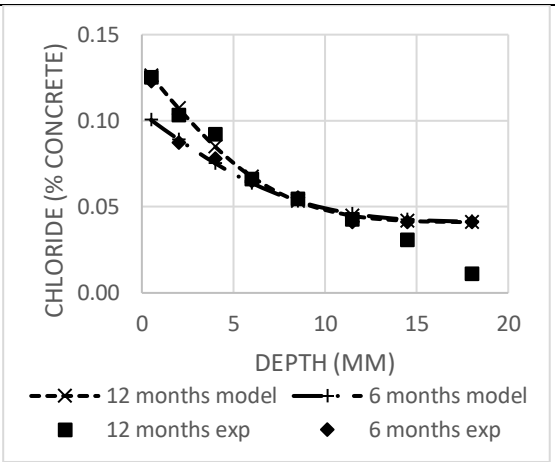 |
| GGBFS | MCI |

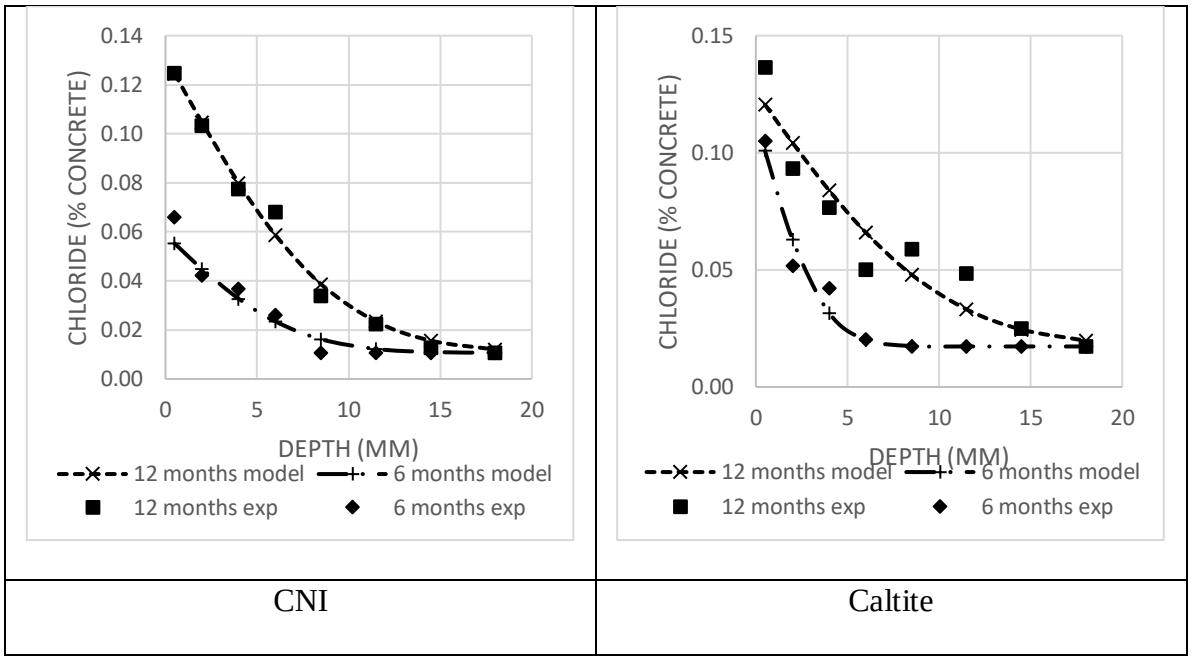


*Figure 6-19:12 and 6 months atmospheric chloride profiles for each mix*

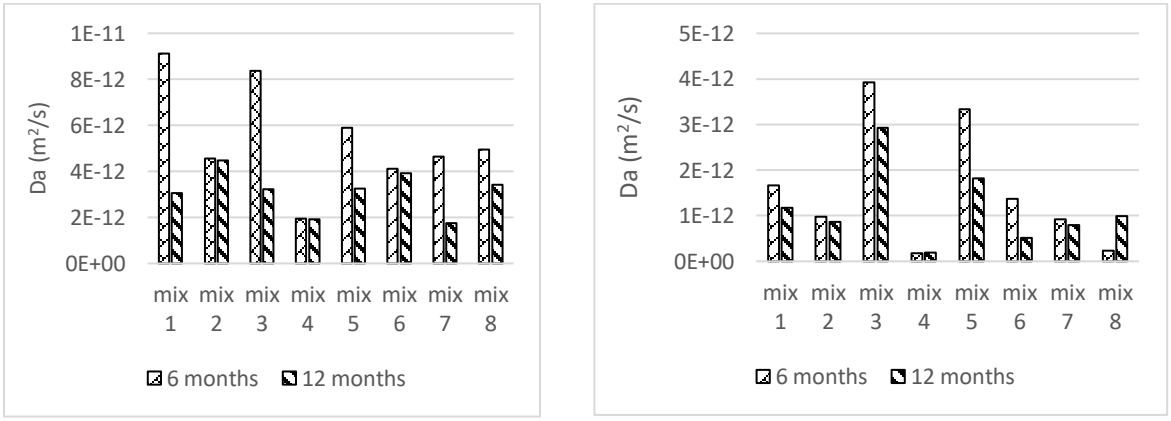


*Figure 6-20: Diffusion coefficient comparison atmospheric(right), tidal (left)*[11]

[11] Mix 1 = Type I. Mix 2= Type V. Mix 3= SF. Mix 4 = FA. Mix 5= GGBFS. Mix 6= MCI. Mix 7= CNI. Mix 8= Caltite.

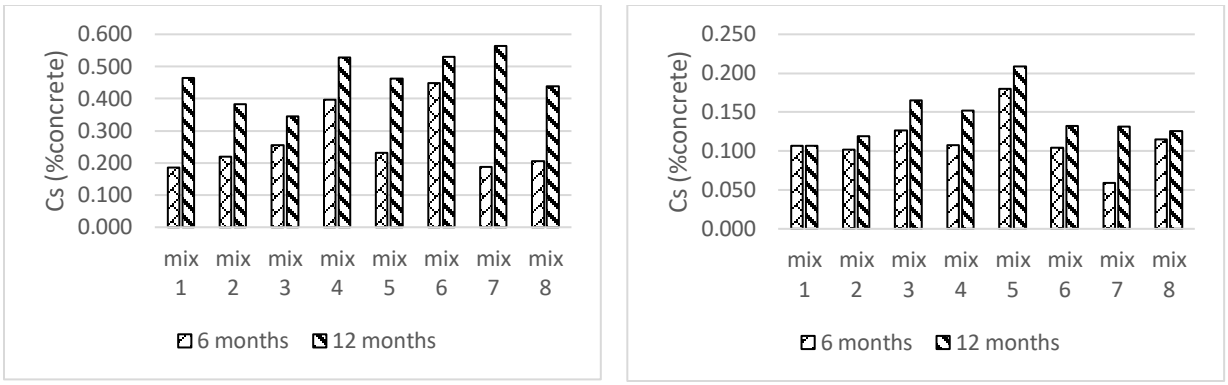


*Figure* 6-21*: Surface Chloride atmospheric (right), tidal (left)*[12]

## 6.8. Linear polarization resistance

As previously explained in earlier chapters, the polarization resistance method was used to calculate the corrosion current density in the atmospheric, splash and tidal zones for reinforcements that were embedded at 12.5 mm, 25.4 mm, 38.1 mm and 50.8 mm away from the surface of the exposure samples. The measurements were taken at 6 and 12 months from exposure to the Arabian Gulf environment. An $I_{corr}$ limit of 0.25 µA/cm$^2$ was taken as the limit of activation since a lower limit was deemed too conservative by many researchers[60]–[62]. A value of 1 µA/cm$^2$ was taken as an indication of high corrosion activity. A general trend was observed where the values of $I_{corr}$ increased with time and decreased with the depth except in some samples in the splash and tidal zones as illustrated in Figures 6-22, 6-23 and 6-24.

[12] Mix 1 = Type I. Mix 2= Type V. Mix 3= SF. Mix 4 = FA. Mix 5= GGBFS. Mix 6= MCI. Mix 7= CNI. Mix 8= Caltite.

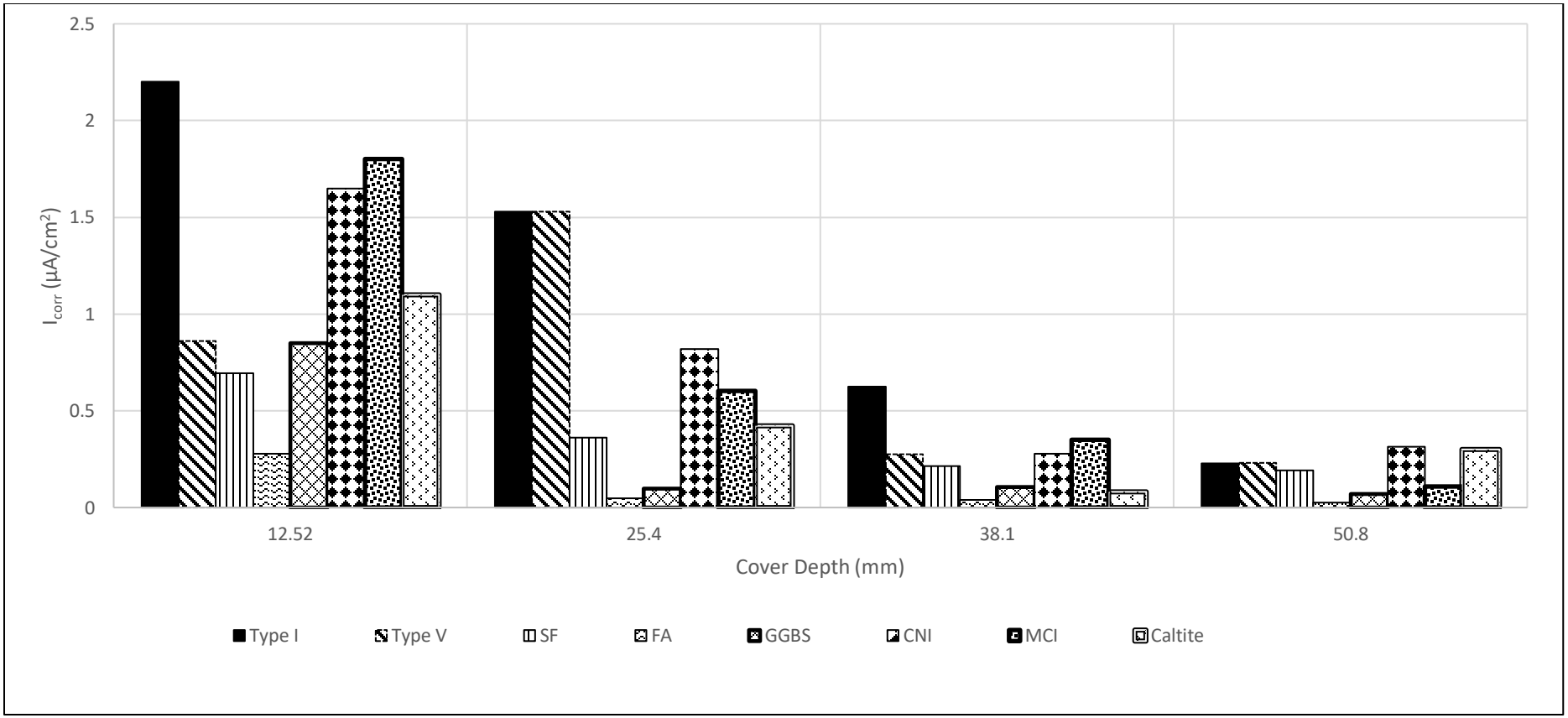


*Figure 6-22: Corrosion current density readings after 12 months in the tidal zone*

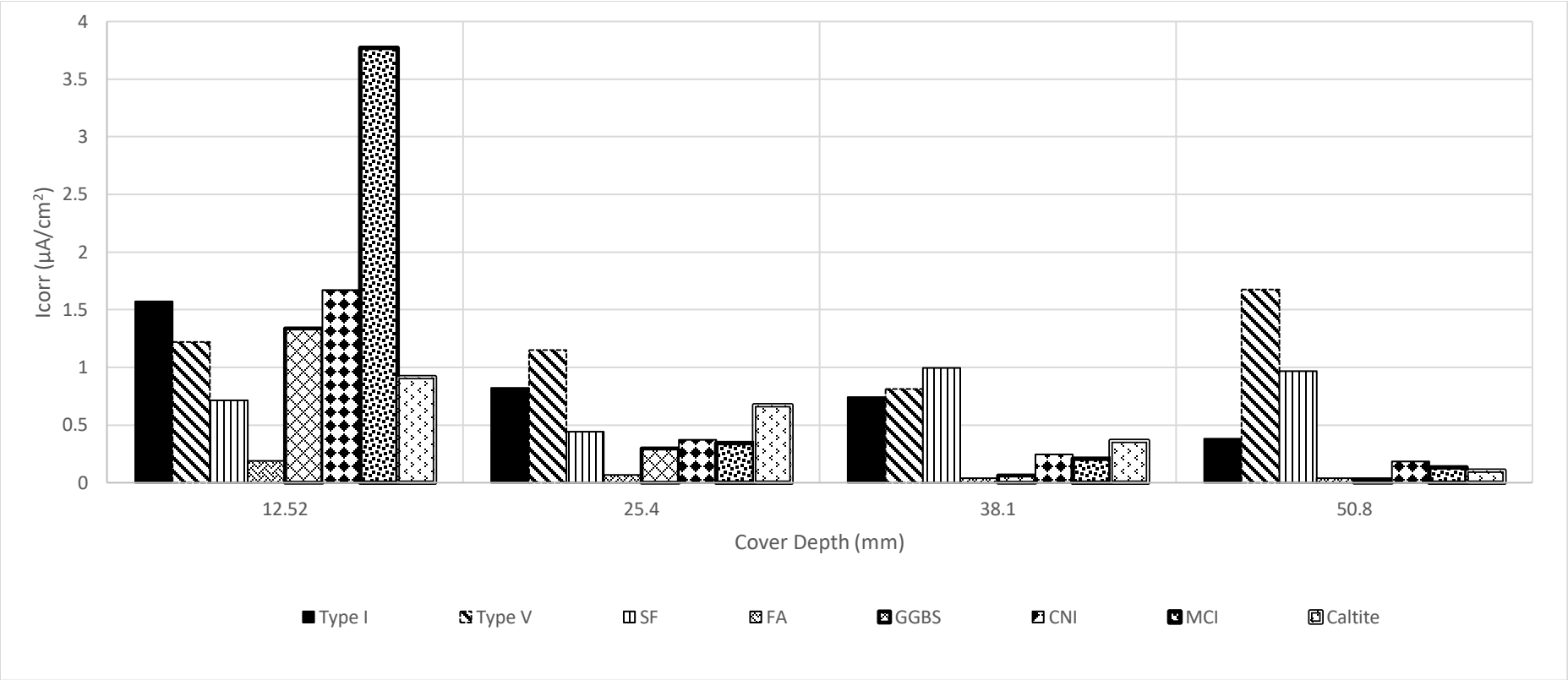


*Figure 6-23:Corrosion current density readings after 12 months in the splash zone*

None of the samples in the atmospheric zone reported a value higher than 0.1 $\mu A/cm^2$ at any depth thus indicating that none of them reached the corrosion activation threshold which coincides with what was reported in the literature for similar mixtures exposed to atmospheric conditions. On the other hand, samples in the splash and tidal zone reported values higher than the activation limit at almost all depths except for fly ash and GGBFS where the corrosion density values were lowered than the activation limit in the first 6 months. In addition, caltite reported a value of less than the activation limit at the final depth only (50.8 mm).

The values of $I_{corr}$ seemed to increase significantly in most mixes during the period from 6 to 12 months however the increase does not seem to follow a certain model. At 12 months, all of the samples reported a high active corrosion status in the first layer except for fly ash where the maximum value did not exceed 0.27 $\mu A/cm^2$ in the first depth. CNI mixture was not able to resist corrosion and reported one the highest values of $I_{corr}$ (2.2 $\mu A/cm^2$) although the samples were not cracked which contradicts Kondratova [62] where he claimed that CNI was effective in resisting corrosion if the samples were uncracked. A justification could be that the exposure conditions in the Arabian Gulf seem to be harsher and the addition of chemical admixtures seems to be ineffective against such environment. The only chemical admixture in this study that seemed to resist corrosion in the slightest was catite and its effectiveness was limited to depths higher than

40 mm. Overall, fly ash and GGBFS seem to be the most effective SCM in resisting corrosion in this study.

The exposure zones role in inducing corrosion seems to agree with what was reported in the literature in terms that the corrosion was worst in the tidal zone for most mixtures (except for MCI where the splash and tidal zones had a relatively similar effect) followed by the splash and atmospheric zones, respectively as shown in Figure 6-24. The role of the cover depth seems to be critical in such a harsh environment and an effective cover of 50 mm and more seems to decrease the risk of corrosion significantly except for fly ash concretes where cover depth less 50 mm could be satisfactory. More research is required to identify the minimum effective cover for each concrete mix.

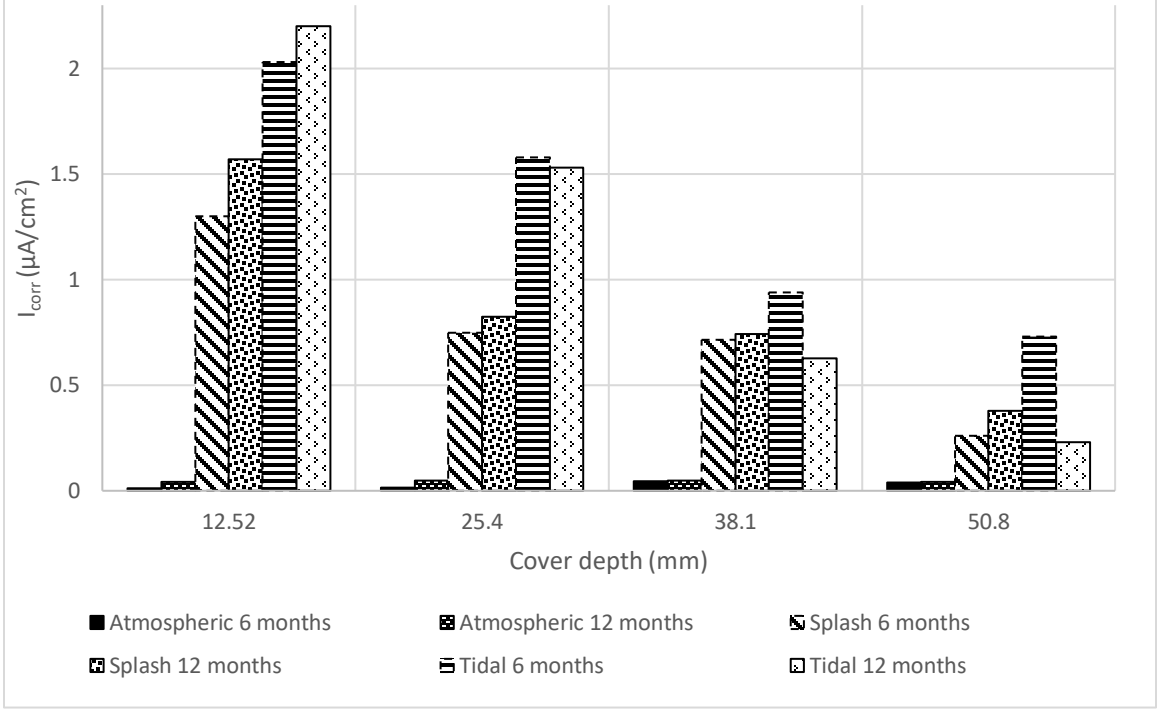
2
1.5
1
0.5
0
$I_{corr}$ (μA/cm²)
12.52
25.4
38.1
50.8
Cover depth (mm)
Atmospheric 6 months
Atmospheric 12 months
Splash 6 months
Splash 12 months
Tidal 6 months
Tidal 12 months

Type I

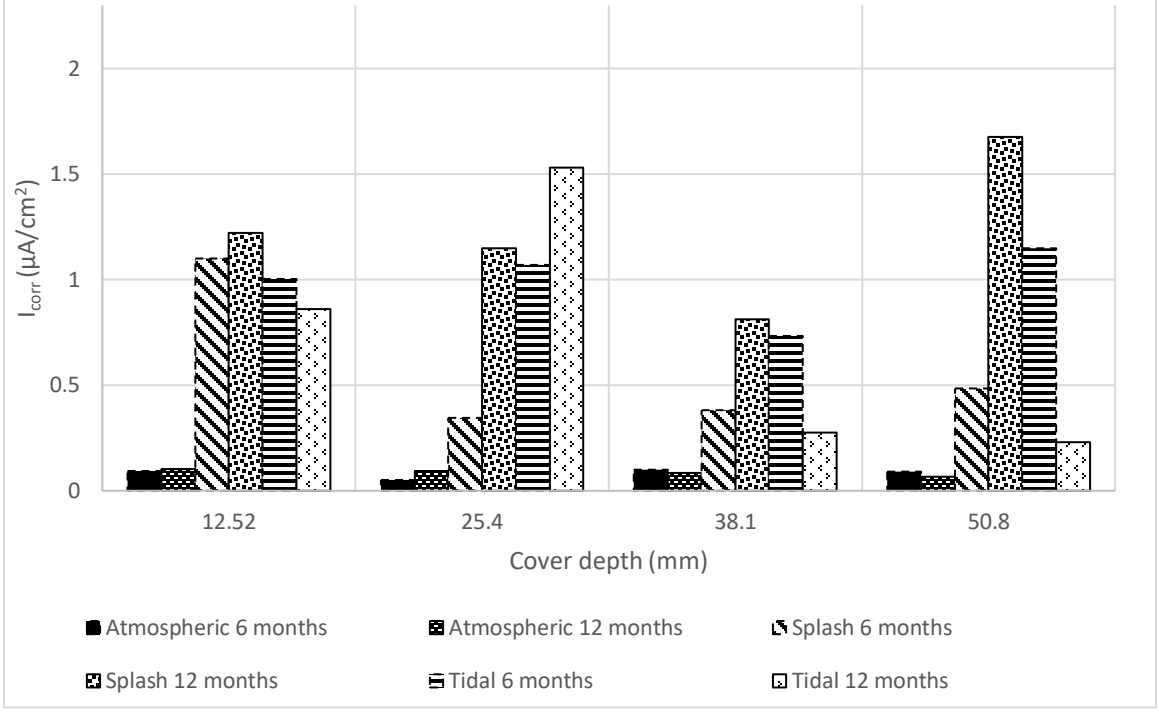
2
1.5
1
0.5
0
$I_{corr}$ (μA/cm²)
12.52
25.4
38.1
50.8
Cover depth (mm)
Atmospheric 6 months
Atmospheric 12 months
Splash 6 months
Splash 12 months
Tidal 6 months
Tidal 12 months

Type V

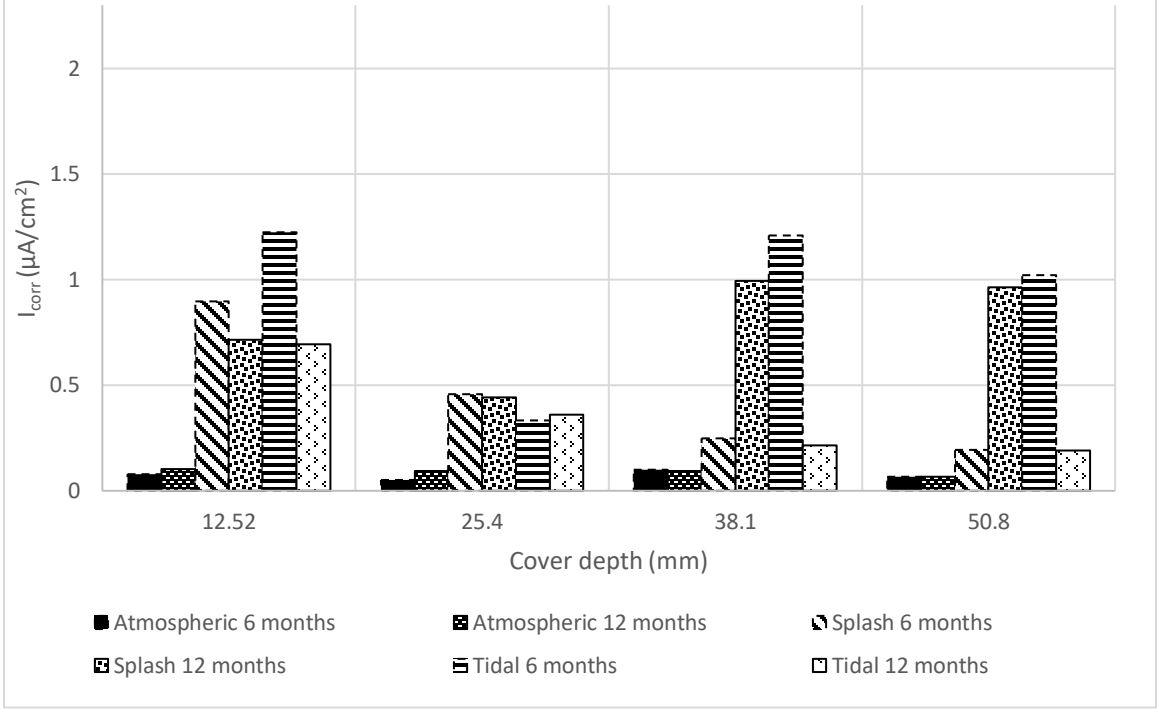
2
1.5
1
0.5
0
$I_{corr}$ (μA/cm²)
12.52
25.4
38.1
50.8
Cover depth (mm)
Atmospheric 6 months
Atmospheric 12 months
Splash 6 months
Splash 12 months
Tidal 6 months
Tidal 12 months

SF

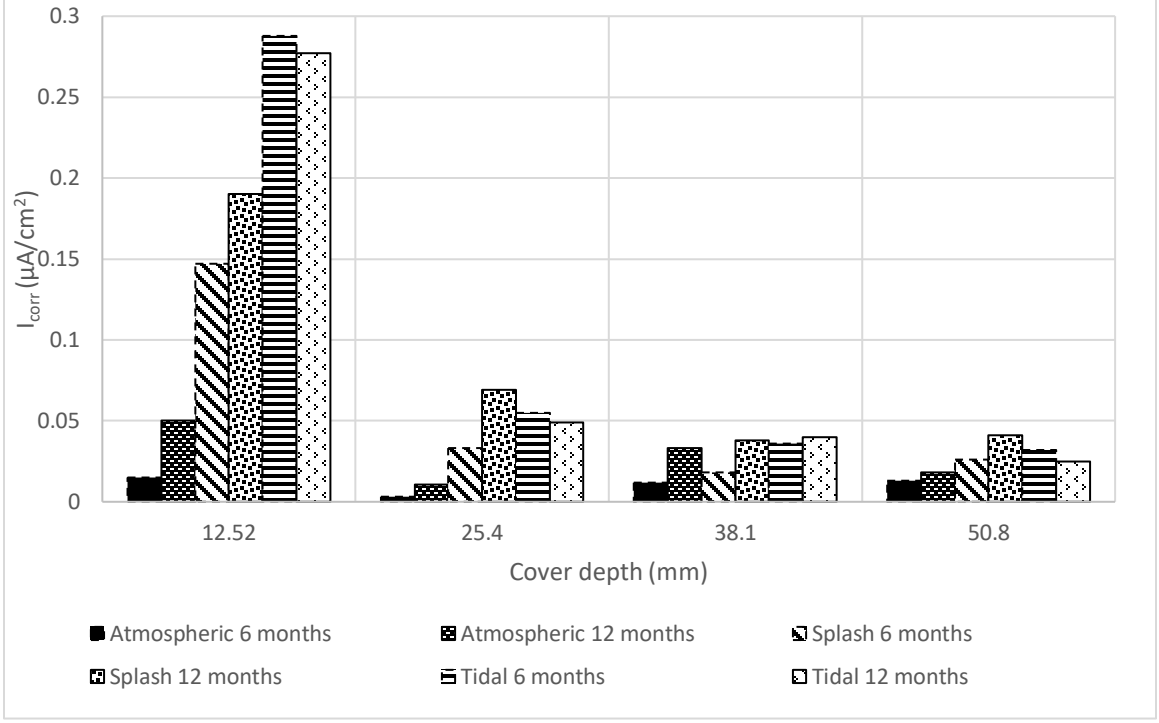
0.3
0.25
0.2
0.15
0.1
0.05
0
$I_{corr}$ (μA/cm²)
12.52
25.4
38.1
50.8
Cover depth (mm)
Atmospheric 6 months
Atmospheric 12 months
Splash 6 months
Splash 12 months
Tidal 6 months
Tidal 12 months

FA

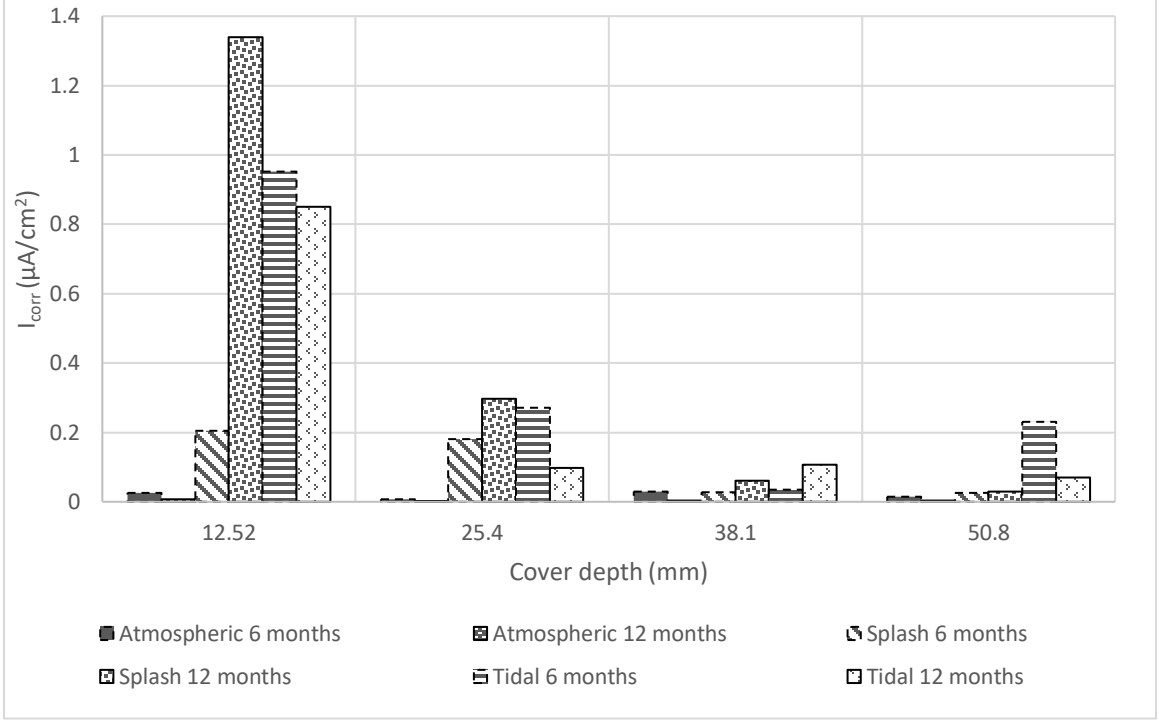
1.4
1.2
1
0.8
0.6
0.4
0.2
0
$I_{corr}$ (µA/cm²)
12.52
25.4
38.1
50.8
Cover depth (mm)
Atmospheric 6 months
Atmospheric 12 months
Splash 6 months
Splash 12 months
Tidal 6 months
Tidal 12 months

GGBFS

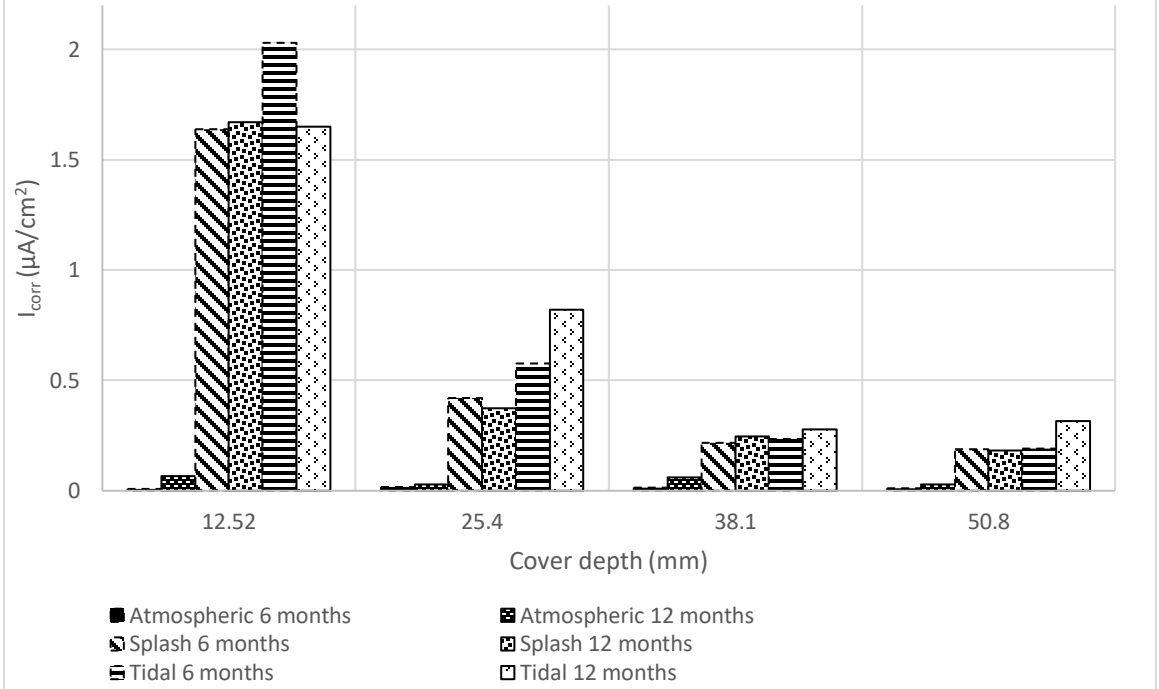
2
1.5
1
0.5
0
$I_{corr}$ (µA/cm²)
12.52
25.4
38.1
50.8
Cover depth (mm)
Atmospheric 6 months
Atmospheric 12 months
Splash 6 months
Splash 12 months
Tidal 6 months
Tidal 12 months

MCI

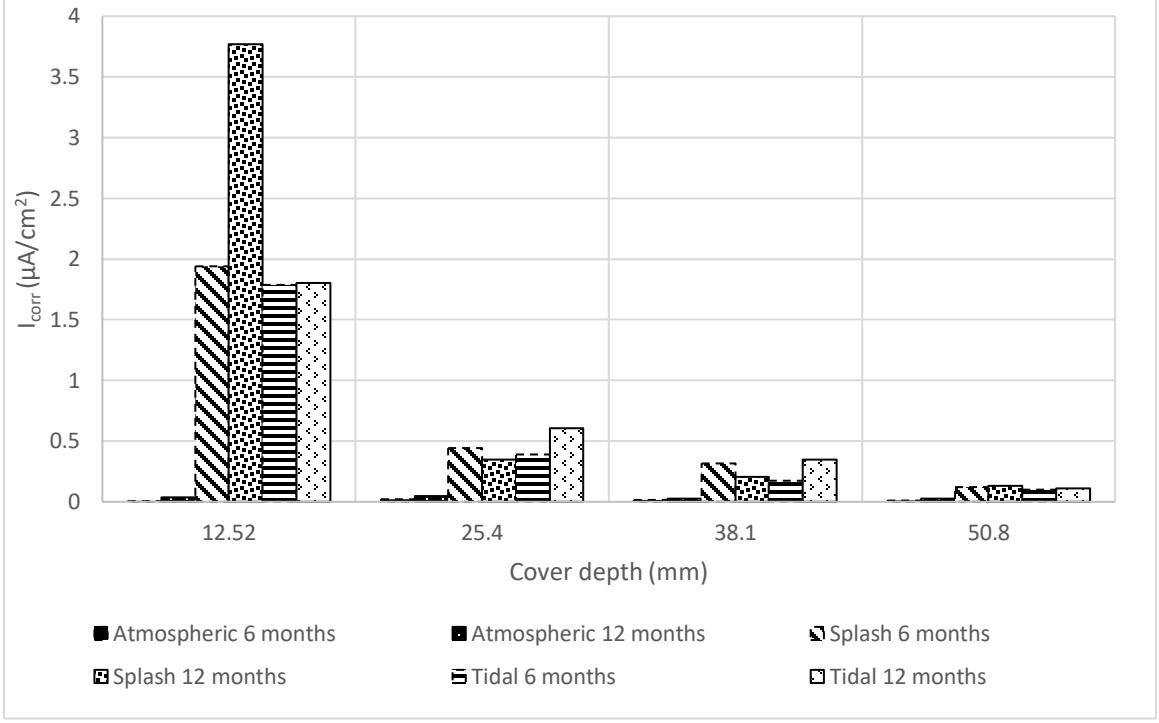
4
3.5
3
2.5
2
1.5
1
0.5
0
$I_{corr}$ (µA/cm²)
12.52
25.4
38.1
50.8
Cover depth (mm)
Atmospheric 6 months
Atmospheric 12 months
Splash 6 months
Splash 12 months
Tidal 6 months
Tidal 12 months

CNI

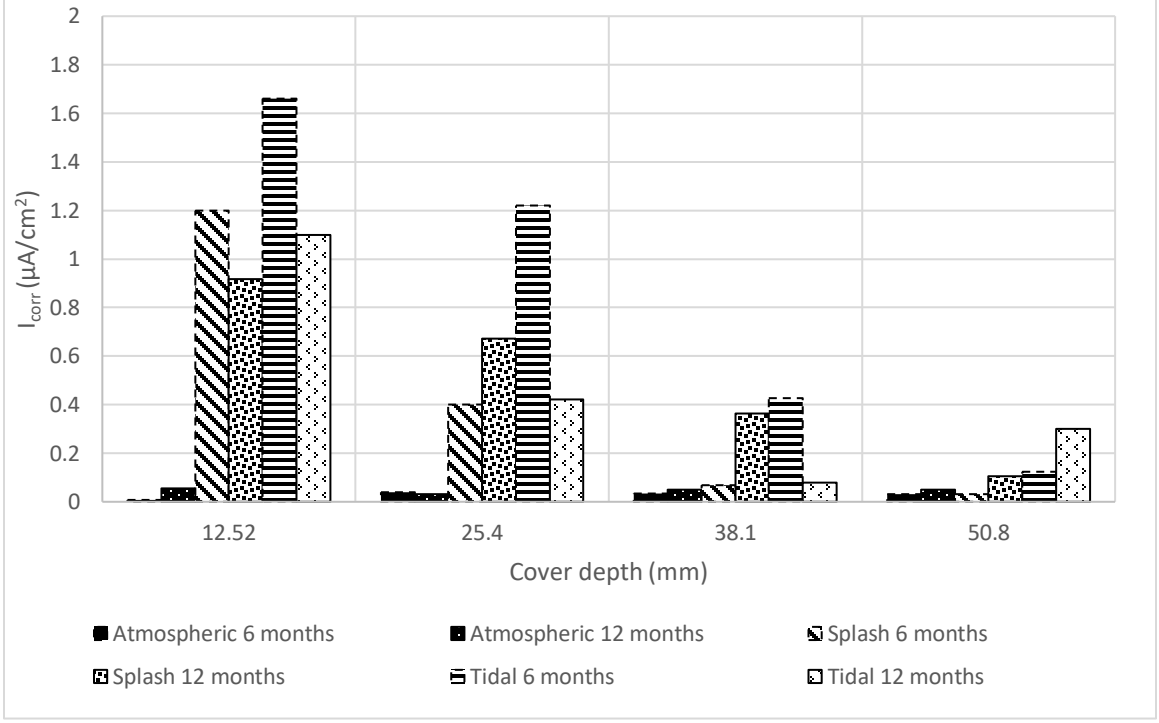


*Figure 6-24: Corrosion current density reading for all of the zones for each mix*

# CHAPTER 7.DISCUSSION

This section addresses three main aspects regarding the results gathered throughout the research project. The first is about modeling the binding results using different models gathered in the literature , suggests the use of a new logarithmic model and discusses which model seems to describe the binding results in the best way. The second section discusses the relationship between the chloride concentration level and the corrosion status and whether the corrosion threshold reported in the literature are conservative or not. The last section considers the overall performance of all the concrete mixtures prepared and tested during this research project and defines the advantages and disadvantages of each mix.

## 7.1. Chloride binding models

The literature suggests four main models to describe the binding capacity ($C_b$) of cement pastes when subjected to the binding experiment setup that was developed by Luping and Nilsson[46] in relation to the free chloride ($C_f$). The four models are: the freundlich isotherm model, the Langmuir isotherm model, the Tuutti linear model and modified Tuutti [79] model that was suggested by Arya et al. [78]. The models are as follow:

1. Freundlich isotherm and it is described by Equation 14

$$C_b = \alpha {C_f}^{\beta} \quad (14)$$

Where α and β are the Freundlich isotherms

2. Langmuir isotherm and it is describe by the following Equation 15

$$C_b = \frac{\alpha C_f}{(1+\beta C_f)} \quad (15)$$

Where α and β are the Langmuir isotherms

3. Tuutti linear model which is described by the following Equation 16

$$C_b = \alpha C_f \quad (16)$$

Where α is the slope of the binding curve

4. Modified Tuutti linear .model which is described by the Equation 17:

$$C_b = \alpha C_f + \beta \quad (17)$$

Where α is the slope of the line and β is the intersection with the y-axis.

This project studied the use of a logarithmic model that is described by the Equation 18:

$$C_b = \alpha \log(C_f) + \beta \quad (18)$$

Where α and β are constants of the model.

As illustrated in Table 7-1, the results of curve fitting the binding data gathered suggest that using the Freundlich isotherm fits the data in this project the best as long as the concentration of the free chloride does not exceed 1 Molar. On the other hand, the

logarithmic model and the Langmuir isotherm model seem to less correlate and produce results that are further away from the actual data at concentration higher than 0.5 Molar while the linear models seems to fit the data the least. This conclusion agrees with what was reported by Luping and Nilsson[46] regarding the Freundlich, Langmuir and Tuutti models and disagrees Mohammed and Hamada [80] who reported a linear relationship between the free and bound chloride. However, the modified linear model could be used to simplify the relationship between the bound and free chloride at high concentrations.

*Table 7-1: Curve fitting results for the binding models*

| Mix | Langmuir | | | Freundlich | | | Tuutti | | Modified Tuutti | | | Logarithmic | | |
|---|---|---|---|---|---|---|---|---|---|---|---|---|---|---|
| | α | β | $R^2$ | α | β | $R^2$ | α | $R^2$ | α | β | $R^2$ | α | β | $R^2$ |
| Type I | 21.7 | 1.09 | **0.979** | 9.1 | 0.421 | **0.991** | 4.43 | **0.373** | 2.96 | 4.64 | **0.924** | 8.14 | 10.34 | **0.947** |
| Type V | 15.3 | 1.05 | **0.963** | 6.6 | 0.420 | **0.993** | 3.24 | **0.554** | 2.42 | 2.56 | **0.865** | 5.67 | 7.47 | **0.938** |
| SF | 18.8 | 1.07 | **0.996** | 7.9 | 0.435 | **0.988** | 3.91 | **0.574** | 2.96 | 2.93 | **0.839** | 7.61 | 9.02 | **0.979** |
| FA | 34.2 | 1.03 | **0.994** | 14.6 | 0.445 | **0.981** | 7.34 | **0.600** | 5.64 | 5.23 | **0.838** | 14.24 | 16.82 | **0.971** |
| GGBFS | 56.5 | 1.46 | **0.990** | 20.5 | 0.434 | **0.991** | 12.90 | **0.570** | 9.58 | 6.79 | **0.837** | 17.36 | 22.42 | **0.987** |
| CNI | 27.9 | 1.39 | **0.984** | 10.1 | 0.393 | **0.987** | 4.79 | **0.448** | 3.48 | 4.08 | **0.810** | 8.84 | 11.34 | **0.982** |
| MCI | 21.4 | 1.10 | **0.989** | 8.9 | 0.425 | **0.995** | 4.38 | **0.552** | 3.28 | 3.41 | **0.848** | 8.32 | 10.11 | **0.975** |
| Caltite | 18.7 | 1.22 | **0.988** | 7.4 | 0.407 | **0.990** | 3.55 | **0.472** | 2.58 | 2.97 | **0.824** | 6.83 | 8.27 | **0.980** |

The difference between the models and how they fit the data is illustrated by an example in Figure 7-1

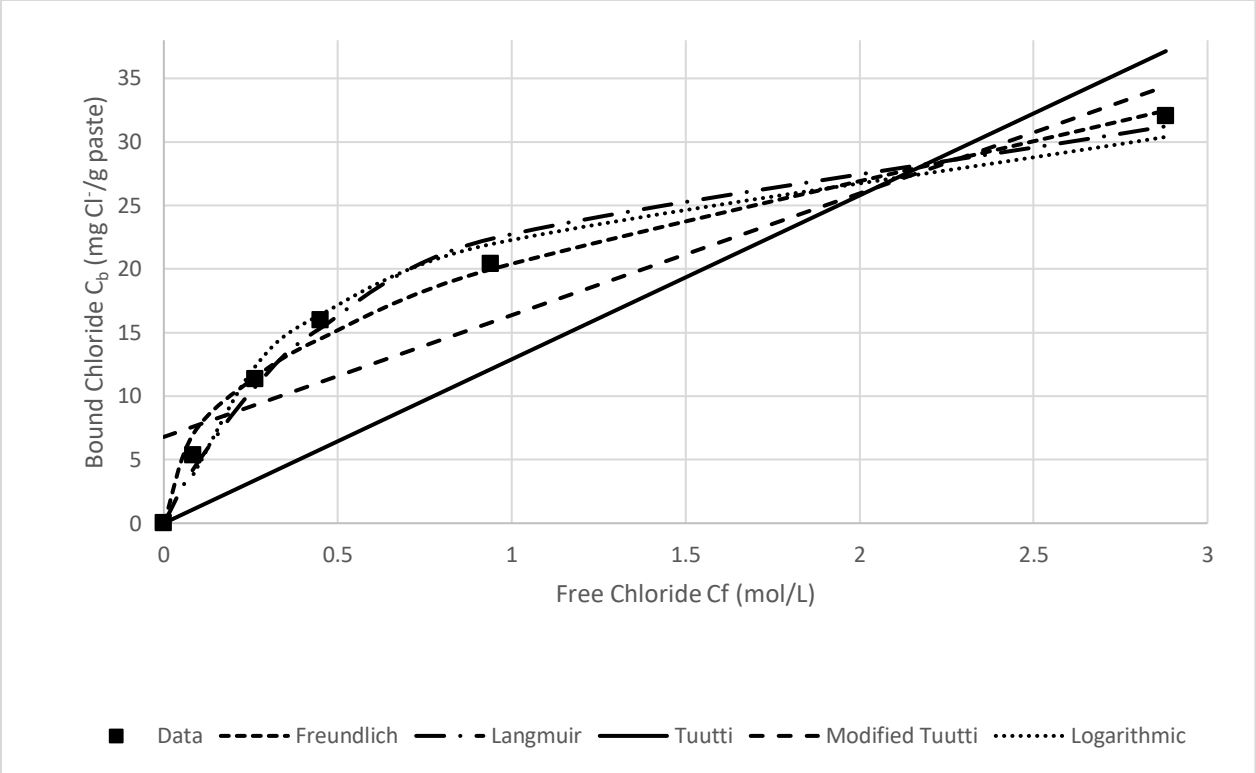


*Figure 7-1:Binding models example*

## 7.2. Chloride threshold and corrosion status

The threshold at which concrete is activated varies based on numerous variables such as the water-to-cement ratio, the exposure conditions, the exposure zone, the chloride cation ($Na^+$, $Ca^{++}$, etc.) , the concrete composition and the SCMs used with the concrete. The literature usually reports the critical total (acid soluble) chloride content ($C_{crit}$) per unit weight of binder to role out the effect of the water-to-cement ratio as Angst et al. reported [41]. The value ranges from 0.04% by weight of binder to 1.96 %. The literature reports the critical value based on case-by-case study and does not generalize. In this project, the reinforcement reached the corrosion activation at different depth and different exposure periods. The concentration at which they were activated is illustrated in Table 7-2. As expected, fly ash concrete and GGBFS concrete recorded the highest chloride values at which they were activated in terms of corrosion (0.795% and 1.129% respectively). This indicates that the limits in literature can be conservative for such mixtures that has a high tolerance and a high binding capacity. The addition of silica fume, CNI and MCI seems to increase the chloride threshold slightly when compared to the standard mix. On the other hand, caltite seems to decrease the chloride threshold slightly. Overall, the addition of different SCMs and chemical admixtures influence the concentration at which reinforcement could reach the activation stage which agrees with reports in the literature and requires further research.

*Table 7-2: chloride concentration at activation depth*

| Mix | Age at activation | Activation at Deepest Cover (mm) | Equivelent Concentration (%wt. binder) |
|---|---|---|---|
| Type I | 6 months | 50.8 | 0.113 |
| Type V | 6 months | 50.8 | 0.187 |
| SF | 6 months | 50.8 | 0.162 |
| FA | 12 months | 12.5 | 0.795 |
| GGBFS | 6 months | 12.5 | 1.129 |
| CNI | 6 months | 50.8 | 0.168 |
| MCI | 6 months | 38.6 | 0.193 |
| Caltite | 6 months | 38.6 | 0.106 |

These results can be used to estimate the time for the fly ash mix and GGBFS mix to show corrosion at deeper layers. Since the ACI 318-08[81] building code states a minimum of 3 inches (76.2 mm) of effective cover for concretes exposed to severe environments and assuming the corrosion to increase linearly, it would require 6 years for fly ash concrete exposed to the tidal zone to be activated at the effective cover depth recommended by the ACI (76.2 mm) and 3 years for GGBFS. On the other hand, it would take less than 1.5 years for the other mixes to get activated giving the assumption that corrosion advances linearly through the depth.

## 7.3. Overall performance of mixes

As illustrated in Table 7-3, the overall performance of the concrete shows that the addition of fly ash and GGBFS seem to improve most of the durability aspects of concrete indicating an improved and balanced micro structures that are water-tight and corrosion resistant unlike silica fume or type V where their addition seemed to improve one or two physical aspects and deteriorate the other aspects. For example, GGBFS reported a binding capacity that is more than 200% the standard mix which when combined with the absorption rate and corrosion activation depth and limit indicate a suitable match for harsh marine environments such as the one covered in this research project. On the other hand, the addition of chemical admixtures such as CNI, MCI or Caltite seem to improve the overall durability slightly. A mix that contain SCMs and chemical admixtures at the same time could improve all of the durability aspects but more research is required in that field.

*Table 7-3: Overall performance*

| Mix | f'c (%)[13] | Total Absorption (%)[13] | Density (%)[13] | Absorp. rate (%)[13] | RCPT Class | Binding (%)[13] | Diffusion[14] | | Corrosion Status[15] | | |
|---|---|---|---|---|---|---|---|---|---|---|---|
| | | | | | | | $C_s$ (% wt concrete) | $D_a$ (E-12 $m^2/s$) | Critical Zone | Activation Depth (mm) | High corrosion Depth (mm) |
| I | - | - | - | - | Moderate | - | 0.63 | 2.06 | Tidal | 50.8 | 25.4 |
| V | 101.9 | 97.8 | 100.4 | 30.7 | High | 67.6 | 0.58 | 2.63 | Tidal | 50.8 | 50.8 |
| SF | 107.8 | 87.1 | 100.4 | 17.0 | Low | 87.3 | 0.62 | 3.98 | Tidal | 50.8 | 50.8 |
| FA | 139.1 | 81.5 | 100.9 | 25.6 | Low | 163.7 | 0.48 | 1.46 | Tidal | 12.5 | None |
| GGBFS | 99.8 | 126.6 | 98.7 | 91.3 | Low | 206.9 | 0.96 | 1.35 | Tidal | 12.5 | 12.5 |
| CNI | 103.9 | 123.4 | 98.7 | 69.7 | Moderate | 105.9 | 0.70 | 3.16 | Tidal | 50.8 | 12.5 |
| MCI | 115.3 | 83.2 | 101.3 | 63.3 | High | 97.1 | 0.77 | 2.71 | Splash | 38.6 | 12.5 |
| Caltite | 100.0 | 87.7 | 98.7 | 50.8 | Moderate | 83.3 | 0.44 | 3.63 | Tidal | 38.6 | 25.4 |

[13] Relative to the standard mix.
[14] At 12 months of laboratory exposure.
[15] At 12 months of exposure in the site.

Another performance is the comparison between the performance of mixes in the laboratory and whether they reported similar performance in the exposure. This could be established by ranking the overall performance of the mixes in the laboratory and comparing to their ranking in the tidal exposure study since it was proven to be the most hostile when it comes to corrosion related durability aspects. As illustrated in Table 7-3, the laboratory performance of the mixes was categorized based mainly on the 12-months diffusion results represented by the diffusion profile and diffusion coefficient. As shown, GGBFS performed the best in terms of diffusion followed by fly ash and type I. on the other end, the performance of silica fume in terms of diffusion was the worst despite it having a more water tight internal structure as evident by its performance in the density test. This categorization does not take into consideration the effect of the binding or corrosion inhibitors since the laboratory experiments covered in this thesis did not test for simulated corrosion which indicates the necessity and importance of exposure studies since they take into consideration the main criteria which is whether the concrete exhibits corrosion or not.

*Table 7-4: categorization of the performance of the laboratory mixes.*

| Rank | Mix | $C_s$ (% wt concrete) | $D_a$ ($m^2/s$) |
|---|---|---|---|
| 1 | GGBFS | 0.96 | 1.35E-12 |
| 2 | FA | 0.48 | 1.46E-12 |
| 3 | Type I | 0.63 | 2.06E-12 |

| | | | |
|---|---|---|---|
| 4 | Type V | 0.58 | 2.63E-12 |
| 5 | MCI | 0.77 | 2.71E-12 |
| 6 | CNI | 0.70 | 3.16E-12 |
| 7 | Caltite | 0.44 | 3.63E-12 |
| 8 | SF | 0.62 | 3.98E-12 |

Regarding the performance of the mixtures in terms of the exposure testing. The corrosion state and depth of active layers after 12 months of exposure in the tidal zone was taken as the main categorization criteria. As shown in Table 7-5, fly ash and GGBFS reported the best performance followed by the chemical admixtures and then by type V and silica fume. One thing that both rankings agree on is the negative influence of silica fume in this project. This can be owed to the silica fume's dosage (6% replacement by weight of cement) being on the lower side as numerous studies reported an optimum dosage of 7.5% and beyond up to 10% [25], [29], [40].

*Table 7-5: Performance ranking based on the exposure testing*

| Rank | Mix | High corrosion Depth (mm) | Activation Depth (mm) |
|---|---|---|---|
| 1 | FA | 0 | 12.5 |
| 2 | GGBFS | 12.5 | 12.5 |
| 3 | MCI | 12.5 | 38.6 |
| 4 | CNI | 12.5 | 50.8 |
| 5 | Caltite | 25.4 | 38.6 |
| 6 | Type I | 25.4 | 50.8 |
| 7 | Type V | 50.8 | 50.8 |
| 8 | SF | 50.8 | 50.8 |

# CHAPTER 8. CONCLUSION

The study of the corrosion durability aspects of concrete mixes utilizing three supplementary cementitious materials (fly ash at 25%, silica fume at 6% and GGBFS at 70% by weight of binder) and three chemical admixtures (calcium nitrite inhibitor at 20 $L/m^3$ of concrete, migrating corrosion inhibitor at 0.6 $L/m^3$ and hydrophobic caltite at 30 $L/m^3$) exposed to the harsh marine environment of the Arabian Gulf establishes that the use of GGBFS and fly ash in such environment can increase the overall durability and life span of concrete structures made with such materials.

The study of the chloride ingress resistance of the previously mentioned concrete mixtures in the laboratory and in the field yielded trends of decreasing diffusion coefficients and increasing surface concentrations with time that were in agreement with the literature generally. The use of fly ash and GGBFS decreased the diffusion coefficeints considerably at all exposure and laboratory conditions and for both exposure periods (29% decrease for fly ash and 35% decrease for GGBFS). The surface concentration were found to be an indication of the binding capacity for both mixtures where an increase comparable to the standard mix was found. The application of silica fume, CNI, MCI and caltite seemed to increase the diffusion coefficient at all exposure periods and all exposure conditions indicating a worse corrosion resistance on their own. The RCPT values seem to reinforce this conclusion since only fly ash and GGBFS were reported to decrease the overall charges passed indicating better chloride resistance and

an overall better chloride-induced corrosion resistance while the other mixes had negative influence on the RCPT values indicating the opposite except for silica fume which in spite of having a low RCPT value reported a high diffusion activity..

The study of the density and sorptivity indicated that fly ash and caltite were able to enhance the micro-structure thus producing a more water-tight micro structure at the age of testing. The role of caltite in providing a hydrophobic nature for the concrete seem to be effective especially at early ages. The addition of GGBFS was found to increase the overall absorption by 26%.

The study of the chloride binding capacity of the mixes following Luping and Nilsson testing setup indicates the addition of fly ash and GGBFS seem to enhance the binding capacity significantly which in turn hinders the movement of chloride deeper into the concrete. The addition of silica fume or the use of type V concrete had an observable negative effect on the binding capacity which can be owed to the lower percentages of alumina salt in such mixes which help in binding the chloride permanently by forming Friedal's salts.

The study of the binding models (Freundlich, Langmuir, Tuutti and modified Tuutti) that were mentioned in the literature in addition to the logarithmic model that was proposed in this study were found to have varying degrees of effectiveness in describing the binding capacity in relation to the free chloride in the environment. The Freundlich model was

found to have the best fit to the binding data gathered in this study as long the free chloride concentration does not exceed 1M which covers the concentrations of chloride in most natural marine environments.

The study of the corrosion status of mixes in the three marine exposure zones (Atmospheric, Tidal and Splash) helped in classifying the zones that were most hostile to concrete in term chloride-induced corrosion. The tidal zone was found to be the harshest environment where 50% samples reported an activation depth of 50 mm (Type I, Type V, silica fume and CNI) after only 12 months of exposure followed by the splash zone. The corrosion risk and corrosion status of samples in the atmospheric zone was found to be considerably lower than the splash and tidal zones where none of the samples reported any activation at any depth after 12 months of exposure. The addition of fly ash and GGBFS was found to increase the corrosion resistance considerably where both mixtures did not report any high activity corrosion even after 12 months of exposure in the tidal zone while other mixes reported a high active corrosion status in the first depth (12.55 mm) after only 6 months of exposure.

The study of the critical chloride thresholds and its relation with the corrosion status for samples in this study indicate that the nature and composition of concrete has a major role in defining the threshold at which depassivation and corrosion activation can occur. In this study, it was found that the addition of fly ash and GGBFS can increase the critical

chloride concentration significantly from 0.1% by weight of binder to 0.8% for fly ash and 1.1% for GGBFS. The threshold was found for other mixtures was found to be between 0.1% and 0.2%. More research is required to identify the exact threshold and the influence of SCMs and chemical admixtures on it.

The study of the corrosion status after one year of exposure to the splash and tidal zones of the Arabian Gulf indicate that the use of the chemical admixtures (MCI, CNI and Caltite) seem to be more effective in reducing corrosion values as the cover depths increases.

# CHAPTER 9.RECOMMENDATIONS

The study of the durability aspects of concretes subjected to the marine environment in the Arabian Gulf in Eastern Province of Saudi Arabia lead to the following recommendation and suggestions for future studies:

- The use of Class F Fly ash and GGBFS in corporation with type I cement can improve the durability of mixtures subjected to similar exposure conditions.
- More research is required into the critical chloride threshold and their relation to the incorporation of SCMs and chemical admixtures in concrete.
- More research is required into the durability of mixtures that contain single or multiple SCMs and chemical admixtures in terms of chlorid-induced corrosion.
- The use of the durability data gathered in this study in developing a service life model that would be used to estimate the service life of structures exposed to the marine environments in the Gulf area.

# REFERENCES


[1] S. H. Kosmatka and M. L. Wilson, *Design and control of concrete mixtures*, 15th ed. Portland Cement Association, 2011.

[2] A. M. Neville, *Properties of Concrete*, 5th ed. Pearson Education Limited, 2011.

[3] K. A. Riding, M. D. A. Thomas, and K. J. Folliard, "Apparent Diffusivity Model for Concrete Containing Supplementary Cementitious Materials," *ACI Mater. J.*, vol. 110, no. No. 6, pp. 705–714, 2013.

[4] E. Ganjian and H. S. Pouya, "The effect of Persian Gulf tidal zone exposure on durability of mixes containing silica fume and blast furnace slag," *Constr. Build. Mater.*, vol. 23, no. 2, pp. 644–652, 2009.

[5] J. Lizarazo-marriaga, L. Guillermo, and L. Yépez, "EFFECT OF SILICA FUME ADDITION ON THE CHLORIDE- RELATED TRANSPORT PROPERTIES OF HIGH-PERFORMANCE CONCRETE TRANSPORTE EN EL CONCRETO DE ALTO DESEMPEÑO," pp. 105–110, 2012.

[6] H. Yazıcı, "The effect of silica fume and high-volume Class C fly ash on mechanical properties , chloride penetration and freeze – thaw resistance of self-compacting concrete," vol. 22, pp. 456–462, 2008.

[7] T. Cheewaket, C. Jaturapitakkul, and W. Chalee, "Long term performance of

chloride binding capacity in fly ash concrete in a marine environment," *Constr. Build. Mater.*, vol. 24, no. 8, pp. 1352–1357, 2010.

[8] B. Topçu, "Influence of fly ash on corrosion resistance and chloride ion permeability of concrete," vol. 31, pp. 258–264, 2012.

[9] R. Luo, Y. Cai, C. Wang, and X. Huang, "Study of chloride binding and diffusion in GGBS concrete," *Cem. Concr. Res.*, vol. 33, no. 1, pp. 1–7, 2003.

[10] H. Z. Lopez-Calvo, P. Montes-Garcia, T. W. Bremner, M. D. a Thomas, and V. G. Jiménez-Quero, "Compressive strength of HPC containing CNI and fly ash after long-term exposure to a marine environment," *Cem. Concr. Compos.*, vol. 34, no. 1, pp. 110–118, 2012.

[11] O. T. de Rincón, V. Millano, M. Aboulhosn, C. Morales, J. Bravo, M. Sánchez, D. Contreras, and Y. Hernández, "Evaluation of Hydrophobic Concrete Coatings in Tropical Marine Environments," *Corrosion*, vol. 67, no. 11, pp. 115001-115001–12, 2011.

[12] L. Schueremans, D. Van Gemert, and S. Giessler, "Chloride penetration in RC-structures in marine environment - Long term assessment of a preventive hydrophobic treatment," *Constr. Build. Mater.*, vol. 21, no. 6, pp. 1238–1249, 2007.

[13] N. C. Malikakkal, “Chloride diffusion in concrete/ prediction of the onset of corrosion in reinforced concrete structures,” King Fahd University of Petroleum and Minerals, 1994.

[14] W. Chalee, C. Jaturapitakkul, and P. Chindaprasirt, “Predicting the chloride penetration of fly ash concrete in seawater,” *Mar. Struct.*, vol. 22, no. 3, pp. 341–353, 2009.

[15] a C. Appleton, “Chloride penetration into concrete in marine environment - Part I1 : Prediction of long term chloride penetration,” *Mater. Struct.*, vol. 32, no. June, pp. 354–359, 1999.

[16] a Costa and A. Appleton, “Chloride penetration into concrete in marine environment -Part I: Main parameters affecting chloride penetration,” *Mater. Struct. Constr.*, vol. 32, no. May, pp. 252–259, 1999.

[17] O. Kayali and B. Zhu, “Corrosion performance of medium-strength and silica fume high-strength reinforced concrete in a chloride solution,” *Cem. Concr. Compos.*, vol. 27, no. 1, pp. 117–124, 2005.

[18] T. Matsumura, K. Shirai, and T. Saegusa, “Verification method for durability of reinforced concrete structures subjected to salt attack under high temperature conditions,” *Nucl. Eng. Des.*, vol. 238, no. 5, pp. 1181–1188, 2008.

[19] T. D. R.K. Dhir, M.A.K. El-Mohr and Dyer, “Developing chloride Resisting Concrete Using PFA,” *Cem. Concr. Res.*, vol. 27, no. 11, pp. 1633–1639, 1997.

[20] H.-W. Song and S.-J. Kwon, “Evaluation of chloride penetration in high performance concrete using neural network algorithm and micro pore structure,” *Cem. Concr. Res.*, vol. 39, no. 9, pp. 814–824, 2009.

[21] a. K. Tamimi, J. a. Abdalla, and Z. I. Sakka, “Prediction of long term chloride diffusion of concrete in harsh environment,” *Constr. Build. Mater.*, vol. 22, no. 5, pp. 829–836, 2008.

[22] M. Valipour, F. Pargar, M. Shekarchi, and S. Khani, “Comparing a natural pozzolan, zeolite, to metakaolin and silica fume in terms of their effect on the durability characteristics of concrete: A laboratory study,” *Constr. Build. Mater.*, vol. 41, pp. 879–888, 2013.

[23] K. Stanish and M. Thomas, “The use of bulk diffusion tests to establish time-dependent concrete chloride diffusion coefficients,” vol. 33, pp. 55–62, 2003.

[24] K. Yun and E. Kyum, “An experimental study on corrosion resistance of concrete with ground granulate blast-furnace slag,” vol. 35, pp. 1391–1399, 2005.

[25] M. Nokken, A. Boddy, R. D. Hooton, and M. D. A. Thomas, “Time dependent diffusion in concrete — three laboratory studies,” vol. 36, pp. 200–207, 2006.

[26] M. D. A. Thomas and P. B. Bamforth, “Modelling chloride diffusion in concrete Effect of fly ash and slag,” vol. 29, pp. 487–495, 1999.

[27] R. Siddique, “Compressive strength , water absorption , sorptivity , abrasion resistance and permeability of self-compacting concrete containing coal bottom,” *Constr. Build. Mater.*, vol. 47, pp. 1444–1450, 2013.

[28] R. D. Hooton, P. Pun, T. Kojundic, and P. Fidjestol, “INFLUENCE OF SILICA FUME ON CHLORIDE RESISTANCE OF CONCRETE,” in *PCI/FHWA International Symposium on High Performance Concrete*, 1997, pp. 245–256.

[29] a. a. Ramezanianpour and V. M. Malhotra, “Effect of curing on the compressive strength, resistance to chloride-ion penetration and porosity of concretes incorporating slag, fly ash or silica fume,” *Cem. Concr. Compos.*, vol. 17, no. 2, pp. 125–133, 1995.

[30] M. Safehian and A. A. Ramezanianpour, “Assessment of service life models for determination of chloride penetration into silica fume concrete in the severe marine environmental condition,” *Constr. Build. Mater.*, vol. 48, pp. 287–294, 2013.

[31] B. Demirel, “Effect of elevated temperature on the mechanical properties of concrete produced with finely ground pumice and silica fume,” vol. 45, pp. 385–

391, 2010.

[32] M. Uysal and V. Akyuncu, “Durability performance of concrete incorporating Class F and Class C fly ashes,” *Constr. Build. Mater.*, vol. 34, pp. 170–178, 2012.

[33] Z. Li, H. K. Venkata, and P. R. Rangaraju, “Influence of silica flour – silica fume combination on the properties of high performance cementitious mixtures at ambient temperature curing,” *Constr. Build. Mater.*, vol. 100, pp. 225–233, 2015.

[34] H. Y. Leung, J. Kim, A. Nadeem, J. Jaganathan, and M. P. Anwar, “Sorptivity of self-compacting concrete containing fly ash and silica fume,” *Constr. Build. Mater.*, vol. 113, pp. 369–375, 2016.

[35] K. Hung, U. J. Alengaram, M. Zamin, M. Yong, J. Liu, and J. Lim, “Assessing some durability properties of sustainable lightweight oil palm shell concrete incorporating slag and manufactured sand,” *J. Clean. Prod.*, vol. 112, pp. 763–770, 2016.

[36] P. Nath and P. Sarker, “Effect of Fly Ash on the Durability Properties of High Strength Concrete,” *Procedia Eng.*, vol. 14, pp. 1149–1156, 2011.

[37] K. Y. Ann, H. S. Jung, H. S. Kim, S. S. Kim, and H. Y. Moon, “Effect of calcium nitrite-based corrosion inhibitor in preventing corrosion of embedded steel in concrete,” *Cem. Concr. Res.*, vol. 36, no. 3, pp. 530–535, 2006.

[38] K. T. Kim, H. W. Kim, H. Y. Chang, B. T. Lim, H. B. Park, and Y. S. Kim, "Corrosion inhibiting mechanism of nitrite ion on the passivation of carbon steel and ductile cast iron for nuclear power plants," *Adv. Mater. Sci. Eng.*, vol. 2015, 2015.

[39] W. Morris and M. Vázquez, "A migrating corrosion inhibitor evaluated in concrete containing various contents of admixed chlorides," *Cem. Concr. Res.*, vol. 32, no. 2, pp. 259–267, 2002.

[40] M. Valipour, F. Pargar, M. Shekarchi, S. Khani, and M. Moradian, "In situ study of chloride ingress in concretes containing natural zeolite, metakaolin and silica fume exposed to various exposure conditions in a harsh marine environment," *Constr. Build. Mater.*, vol. 46, pp. 63–70, 2013.

[41] U. Angst, B. Elsener, C. K. Larsen, and Ø. Vennesland, "Critical chloride content in reinforced concrete — A review," *Cem. Concr. Res.*, vol. 39, no. 12, pp. 1122–1138, 2009.

[42] G. R. Meira, C. Andrade, C. Alonso, I. J. Padaratz, and J. C. Borba, "Modelling sea-salt transport and deposition in marine atmosphere zone - A tool for corrosion studies," *Corros. Sci.*, vol. 50, no. 9, pp. 2724–2731, 2008.

[43] C. Andrade and C. Alonso, "Corrosion rate monitoring in the laboratory and on-

site," *Constr. Build. Mater.*, vol. 10, no. 5, pp. 315–328, 1996.

[44] C. Andrade and C. Alonso, "On-site measurements of corrosion rate of reinforcements," *Constr. Build. Mater.*, vol. 15, no. 2–3, pp. 141–145, 2001.

[45] K. Y. Ann, J. H. Ahn, and J. S. Ryou, "The importance of chloride content at the concrete surface in assessing the time to corrosion of steel in concrete structures," *Constr. Build. Mater.*, vol. 23, no. 1, pp. 239–245, 2009.

[46] T. Luping and L.-O. Nilsson, "Chloride binding capacity and binding isotherms of OPC pastes and mortars," *Cem. Concr. Res.*, vol. 23, no. 2, pp. 247–253, 1993.

[47] M. D. a. Thomas, R. D. Hooton, a. Scott, and H. Zibara, "The effect of supplementary cementitious materials on chloride binding in hardened cement paste," *Cem. Concr. Res.*, vol. 42, no. 1, pp. 1–7, 2012.

[48] M. Islam and M. Islam, "Strength and durability characteristics of concrete made with fly-ash blended cement," *Aust. J. Struct. Eng.*, vol. 14, no. 3, pp. 303–319, 2013.

[49] R. K. Dhir, M. a K. El-Mohr, and T. D. Dyer, "Chloride binding in GGBS concrete," *Cem. Concr. Res.*, vol. 26, no. 12, pp. 1767–1773, 1996.

[50] A. Delagrave, J. Marchand, J. Ollivier, S. Julien, and K. Hazrati, "Chloride Binding Capacity of Various Hydrated Cement Paste Systems," vol. 7355, no. 97.

[51] Q. Yuan, C. Shi, G. De Schutter, K. Audenaert, and D. Deng, “Chloride binding of cement-based materials subjected to external chloride environment – A review,” *Constr. Build. Mater.*, vol. 23, no. 1, pp. 1–13, 2009.

[52] M. Akiyama, D. M. Frangopol, and M. Suzuki, “Integration of the effects of airborne chlorides into reliability-based durability design of reinforced concrete structures in a marine environment,” *Struct. Infrastruct. Eng.*, vol. 8, no. 2, pp. 125–134, 2012.

[53] C. Andrade, C. Alonso, and J. Sarŕa, “Corrosion rate evolution in concrete structures exposed to the atmosphere,” *Cem. Concr. Compos.*, vol. 24, no. 1, pp. 55–64, 2002.

[54] M. Shekarchi, A. Rafiee, and H. Layssi, “Long-term chloride diffusion in silica fume concrete in harsh marine climates,” *Cem. Concr. Compos.*, vol. 31, no. 10, pp. 769–775, 2009.

[55] M. a. Mustafa and K. M. Yusof, “Atmospheric chloride penetration into concrete in semitropical marine environment,” *Cem. Concr. Res.*, vol. 24, no. 4, pp. 661–670, 1994.

[56] G. R. Meira, C. Andrade, C. Alonso, J. C. Borba, and M. Padilha, “Durability of concrete structures in marine atmosphere zones - The use of chloride deposition

rate on the wet candle as an environmental indicator," *Cem. Concr. Compos.*, vol. 32, no. 6, pp. 427–435, 2010.

[57] S.-W. Pack, M.-S. Jung, H.-W. Song, S.-H. Kim, and K. Y. Ann, "Prediction of time dependent chloride transport in concrete structures exposed to a marine environment," *Cem. Concr. Res.*, vol. 40, no. 2, pp. 302–312, 2010.

[58] S. K. Roy, Liam Kok Chye, and D. O. Northwood, "Chloride ingress in concrete as measured by field exposure tests in the atmospheric, tidal and submerged zones of a tropical marine environment," *Cem. Concr. Res.*, vol. 23, no. 6, pp. 1289–1306, 1993.

[59] P. Sandberg, L. Tang, and a Andersen, "Recurrent studies of chloride ingress in uncracked marine concrete at various exposure times and elevations," *Cem. Concr. Res.*, vol. 28, no. 10, pp. 1489–1503, 1998.

[60] O. Trocónis de Rincón, M. Sánchez, V. Millano, R. Fernández, E. a. de Partidas, C. Andrade, I. Martínez, M. Castellote, M. Barboza, F. Irassar, J. C. Montenegro, R. Vera, a. M. Carvajal, R. M. de Gutiérrez, J. Maldonado, C. Guerrero, E. Saborio-Leiva, a. C. Villalobos, G. Tres-Calvo, a. Torres-Acosta, J. Pérez-Quiroz, M. Martínez-Madrid, F. Almeraya-Calderón, P. Castro-Borges, E. I. Moreno, T. Pérez-López, M. Salta, a. P. de Melo, G. Rodríguez, M. Pedrón, and M. Derrégibus, "Effect of the marine environment on reinforced concrete

durability in Iberoamerican countries: DURACON project/CYTED," *Corros. Sci.*, vol. 49, no. 7, pp. 2832–2843, 2007.

[61] M. a. Pech-Canul and P. Castro, "Corrosion measurements of steel reinforcement in concrete exposed to a tropical marine atmosphere," *Cem. Concr. Res.*, vol. 32, no. 3, pp. 491–498, 2002.

[62] I. L. Kondratova, P. Montes, and T. W. Bremner, "Natural marine exposure results for reinforced concrete slabs with corrosion inhibitors," *Cem. Concr. Compos.*, vol. 25, no. 4–5, pp. 483–490, 2003.

[63] ASTM International, "ASTM C 642 Standard Test Method for Density, Absorption, and Voids in Hardened Concrete," *Annu. B. ASTM Stand.*, no. March, pp. 1–3, 1997.

[64] ASTM International, "Standard Test Method for Measurement of Rate of Absorption of Water by Hydraulic-Cement Concretes," *ASTM Int.*, vol. 41, no. 147, pp. 1–6, 2013.

[65] ASTM International, "Determining the Apparent Chloride Diffusion Coefficient of Cementitious Mixtures by Bulk Diffusion 1," *ASTM Int.*, vol. 4, pp. 1–7, 2003.

[66] ASTM International, "Standard Test Method for Compressive Strength of Cylindrical Concrete Specimens 1," vol. 4, no. October, pp. 1–7, 2014.

[67] GAMRY, “Getting Started With Your First Experiment : DC105 Corrosion Techniques- Polarization Resistance,” *Gamry Appl. Notes*, pp. 3–7, 2014.

[68] ASTM International, “Standard Test Method for Electrical Indication of Concrete ’ s Ability to Resist Chloride,” *Annu. B. ASTM Stand.*, no. 95 mm, pp. 1–6, 2008.

[69] SBC, “Saudi Building National Committee.” [Online]. Available: https://sbc.gov.sa. [Accessed: 01-Jan-2016].

[70] S. M. Mosaddad and M. Delphi, “A Numerical Study of Thermocline in the Persian Gulf,” *Middle-East J. Sci. Res.*, pp. 772–780, 2013.

[71] ASTM International, “Standard Test Method for Acid-Soluble Chloride in Mortar and Concrete.” ASTM international, West Conshohocken, PA, pp. 3–5, 2006.

[72] C. Hall, “Water sorptivity of mortars and concretes: a review,” *Mag. Conrete Res.*, vol. 41, no. 147, pp. 51–61, 1989.

[73] German Instruments, “Proove It manual.” 2014.

[74] T. Cheewaket, C. Jaturapitakkul, and W. Chalee, “Initial corrosion presented by chloride threshold penetration of concrete up to 10 year-results under marine site,” *Constr. Build. Mater.*, vol. 37, pp. 693–698, 2012.

[75] W. U. Ling-jie, Z. Yong-jun, K. O. U. Xin-jian, and J. Meng, “Reliability-based service life prediction of existing concrete structures under marine environment,”

pp. 3608–3614, 2015.

[76] S. V. Nanukuttan, L. Basheer, W. John McCarter, D. J. Robinson, and P. a. Muhammed Basheer, “Full-scale marine exposure tests on treated and untreated concretes-initial 7-year results,” *ACI Mater. J.*, vol. 105, no. 1, pp. 81–87, 2008.

[77] M. V. a. Florea and H. J. H. Brouwers, “Chloride binding related to hydration products,” *Cem. Concr. Res.*, vol. 42, no. 2, pp. 282–290, 2012.

[78] C. Arya, N. R. Buenfeld, and J. B. Newman, “Factors influencing chloride-binding in concrete,” *Cem. Concr. Res.*, vol. 20, no. 2, pp. 291–300, 1990.

[79] T. K., “Analysis of pore solution squeezed out of cement and mortar.,” *Nord. Concr Res*, vol. 1, no. 25, pp. 1–16, 1982.

[80] M. TU and H. H., “Relationship between free chloride and total chloride contents in concrete,” *Cem Concr Res*, vol. 33, no. 14, pp. 87–90, 2003.

[81] ACI, *Building Code Requirements for Structural Cocnrete*. ACI, 2008.

# VITAE

| | |
|---|---|
| Name | :Ibrahim Nabil Ali Al-Duais |
| Nationality | :Yemeni |
| Date of Birth | 12-Jan-1992 |
| Email | :Ibrahim.ce92@gmail.com |
| Address | :Student Housing, KFUPM, Dhahran, Saudi Arabia |
| Academic Background | :Bachelor of Science in Civil and Environmental Engineering from KFUPM with second Honors awarded in 2014. |